Human Pegivirus Infection of the Central Nervous System: Neural Cell Tropism and Neuroimmune Responses

by

Matthew Anthony Lynn Doan

A thesis submitted in partial fulfillment of the requirements for the degree of

Master of Science

in

NEUROSCIENCE

Neuroscience and Mental Health Institute
University of Alberta

Abstract

Human pegivirus (HPgV) is a positive sense, single-stranded RNA virus of the *Flaviviridae* family that is best characterized in the context of peripheral lymphocyte infection. Our group recently reported HPgV infection in the central nervous system (CNS) of two patients with fatal leukoencephalitis wherein HPgV NS5A antigen was detected chiefly in glial cells in cerebral white matter. Brain derived viral sequences from these patients revealed an 87-nucleotide deletion in the HPgV *NS2* gene that had not been previously characterized. Other related members of the *Flaviviridae* family, including Zika virus (ZIKV) and West Nile virus (WNV), are known to cause encephalitis, establishing a precedent that prompted further investigation into HPgV as a putative causative agent of encephalitis. To date, HPgV has not been shown to be an etiological agent in any disease and HPgV neurotropism has yet to be investigated.

In this thesis, HPgV was shown to infect, replicate, and spread in human fetal astrocytes *in vitro*. As HPgV has been described as a lymphotropic virus, this finding expands our understanding of HPgV tropism and provides new evidence that HPgV can infect CNS cells. Human microglia, the resident macrophages of the brain, were also identified as being permissive to HPgV infection. Using a HPgV viral clone containing the 87-nucleotide deletion in the *NS2* gene, HPgV WT and ΔNS2 were tested in parallel and HPgV ΔNS2 showed greater infectivity, replication and spread in human astrocytes.

Antiviral and proinflammatory responses to HPgV infection were also examined in human astrocytes and microglia. Similar transcriptional profiles in HPgV WT and ΔNS2-infected astrocytes were observed following infection of human astrocytes. In contrast, human microglia showed differential induction of proinflammatory genes such as interferon, following HPgV ΔNS2 infection compared to HPgV WT. Further, cell death mechanisms were not activated in either microglia nor astrocytes following infection with either HPgV WT or ΔNS2, unless infection was combined with a second stimulus in the form of an inflammatory cytokine. Within the human CNS, analysis of frontal cortical samples showed that HPgV infection was associated with the suppression of several antiviral and proinflammatory genes compared to uninfected patient samples. RNA deep sequencing analysis of patients in this cohort recapitulated the suppression of various antiviral pathways in the CNS of HPgV-infected patients and revealed the induction of specific neuroinflammatory pathways. *NOS2*, which can either exert proinflammatory or immunomodulatory effects, was identified by RNA sequencing as markedly induced in the CNS of HPgV-infected patients.

This thesis provides previously unrecognized evidence that HPgV infects, replicates and spreads in primary human astrocyte and microglia cultures, and an 87-nucleotide deletion in the HPgV *NS2* gene modulates these viral properties *in vitro*. In addition, the differential immune responses observed following HPgV WT and ΔNS2 infection suggested that the *NS2* gene might also modulate host immune

responses. Lastly, the identification and analysis of seven new HPgV-infected patients offered an opportunity to investigate the host responses in the CNS, which had not previously been possible. These findings represent a substantial advance in the understanding of HPgV biology within the context of the CNS.

Preface

All experiments in this thesis were performed by Matthew Doan with the exception of: (i) Figure 5.3, which was imaged and quantified by Dr. Brienne McKenzie, a post-doctoral fellow and (ii) the Ingenuity™ analysis that produced Figure 5.6 and Figure 5.7 were performed by William Branton, a technician in the Brain Power Lab. Human cortex samples were provided from the National Neuro-AIDS Tissue Consortium (NNTC) through a collaboration with Dr. Benjamin Gelman, University of Texas Medical Branch. Human cortex and white matter samples from patients LE-1 and LE-2 that were imaged in Figure 5.3 were provided by Dr. Frank van Landeghem, University of Alberta. RNA sequencing was performed at the Institut de Recherches Cliniques de Montréal (IRCM). Sanger sequencing to identify mutations in Figure 3.3A and Figure 3.3C were performed by the TAGC facility, University of Alberta. I performed subsequent analysis of Sanger sequencing data.

The use of human tissues was approved (Pro0002291, Pro00027660) by the University of Alberta Human Research Ethics Board (Biomedical) and written informed consent was received for all samples.

Acknowledgements

I would first like to thank my supervisor, Dr. Christopher Power, for providing me the opportunity to join his group and for the mentorship, scientific insight and guidance he provided during my tenure in the Brain Power Lab. Being part of a translational laboratory allowed me to think and evolve as a scientist in a unique way. I am grateful to both the Alberta MS Network for funding my summer studentship and to the Canadian Institutes of Health Research (CIHR) for funding my MSc studies. I would also like to thank my committee members, Dr. Gregg Blevins and Dr. Tom Hobman for their invaluable support, insight, and mentorship during my degree. To Dr. Bradley Kerr, Amber Lapointe and the rest of the NMHI team, thank you for your unwavering support and assistance throughout my time as a graduate student. I would also like to express my gratitude to Dr. Jack Stapleton from the University of Iowa for his helpful insight and scientific support early in my studies.

To current and past members of the Brain Power Lab, I would like to thank each of you for your scientific contributions and individual expertise you offered to my project. I would like to thank my first scientific mentor in the lab, Manmeet, for her guidance, friendship and scientific knowledge that helped me in my studies. Brie, thank you for your incredible mentorship and friendship that certainly improved me as a scientist and as a person. Will, and Jason, thank you for your friendship and numerous scientific and non-scientific discussions over the years. Also, thank you to

Carla for your ongoing kindness, mentorship, and guidance throughout my undergraduate and graduate journey.

Finally, I would like to thank my friends for their encouragement along the journey. And to my family I offer my utmost gratitude for your ongoing love, support, and encouragement that made it possible for me to accomplish this degree.

Table of Contents

List of Tables

Chapter I

Chapter II

Chapter V

List of Figures

Chapter I

Chapter III

Chapter IV

Chapter V

Appendix

List of Abbreviations

ALR	AIM2-like receptor
anti-LGI1	Anti-leucine-rich, glioma inactivated 1
anti-NMDAR	Anti-*N*-methyl-D-aspartic acid
ART	Antiretroviral therapy
BBB	Blood-brain barrier
BMEC	Brain microvascular endothelial cell
CCR	C-C chemokine receptor
CD	Cluster of differentiation
CLR	C-type lectin receptor
CNS	Central nervous system
COX	Cyclooxygenase
CSF	Cerebrospinal fluid
CXCR	C-X-C chemokine receptor
CYTOF	Cytometry by time of flight
ddPCR	Droplet digital PCR
DENV	Dengue virus
dsRNA	Double stranded ribonucleic acid
EAE	Experimental autoimmune encephalomyelitis
EEG	Electroencephalogram
eNOS	Endothelial NOS
EPgV	Equine pegivirus
FIV	Feline immunodeficiency virus
FOV	Field of view
GBS	Guillain-Barré syndrome
GBVC	GB virus C
GE	Genomic equivalents
GFAP	Glial fibrillary acidic protein
HAAA	Hepatitis-associated aplastic anemia
HAND	HIV-1-associated neurocognitive disorders
HBV	Hepatitis B virus
HBCA	Human brain cortical astrocytes
HCV	Hepatitis C virus
HFA	Human fetal astrocytes
HFM	Human fetal microglia
HGV	Hepatitis G virus
HIV-1	Human Immunodeficiency virus type 1
HIVE	HIV-1 encephalitis
HL	Hodgkin's Lymphoma
HPgV	Human pegivirus
HSV-1	Herpes simplex virus type 1
IDU	Intravenous drug user
IF	Immunoflourescent
IFN	Interferon
IFNAR	Interferon-alpha/beta receptor
IFNα	Interferon alpha

IFNβ	Interferon beta
IHC	Immunohistochemical
IL	Interleukin
IL-1RA	Interleukin-1 receptor alpha
iNOS	Inducible NOS
IRCM	Institut de Recherches Cliniques de Montréal
IRF3	Interferon regulatory factor 3
ISG	Interferon-stimulated gene
JAK	Janus kinase
JEV	Japanese encephalitis virus
LDH	Lactate dehydrogenase
MAVS	Mitochondrial antiviral signalling protein
MBP	Myelin basic protein
MFI	Mean fluorescent intensity
MIP	Macrophage inflammatory protein
MOI	Multiplicity of infection
MOMP	Mitochondrial outer membrane permeabilization
MR	Magnetic resonance
MRI	Magnetic resonance imaging
MS	Multiple sclerosis
MSM	Men who have sex with men
MVEV	Murray Valley encephalitis virus
NCCD	Nomenclature Committee on Cell Death
NF-κB	Nuclear factor kappa-light-chain-enhance of activated B cells
NHL	Non-Hodgkin's Lymphoma
NK	Natural killer
NLR	NOD-like receptor
nNOS	Neuronal NOS
NNTC	National Neuro-AIDS Tissue Consortium
NO	Nitric oxide
NOS	Nitric oxide synthase
ODC	Other disease control
ORF	Open reading frame
PAMP	Pathogen-associated molecular pattern
PBMC	Peripheral blood mononuclear cells
PCR	Polymerase chain reaction
PG	Prostaglandin
PPgV	Porcine pegivirus
PRR	Pattern recognition receptor
qPCR	Semi-quantitative PCR
qRT-PCR	Semi-quantitative-real-time PCR
RCD	Regulated cell death
RFC	Relative fold change
RIG-I	Retinoic acid-inducible gene 1
RLR	RIG-I-like receptor
RNA	Ribonucleic acid
RNA-seq	RNA sequencing
ROI	Region of interest

ROS	Reactive oxygen species
RT-dPCR	Real-time digital PCR
SDF	Stromal cell-derived factor
SEM	Standard error of the mean
SIV	Simian immunodeficiency virus
SPgV	Simian pegivirus
ssRNA	Single stranded ribonucleic acid
STAT	Signal transducer and activator of transcription
TAM	TYRO3, AXL and MER
TBEV	Tick-borne encephalitis virus
TCR	T-cell receptor
TDAV	Theiler's disease-associated virus
Th1	T helper 1
Th2	T helper 2
TIM	T-cell immunoglobulin and mucin domain
TLR	Toll-like receptor
TNF-α	Tumour necrosis factor alpha
TRIF	TIR-domain containing adapter-inducing interferon-β
USA	United States of America
UTR	Un-translated region
VGKC	Voltage-gated potassium channel
WNV	West Nile virus
WM	White matter
WT	Wild type
ZIKV	Zika virus

Chapter I: Introduction

1.1 Encephalitis

1.1.1 Clinical overview

Encephalitis is a severe and potentially fatal disorder characterized by inflammation of the brain parenchyma and associated neurological dysfunction[1,2]. The word encephalitis is derived from the ancient Greek terms *enkephalos* (brain) and *itis* (inflammation). In developed countries, the incidence rate of encephalitis is approximately 7 cases per 100,000 people[1,3]. Typically, encephalitis presents with clinical symptoms including headaches, fevers, encephalopathy, seizures, and other neurological dysfunctions and deficits[4,5]. Common causes of encephalitis include acute viral infections of the central nervous system (CNS) and autoimmune disorders; however, the etiology of encephalitis is unclear in 40-80% of patients, and new pathogens are increasingly being discovered that have associations with encephalitis[1,3]. Children and the elderly are particularly vulnerable to encephalitis, especially that of viral origin[6]. The incidence of encephalitis in children in both the United States of America (USA) and England has increased over the past 10 years, potentially due to increased usage of immunosuppressive therapies[7].

The most recent diagnostic criteria for encephalitis established by the International Encephalitis Consortium include the presence of encephalopathy, or altered consciousness for at least a 24-hour period, and the presence of two of the following: (i) fever, (ii) seizures or other focal neurological findings, (iii) CSF pleocytosis (increased white blood cell count), (iv) abnormal neuroimaging

suggesting encephalitis, or (v) electroencephalogram (EEG) results suggesting encephalitis[8,9].

1.1.2 Neuropathology and pathogenesis

Although the causes of encephalitis are diverse (as discussed below), the neuropathological presentation is remarkably consistent. In the brain parenchyma, encephalitis is usually characterized by intense and dysregulated neuroinflammation, breakdown of the blood-brain barrier (BBB), massive infiltration of circulating lymphocytes, and sustained activation of astrocytes and microglia[10]. This neuroimmune response is associated with the release of neurotoxic inflammatory mediators such as cytokines and reactive oxygen species (ROS), which can lead to bystander tissue damage, neuronal damage and neurological dysfunction[11]. Gliosis characterized by activation of microglia, the resident macrophages of the brain, and astrocytes is often found during encephalitis[12]. Early histological studies of humans who have died due to viral encephalitis have shown striking inflammatory responses present in post mortem tissue[13].

1.1.3 Causes of encephalitis

Viral

The most common cause of encephalitis is viral infection, with herpes simplex virus type 1 (HSV-1) infection being the most prominent[14]. To cause direct infection of the

CNS, a virus must cross the BBB and find a host cell permissive to maintaining viral replication. Three common routes for viruses to enter the CNS compartment are: (i) the virus travels along a peripheral nerve with subsequent infection of neurons in a (trigeminal) ganglion or CNS neurons, (ii) systemic viremia that leads to viral translocation across the BBB, or (iii) a 'Trojan Horse' mechanism wherein the virus employs immune cells trafficking to the brain parenchyma to transport the virus into the CNS[15]. Encephalitis due to viral infection can either be the sole neurologic manifestation following infection, or it may occur in conjunction with myelitis, neuritis or meningitis[16].

Autoimmune

Autoimmune encephalitis refers to a family of related disease processes that share similar clinical features but are differentiated by specific antibody subtypes that drive the immune attacks on the CNS[17]. Current literature suggests that two broad categories of antibody-mediated encephalitis exist, comprised of (i) paraneoplastic (neoplasm-associated) disorders with induced antibodies targeting intracellular antigens (e.g. anti-Hu), and (ii) non-paraneoplastic syndromes wherein autoantibodies target extracellular antigens such as ion channels and receptors (e.g. anti-NMDA receptor antibodies)[17,18]. Autoimmune encephalitis is usually associated with antibodies that target CNS antigens and the pathology is likely mediated by an accompanying cytotoxic T cell response[19]. Common autoantibodies that are associated with non-paraneoplastic autoimmune encephalitis include anti-*N*-

methyl-$_{D}$-aspartic acid (anti-NMDA) receptor antibody, anti-leucine-rich, glioma inactivated 1 (anti-LGI1) antibody and the voltage-gated potassium channel (VGKC) antibody[20]. A common presenting sign in these patients are seizures[18].

Other types of encephalitides

Bacteria and fungi are rare causes of encephalitis, with reports of 3% and 1% in encephalitis patients from previous studies, respectively[15]. These infectious agents typically cause meningitis although under certain conditions, encephalitis may occur following invasion of the brain by either bacteria or fungi[21]. Noninfectious mimics of encephalitis also exist under certain circumstances, including but not limited to vascular disease, neoplasms and certain drug intoxication effects[22].

For the remainder of this thesis, I will focus upon the molecular drivers of neuropathology in the context of viral encephalitis, as it is most pertinent to the virus studies in this thesis.

1.2 Mechanisms of antiviral immunity in the central nervous system

1.2.1 Innate and adaptive immunity in the brain

Innate Immunity

The innate immune response in the CNS is the first line of defense against viral infections and other harmful microbes/molecules that might enter from the periphery. All major CNS cell types (including neurons, oligodendrocytes, astrocytes, and resident microglia/trafficking macrophages) express pattern recognition receptors (PRRs) and can participate in the detection of viral genomes and virus-encoded proteins, with astrocytes and microglia serving as the predominant effectors of the CNS innate immune response[23]. Several PRR families assist in the recognition of pathogen-associated molecular patterns (PAMPs), including the Toll-like receptors (TLRs), NOD-like receptors (NLRs), AIM2-like receptors (ALRs), RIG-I-like receptors (RLRs) and C-type lectin receptors (CLRs), among others[24,25]. These PRRs may be present on the plasma membrane (TLRs/CLRs), within the cytoplasm (NLRs/RLRs/ALRs), or on endolysosomes (TLRs)[25]. Ultimately, the ligation of PRRs leads to the activation of proinflammatory transcription factors that direct antiviral immunity.

Cytokines, chemokines, and other inflammatory mediators

PRR ligation leads to the activation and nuclear translocation of central proinflammatory transcription factors such as nuclear factor kappa-light-chain-enhancer of activated B cells (NF-κB), a crucial proinflammatory regulator responsible for (among other things), the synthesis and release of cytokines such as interleukin (IL)-1α, IL-1β, IL-6, tumor necrosis factor alpha (TNF-α), and IL-12[26]. Such cytokines have a wide variety of autocrine and paracrine effects in the CNS, including engagement of additional intracellular proinflammatory signaling pathways, disruption of the BBB, recruitment and migration of immune cells, and activation of specific immune cell phenotypes[27].

In both murine and cell culture models of viral encephalitis, IL-1β has been shown to be elevated following viral infection; it can result in fever, increased BBB permeability, and the production of additional proinflammatory cytokines and inflammatory mediators[14].

Although crucial for clearance of viruses, many immune mediators exert off-target effects that can contribute to neuroinflammation and tissue damage during viral infections. For example, TNFα and IL-1β have well-documented cytotoxicity against both neurons and oligodendrocytes through a variety of mechanisms, including glutamate excitotoxicity and pyroptosis[28]. Thus, antiviral mechanisms might have detrimental effects on the delicate CNS microenvironment.

Although cytokines are essential for minimizing viral spread and localizing infection, innate immune responses are rarely sufficient in abrogating viral infection of the CNS[26]. Cytokines, including IL-1β, IL-6 and TNF-α, can cause disruption of the BBB and allow leukocyte infiltration into the CNS to access the infection[29]. This phenomenon is assisted by the release of chemokines, including RANTES, MIP-1α and IP-10, a unique group of cytokines that have longer-range effects and promote the recruitment of both innate and adaptive immune cells to the site of infection[30].

In the context of encephalitis, inflammatory mediators including ROS, prostaglandins (PGs) and nitric oxide (NO) play a crucial role in propagating CNS inflammation. The production of ROS mediates several secondary mechanisms of tissue damage during viral encephalitis, including affecting signaling pathways that stimulate further production of cytokines and chemokines by microglia[31]. The overabundance of ROS is detrimental though, and leads to the deterioration of neuronal cells and plays a significant role in exacerbating neuroinflammation and tissue damage, with significant connections between ROS and neurodegenerative diseases including Alzheimer's disease, Parkinson's disease and ageing[32].

Two major classes of PG generating enzymes include cyclooxygenase-1 (COX-1) and COX-2. COX-2 is inducible under inflammatory conditions and has been shown to localize to neurons, astrocytes and endothelial cells in the CNS[33]. During encephalitis

and other inflammatory conditions, PGs can regulate the chemokine gradient in the CNS[33].

Nitric oxide synthase (NOS) has three isoforms in the CNS including: (i) NOS1 or neuronal NOS (nNOS), in neurons, (ii) NOS2, or inducible NOS (iNOS), in microglia and some astrocytes and, (iii) NOS3, or endothelial NOS (eNOS) in endothelial cells and astrocytes[33]. Of particular interest, iNOS is not constitutively expressed by astrocytes and microglia, although inflammatory stimuli such as inflammatory damage, astrogliosis, or viral infection, induce its expression[34,35]. The overproduction of NO in the CNS has been identified as a major cause for several neurological diseases[36]. iNOS is also involved in catabolizing arginine in the CNS, whilst a similar molecule, indoleamine 2,3-dioxygenase (IDO), is involved in tryptophan metabolism in the CNS[37]. Both iNOS and IDO are induced by IFNγ expression and have been shown to regulate viral, bacterial and parasitic replication in humans[38]. These factors in combination with the production of cytokines and chemokines alter the inflammatory milieu of the CNS during encephalitis.

Interferon responses and host restriction factors in the brain

Depending upon the specific ligand detected, different PRRs transmit the danger signal to the nucleus through a series of different downstream second messenger proteins. For example, in the brain, astrocytes, neurons, and microglia constitutively express TLR-3, TLR-7 and TLR-9[26]. TLR-3 detects double stranded ribonucleic acid

(dsRNA) inside of endosomes after uptake by endocytosis, and its engagement induces the type I interferon (IFN) response downstream of TIR-domain containing adapter-inducing interferon-β (TRIF) activation and interferon regulatory factor 3 (IRF3) nuclear translocation[39]. Another well-known antiviral defense mechanism is the retinoic acid-inducible gene 1 (RIG-I) sensor, which detects dsRNA and signals through the mitochondrial antiviral signaling protein (MAVS), located on the mitochondrial surface[40]. This pathway, similar to TLR3, induces IRF3/7 translocation and IFN induction. Previous work in this area has shown that both the hepatitis C virus (HCV) protease and the human pegivirus (HPgV) protease can cleave MAVS in an effort to evade the innate immune response[39,41].

Type I interferons (IFNα/β) are essential cytokines that limit viral replication and further viral infection. Multiple interferon-stimulated genes (ISGs), including IRF1 and MX1, are induced following activation of IRF3/7[42]. IFNα/β are released and act in an autocrine and paracrine manner through the Janus kinase/signal transducer and activator of transcription (JAK/STAT) pathway to promote viral clearance; this pathway has been well-studied in various CNS cell types, including neurons[43]. Loss of the type I IFN-α/β receptor (IFNAR) in mice renders these animals more susceptible to CNS viral infection and encephalitis, illustrating the importance of IFNs to combatting viral neuropathogenesis[26]. The loss of IFNAR affects the severity viral infections of the CNS in several ways, and it was observed that in the knock-out

mice mentioned above, two members of the *Flaviviridae* family, WNV and Murray Valley encephalitis virus (MVEV), have increased viral load and neurovirulence[44,45].

Adaptive immunity

Adaptive immunity is characterized by long-lived, antigen-specific immune (memory) responses, mediated primarily by B and T lymphocytes. Professional antigen-presenting cells, such as dendritic cells, also participate in the generation of the adaptive immune response through the presentation of antigenic peptides. During homeostasis, the brain parenchyma is seemingly devoid of adaptive immune cells, which are primarily compartmentalized to specific CNS structures such as the meninges and choroid plexus[46]. Early observations regarding the relative lack of adaptive immune cells within the brain parenchyma were fundamental to the enduring concept of the CNS as an "immune privileged" environment. However, the immune cell composition of the brain changes vastly under neuroinflammatory conditions, a phenomenon which has been recently interrogated with single-cell resolution using techniques such as single cell RNA-seq and mass cytometry (cytometry by time of flight (CYTOF))[47].

In the context of viral infection, antigen-specific CD4+ and CD8+ T lymphocytes accumulate in the CNS and can mediate antiviral immunity[48]. The infiltration of both CD8+ and CD4+ T cells play an important role in clearing viruses and other pathogens from the CNS[49]. The degree to which the adaptive immune response is

functionally effective in clearing CNS infections is highly variable. For example, Zika virus (ZIKV) infection has been shown to be independent of both B and T lymphocytes based upon observations that *Rag1* knockout mice have a similar disease course to wild-type animals[50]. However, both the adaptive and innate arms of the immune system are necessary to not only control WNV infection in humans, but to also clear the virus and reduce the ensuing immunopathogenesis[51].

1.2.2 Cell death mechanisms in encephalitis

If an individual cell is unable to contain a viral infection, it is advantageous to the host organism to remove that cell through a process of regulated cell death (RCD) instead of permitting unrestricted viral replication. Many forms of RCD exist[52], of which apoptosis and pyroptosis are two of the most pertinent for viral infections.

Apoptosis

Apoptosis is the most common cell death mechanism by which damaged, infected or excess cells are eliminated[53]. Although exceptions exist, apoptosis is widely considered to be non-immunogenic, thus preventing the release of proinflammatory molecules that would otherwise drive a cycle of local inflammation; for this reason, in moderation, apoptosis represents one of the least harmful forms of cell death in the CNS and is widely observed during normal CNS development[52].

According to the Nomenclature Committee on Cell Death (NCCD), apoptosis may be either intrinsic (initiated by microenvironmental alterations that cause mitochondrial outer membrane permeabilization (MOMP) leading to direct activation and execution by caspase-3) or extrinsic (initiated by microenvironmental alterations that are detected by plasma membrane receptors, leading to activation of caspase-8 and execution by caspase-3)[52]. The process of apoptotic cell death is thus conceptualized as a widespread, systematic and protease-driven destruction of cellular structures, wherein executioner caspase-3 and -7 target hundreds of protein substrates to mediate a highly coordinated process of cellular dismantling[54].

Virus-induced apoptosis of neurons in the CNS was first reported in Sindbis virus-induced encephalitis[55]. Nonetheless, because apoptosis is a commonly utilized mechanism to remove infected cells, many viruses have evolved methods of modulating apoptotic responses. Viruses from the flavivirus family have several different proteins involved in regulating apoptosis of infected cells within the host, either creating pro-survival or pro-apoptotic environments[56]. As an example, both Japanese encephalitis virus (JEV) and Dengue virus (DENV) activate ER-associated protein degradation machinery in order to protect infected cells from cell death[56]. Taken together, viral modulation of apoptotic mechanisms can influence the ability for the virus to spread within the host and cause virulence.

Pyroptosis

On the other end of the inflammatory spectrum, pyroptosis is a highly proinflammatory form of cell death that may occur during viral infections. Based on NCCD guidelines, pyroptosis depends on the formation of gasdermin pores in the plasma membrane following perturbations of intracellular or extracellular homeostasis leading to activation of proinflammatory caspases[52]. Unlike apoptosis, pyroptosis is mediated primarily by the proinflammatory caspases-1/-4/-5/-11 and ultimately results in cell membrane rupture and lysis, perpetuating a cycle of local inflammation.

Many viruses that cause CNS infections have been shown to induce pyroptosis in the host as an attempt to combat viral infection. ZIKV has been shown to increase IL-1β, NLRP3 and caspase-1 transcripts in glial cell lines, all important in the execution of pyroptosis[57]. Similarly, pyroptosis has been described during HIV-1 infection as a pathway by which CD4+ T cells are depleted during infection[58]. At the same time, multiple viruses have also developed ways of circumventing pyroptosis. For example, Enterovirus 71 can cleave and inactivate the pyroptosis executioner protein, gasdermin D[59].

1.3 Human encephalitis-associated viruses

With viral encephalitis representing about 50% of encephalitis cases in the United States[6], it is necessary to understand how different viruses affect the CNS and the similarities and differences present during infection.

1.3.1 Herpes simplex virus type 1 (HSV-1)

Herpes simplex associated encephalitis is almost exclusively caused by HSV-1, with most infections acutely occurring in early childhood or in adults over the age of 50[16]. The pathophysiology of CNS infection is not fully understood, although HSV-1 encephalitis is typically initiated by either primary infection or viral reactivation from within the host[16]. Most patients present with acute or rapid onset of typical encephalitis-associated signs including fever, headache, confusion and altered behavior, although more serious deficits including seizures and cranial neuropathies are also seen in HSV-1 encephalitis cases[16]. Approximately a third of all patients become comatose, with manifestations evolving over the course of infection[16]. HSV-1 encephalitis usually begins unilaterally with only one half of the brain affected, with brain areas including the anterior and medial temporal lobes, frontal lobes, thalamus and insular cortex being selectively targeted[16].

1.3.2 Human immunodeficiency virus type 1 (HIV-1)

HIV-1 is a retrovirus that causes a persistent infection that progresses to death in persons without antiretroviral therapy (ART) intervention[60]. The initial recognition that HIV-1 affected the CNS came in 1983, when 50 patients were analyzed, revealing a high prevalence of chronic progressive encephalopathy, later termed HIV-1 dementia[61]. Continued studies have now shown that approximately 20-50% of HIV-1 infections lead to HIV-1-associated neurocognitive disorders (HAND) that can include HIV-1 encephalitis (HIVE)[4,62]. The neuronal damage and death seen in HIVE is caused indirectly, wherein HIV-1 infects macrophages and microglia but not neurons[63]. This leads to accompanying neuronal injury that is indirectly caused by the release of inflammatory molecules and viral proteins by infected glial cells, damaging neurons and leading to abundant inflammation[64-66]. HIVE typically appears late during the course of infection, when the patients are severely immunocompromised and results in atrophy, neuroinflammation and BBB perturbation affecting both the white and grey matter[67].

1.3.3 Flaviviruses

The *Flaviviridae* family has several members that are known to be neurotropic, most being prominent arthropod viruses that are associated with encephalitis cases in North America[68]. The *Flavivirus* genus consists of positive-single stranded enveloped RNA viruses that typically include attachment molecules that are essential for binding to host cell receptors[68]. In general, it is known that many

members of the *Flaviviridae* family rely on multiple cellular proteins and host cell receptors for infection and viral propagation within the CNS[68]. Common receptors used by flaviviruses include members of the CLR family and phosphatidylserine receptors composed of TIM (T-cell immunoglobulin and mucin domain) and TAM (TYRO3, AXL and MER)[69]. Once attached to the cell, these viruses are sequestered into membrane-bound vesicles where they are transported by the endocytotic pathway through the cytosol until the viral envelope fuses with the endosomal membrane and the viral nucleocapsid is released into the cytoplasm of the host cell[68]. The viruses in this family that are known to be neurotropic include Zika virus (ZIKV), West Nile virus (WNV), Japanese encephalitis virus (JEV), Dengue virus (DENV) Tick-borne encephalitis virus (TBEV) and Murray Valley encephalitis virus (MVEV). Below I will focus on how each virus listed above enters the CNS as well as the associated clinical features.

Zika virus (ZIKV)

ZIKV is an arbovirus and was first isolated from a sentinel monkey in Uganda in 1947[70], and since then has been shown to cause neurological disease in adults and microencephaly in fetuses[50]. The most recent outbreak of ZIKV in 2015 spread to over 48 countries in the Americas wherein over 171,553 cases were reported as of November 2016[71].

Viral neuroinvasion and neurotropism

Several mechanisms of ZIKV transmission into the CNS are proposed, all of which resemble what has been described previously in the above sections. The capacity for ZIKV pathogenesis to be unaffected by interferon exposure suggests the virus has the ability to evade or dismantle certain aspects of host viral defense mechanisms and may potentially aid its efforts to gain access to the CNS[72]. Once inside the CNS, it is believed that astrocytes are the main reservoir for ZIKV[73]. Other studies have shown that ZIKV can directly infect human cortical neuron progenitor cells and neural progenitor cells *in vitro*[74]. ZIKV can also infect neurospheres and brain organoid cultures thus reducing their viability and growth, resembling the microencephaly phenotype[75].

Clinical manifestations

The major neurological clinical manifestation is microcephaly in newborns and Guillain-Barré syndrome (GBS) in adults. GBS is characterized as a rapid-onset weakness and sensory loss caused by damage of peripheral nerves by the immune system[74]. Microcephaly meanwhile, is a condition in which the brain of a fetus does not fully develop, resulting from prenatal ZIKV infection causing encephalitis that is manifested in newborns[71].

West Nile virus (WNV)

WNV is currently the second most common cause of encephalitis worldwide and was first introduced to North America in 1999[51]. WNV has been found across the globe, most prominently in the United States, North Africa and Europe[16]. Similar to ZIKV, it is a member of the *Flaviviridae* family, is an arbovirus and has associations with encephalitis. Encephalitis is the most common neurological presentation of WNV infection, with approximately 50%-60% of neuroinvasive infections being classified as encephalitis[16].

Viral neuroinvasion and neurotropism

WNV has been shown to cross the BBB leading to neuronal cell infection and ensuing cell death, gliosis, and an influx of leukocytes leading to inflammation[76]. Neuroinvasion is dictated by viral structure proteins, in particular the E protein of WNV[51]. Although the determinants of neuroinvasion are not fully known, it is believed that WNV can gain entry to the CNS through several routes including, (i) binding and penetration through epithelial cells lining brain capillaries, (ii) breakdown of the BBB leading to WNV entry, (iii) infection of olfactory neurons which spreads into the CNS to the olfactory bulb or (iv) a 'Trojan Horse' mechanism that was described previously[51]. After initial systemic infection and replication inside the host, WNV can enter the CNS and propagate within neuron and myeloid cells[51].

Clinical manifestations

In approximately 1 in 150 WNV-infected patients, neurological involvement is evident, termed 'neuroinvasive disease'[77]. WNV has a tendency to infect the brainstem early during CNS invasion, but can also affect the basal ganglia, thalamus and cerebellum[16]. Patients with WNV encephalitis present with typical encephalitis features, although additional movement disorders are common including tremor, parkinsonism and dyskinesia[16].

Japanese encephalitis virus (JEV)

In low income countries, JEV has become one of the most common causes of encephalitis, with approximately 60% of the world population living in JEV endemic areas[78]. Further, JEV is the most common cause of encephalitis in Asia with an estimated 35,000- 50,000 reported cases annually[15]. Although JEV-associated encephalitis is fatal in 25% of symptomatic cases, infection is asymptomatic in approximately 90% of cases[78,79]. In the majority of cases, children and young adults are predominantly affected[16].

Viral neuroinvasion and neurotropism

Little is known regarding the mechanisms by which JEV enters the CNS, although it is known that viral entry and neuronal infection precede the breakdown of the BBB in animal models of disease[80]. Several proposed models for how JEV enters have been proposed, including (i) the infection of endothelial cells lining brain capillary

networks wherein the virus penetrates into the CNS and can infect microglia and astrocytes, before spreading to neurons or (ii) JEV-infected immune cells travel to the CNS through physiological routes including the choroid plexus into the ventricular space[80].

Clinical manifestations

One of the most common outcomes of JEV encephalitis is seizures, with tremors and overall rigidity presented frequently as well[16]. Typically, the basal ganglia, thalamus and brainstem are most affected following neuroinvasion although JEV is often focal and therefore few brain regions are affected[80]. In endemic regions, JEV typically infects children, although in newly affected areas JEV encephalitis has been seen in both children and adults[81].

Dengue virus (DENV)

Commonly found in India, China, Southeast Asia, Africa and South America, DENV is an arbovirus that has neurological manifestations in approximately 10% of patients with DENV infection[16]. Four serotypes of DENV exist, all of which are able to cause Dengue fever and neurological disease[82]. Since the most common and well-characterized complication of DENV infection is Dengue fever, little literature exists regarding DENV-associated encephalitis. In order to diagnose DENV encephalitis, CNS involvement and the presence of DENV RNA or antibodies must be present within the CSF or brain parenchyma itself[83].

Viral neuroinvasion and neurotropism

Early studies suggested that DENV did not enter the CNS, although this has been disproven over time with the detection of viral antigen, RNA and antibodies being present within the CNS[82]. The ability for the virus to penetrate the CNS is not well characterized, although many indirect effects of peripheral infection including the immune response, metabolic abnormalities, shock, and liver failure all are important in creating conditions allowing DENV to infiltrate the CNS[84].

Clinical manifestations

Encephalitis is not normally seen following DENV infection and in patients with DENV encephalitis, CSF cellularity appears normal in 75% of patients[82]. Clinical symptoms are therefore not outlined in the diagnosis for DENV encephalitis, although case reports have suggested that the criteria include (i) a fever, (ii) cerebral involvement, (iii) the presence of antibodies to DENV in the CSF and (iv) exclusion of other viral pathogens present[85]. A recent report showed chronic encephalitis associated with DENV infection of the CNS in an individual with progressive dementia[86].

Tick-borne encephalitis virus (TBEV)

TBEV consists of three subtypes including the (i) European (TBEV-Eu), (ii) Siberian (TBEV-Si) and (iii) Far Eastern (TBEV-FE)[87] subtypes. Each viral subtype is found across Eastern Europe and into Eastern Asia, although the different subtypes are all

carried by different strains of ticks. Different viral subtypes are also associated with varying degrees of pathogenesis within a host[88]. TBEV is transmitted to humans from the saliva of a tick within minutes of a bite and can be sustained within multiple generations of ticks[87].

Viral neuroinvasion and neurotropism

TBEV enters the brain through the hematogenic pathway using infected blood cells[88]. Similar to other flaviviruses, the exact mechanism is unknown although the common viral entry routes have been proposed: (i) infection of olfactory neurons or peripheral nerves, (ii) viral infection of endothelial cells lining brain vessels, (iii) crossing of the BBB following infection or (iv) a 'Trojan Horse' mechanism relying on viral infection of infected leukocytes that traffic into the CNS[88]. Once inside the CNS, the virus causes brain damage through several mechanisms including cytotoxic T cell infiltration, microglial activation and proliferation, neural degeneration and inflammatory cell death[88].

Clinical manifestations

Viral infection is broken down into two stages, with the second stage including a clinical spectrum ranging from mild meningitis to overt encephalitis[87]. TBEV preferentially affects large neurons in the grey matter including the basal ganglia, medulla oblongata, spinal cord, brainstem or cerebellar Purkinje cells[4]. Within

patients, TBEV-Fe causes the most severe forms of CNS disease with mortality rates ranging from 5-20% among infected patients[77].

Murray Valley encephalitis virus (MVEV)

Similar to other flaviviruses, MVEV is an arbovirus that is endemic to Australia and New Guinea. The majority of MVEV cases occur during outbreaks, such as that which occurred in 1974 when 58 cases of MVEV-associated encephalitis cases were identified[89]. Since then, it is believed that MVEV was contained within zoonotic foci within Australia until the next outbreak, which occurred in 2011, with 17 confirmed cases[90].

Viral neuroinvasion and neurotropism

Little is known about how MVEV gains access to the CNS or its pathogenesis within the CNS, although one study reported that MVEV preferentially induces neuronal injury in the olfactory lobe and hippocampus within 5 days of infection[91]. A recent study described a single MVEV encephalitis case (out of three total) in which viral antigens and RNA were detected solely in neurons, suggesting this virus is primarily neuronotropic[92].

Clinical manifestations

MVEV cases present in a seasonal pattern, with most occurring between February and June[93]. It is thought that anywhere between 1 in 150 to 1 in 1000 infections result in neurological disease, including encephalitis[94]. MVEV encephalitis have a variety of presentations, but four clinical patterns have been observed during MVEV encephalitis which are (i) relentless progression to death, (ii) spinal cord involvement causing paralysis, (iii) brainstem involvement and tremor or (iv) encephalitis followed by complete recovery[94]. The fatality rate following MVEV encephalitis is high, approaching 25%[89].

Hepatitis C virus (HCV)

HCV is an enveloped single-stranded RNA (ssRNA) virus in the *Flaviviridae* family. HCV is known to be hepatotropic and cause hepatitis in its host; it is the virus most closely related to HPgV in terms of its genome structure[95]. An estimated 71 million people worldwide are chronically infected and many of these individuals are unable to access the healthcare necessary to treat HCV[96]. In terms of HCV neurotropism, many reports have shown that HCV ribonucleic acid (RNA) can be detected in the CNS, although the presence of negative strand RNA (signifying viral replication) has not completely been validated[97]. Viral RNA has been detected from isolated microglia and astrocytes, although neither viral antigen nor HCV receptors have been detected *in vivo* on human microglia or astrocytes[97]. A study has also reported that brain microvascular endothelial cells (BMEC), a major component of the BBB,

support HCV replication *in vitro*[98]. Overall, both the notion that HCV is neurotropic and the possible association with encephalitis remain controversial.

1.4 Human pegivirus (HPgV)

1.4.1 Viral classification

HPgV is a positive sense, single-stranded RNA virus and a member of the *Flaviviridae* family. Since its discovery in 1967, HPgV has alternatively been known as GB virus C (GBV-C) and hepatitis G virus (HGV), after a surgeon with the initials G.B. used human sera from patients with presumed viral hepatitis to cause hepatitis in marmosets[99]. The classification of HGV was subsequently predicated on the assumption that the virus was hepatotropic although later evidence proved the virus did not replicate in the liver and the HGV was eventually renamed human pegivirus, in which "pegivirus" represents "persistent G" virus[100].

At least 7 different HPgV genotypes exist across the world, with HPgV genotype 2 being most prevalent in North America and Europe[101]. HPgV genotype 1 and 5 are predominantly found in Africa. The main genotype in China is genotype 3 although genotype 7 has also been detected in China as well[101]. One study identified that in populations of intravenous drug users (IDUs) genotype 7 was most prevalent in the Yunnan province in China, while another study in Beijing, China demonstrated that genotype 3 was most common in men who have sex with men (MSM)

populations[102,103]. Based on these studies, it initially seemed plausible that the route of transmission might dictate the genotype of HPgV present within a given population, although this was disproven[104]. Finally, HPgV genotypes 4 and 6 are predominantly found in Asian countries as well, including Japan, China and the Philippines[101].

1.4.2 Epidemiology

Transmission of HPgV can be either vertical (maternal-fetal transmission) or horizontal (sexual exposure or exposure through contaminated blood products)[105]. The prevalence of HPgV infection in the general population ranges from 1-4% in developed countries, with up to 20% prevalence in developing nations[106-108]. Previous studies have suggested that women are about two times more likely than men to be infected with HPgV, although conclusive evidence regarding sex differences influencing viral infection has yet to be provided[109]. Based upon the transfusion frequency worldwide, at least 7,000 people worldwide are expected to receive HPgV contaminated blood products each day[95].

1.4.3 Viral genome

The genome (approximately 9.5 kb in size) contains a long open reading frame (ORF) flanked by 5' and 3' untranslated regions (UTRs) and is organized similarly to the HCV genome[106,110,111], although the capsid-encoding domain remains to be

defined. The ORF is translated to form a single polyprotein which is post-translationally cleaved by both viral and host proteases[110]. Cleavage of this polyprotein is predicted to generate two envelope proteins, E1 and E2, along with six non-structural proteins (NS2, NS3, NS4A, NS4B, NS5A and NS5B) including a helicase, a protease, and a RNA-dependent RNA polymerase[112]. HPgV viral proteins and their putative functions in viral replication and during HIV-1 co-infection can be found below [Table 1.1].

Table 1.1: HPgV proteins and their putative functions.

Protein	***Putative Function***
E1	Forms a heterodimer with E2 and inserted into viral envelope[113]
E2	Viral entry into the cytosol[114] Inhibits CXCR4 -and CCR5-tropic HIV-1 replication[108]
NS2	Viral protease[113]
NS3	NTPase and helicase functions (C-terminal)[113] Trypsin-like serine protease (N-terminal)[113]
NS4A	Co-factor for serine protease[115]
NS4B	Enhances stability and enzymatic activity of NS3/NS4A protease[115]
NS5A	Promotes Th1 polarization[108] Inhibits CXCR4 -and CCR5-tropic HIV-1 replication[108]
NS5B	RNA-dependent RNA polymerase[113]

1.4.4 T-cell modulation

HPgV E2 has been extensively studied and has been shown *in vitro* to inhibit T-cell receptor (TCR)-mediated T cell activation by competing for Lck phosphorylation sites[116]. This phenomenon was seen in HPgV-infected human CD4+ and CD8+ T lymphocytes, and uninfected bystander cells[116]. Further, the E2 peptide has been shown to inhibit IL-2, an essential cytokine necessary for the activation,

proliferation and function of T cells[117]. Further, IL-2 is also an inducer of proinflammatory cytokines including IL-6, IL-1β and TNFα[118]. Taken together, these two observations highlight the ability of the virus to modulate host immune activation following HPgV infection, improving its ability to sustain a productive infection within a host.

1.4.5 Tissue tropism

As previously mentioned, HPgV was initially named hepatitis G virus, which was eventually changed after it was determined that the virus was unable to replicate in the liver. The NS5B RNA-dependent RNA polymerase transcribes negative strand RNA, which then undergoes additional transcription for positive strand RNA to be produced. Detection of the negative strand RNA by polymerase chain reaction (PCR) is indicative of viral transcription within the host. The lack of hepatic disease is related to the tissue tropism of the virus, which now includes primarily B and T lymphocytes (CD4+ and CD8+), the spleen and bone marrow[119]. This data suggests that HPgV is a lymphotropic virus, with a selective preference of lymphocytes for replication. Peripheral blood mononuclear cells (PBMCs) isolated from HPgV+ patients are not informative *ex vivo* because the negative strand RNA is found in very low concentration[120].

1.4.6 Disease associations

Recently an association with HPgV positivity and lymphoma in patients from North America has been reported[121,122]. Two studies dating back to the late 1990's initially identified significant associations in patients with hematological disease, albeit with a limited number of patients (47 and 69, respectively)[123,124]. Similar studies continued in patient populations with lymphomas, and consistently individuals with HPgV infection were more likely to have the disease, compared to HPgV negative indivduals[125,126]. A Canadian study recently investigated 553 non-Hodgkin's lymphoma patients and found that HPgV was present in 4.5% of cases, compared to only 1.8% of controls[122]. Additionally, a North American study using 2094 patient samples found that 7.8% of individuals with lymphoma were positive for HPgV, compared to 3.3% of controls[121]. The identification of HPgV as a potential risk factor for lymphoma is important due to the fact that in the United States, lymphoid neoplasms (including Hodgkin's lymphoma (HL), non-Hodgkin's lymphoma (NHL) and others) represent the sixth most common type of cancer[119]. Meta-genomic analysis studies support this claim, and further show stronger associations with HPgV and lymphomas from cases tested in Southern Europe, compared to what is observed in North America[119].

Other studies suggest that HPgV might be a causative agent of hepatitis-associated aplastic anemia (HAAA). A case report from 1996 was the first to describe an individual with HAAA who tested positive for HPgV RNA by PCR[127]. This was

followed up by another case report in 1999[128] and then more recently in 2011[129]. HAAA is a rare condition and occurs when aplastic anemia (a disease where the bone marrow does not replenish enough new blood cells) follows an attack of acute hepatitis[129]. Although these reports have described a potential association between HPgV infection and HAAA, no causation has been proven.

1.4.7 Other pegiviruses

Pegiviruses were recently classified by species (n=11) [Pegivirus A-K] within the *Pegivirus* genera[130], with HPgV classified as *Pegivirus C*. In other species, pegiviruses are still being examined for their infectivity and potential virulence inside the host. Studies of porcine pegivirus (PPgV) have identified a prevalence of 2-15% in pigs across the world[131]. Theiler's disease-associated virus (TDAV) and equine pegivirus (EPgV) are both members of the *Pegivirus* genus and both are known to infect horses[132]. A recent study used simian pegivirus (SPgV) along with simian immunodeficiency virus (SIV) in cynomolgus macaque models in an attempt to recapitulate HPgV and HIV-1 co-infection in humans. They found that SPgV exists in high titers throughout infection, although no effects on SIV viral load, CD4+ T cell death were observed in co-infected animals compared to SIV mono-infected macaques[133].

1.5 HPgV neurotropism

1.5.1 Early viral detection in the CNS

The first investigation of HPgV in the CNS occurred in 1998 in which the CSF of 17 patients who had been hospitalized for encephalitis were screened for HPgV RNA[134]. At the time investigators were unable to identify HPgV sequences in the CSF from these patients. Concurrently, this group also screened PBMCs from 9 individuals suffering from chronic HCV infection, and were also unable to detect any HPgV RNA[135].

1.5.2 The utilization of RNA-Seq for HPgV diagnosis

The growing application of RNA sequencing (RNA-seq) has created new avenues for detecting rare viral infections in humans. Several more recent case reports have implemented RNA-seq and subsequently successfully identified HPgV in the CNS. The first report of HPgV in the CNS compartment occurred in 2012, wherein RNA-seq identified over one-thousand HPgV reads in post-mortem brain tissue from an individual with multiple sclerosis (MS)[107]. The authors identified both positive and negative strand HPgV viral RNA using semi-quantitative PCR (qPCR), suggesting active replication in the CNS of this individual[107]. No HPgV RNA was detected in 53 other brain specimens[107]. At the time, they could not identify HPgV antigen using IHC techniques. The immune status of this MS patient was unknown, although MS is often treated with immunosuppressive therapies (e.g., corticosteroids). Another study identified HPgV RNA in the CSF of an individual with severe immune

suppression resulting from coincident HIV-1, toxoplasmosis and fungal infections leading to encephalitis[136]. They hypothesized that the ongoing immune suppression in combination with the degradation of the BBB from the fungal and bacterial infections resulted in an opportunistic HPgV invasion into the CSF, although they did not further investigate viral replication or attempt to detect viral antigen in the CNS[136]. Similarly, HPgV was detected in the CSF of one individual using a pan-microbial array with subsequent RNA-seq analysis after admission to a local hospital[137]. The group tested CSF for HPgV RNA from an additional 53 patients that were all negative. Of interest, one study using next-generation sequencing of human CSF samples identified HPgV as the most likely cause of chronic meningitis in one individual, although at the time they decided it was a bystander infection and not involved in causing disease[138].

As the number of identified HPgV CNS infections continued to rise, the diversity (or lack thereof) between viral sequences from matched serum and CSF samples had yet to be investigated. In 2018, a study detected HPgV sequences in 3 patients out of 96 who had encephalitis[139]. Interestingly, the authors found that viral sequences differed between matched CSF and serum samples, suggesting that viral replication occurred in both sites. Further, the observed mutations in the HPgV genome were localized primarily in the E2 region of the genome and were characterized as either containing B-cell epitopes or being involved in cell fusion[139]. An additional study

also employed RNA-seq to identify HPgV sequences from the brain of an individual with encephalitis[140].

1.5.3 HPgV antigen, viral diversity and subsequent neuroimmune response characterization

The only study to detect viral antigen in the CNS compartment was published by our group; we initially detected HPgV in brain tissues from two patients with brainstem encephalitis using RNA-seq and verified by semi-quantitative-real-time PCR (qRT-PCR) analysis[1]. An additional 66 patients with other disorders were screened using qRT-PCR, although no HPgV RNA sequences were detected[1]. To follow up on our initial observations, we employed both immunohistochemical (IHC) and immunofluorescent (IF) techniques and were able to identify HPgV NS5A antigen in oligodendrocytes, astrocytes and CD3+ T-cells in the brain tissue of these individuals[1]. Moreover, we identified a novel deletion in the HPgV *NS2* domain that was present in brain-derived virus from both of our two index cases but was not evident in previously published HPgV sequences. Of interest, both patients suffered from a malignancy (T-cell lymphoma and lung adenocarcinoma), which might have resulted in the systemic immunosuppression necessary for an opportunistic HPgV infection of the CNS.

1.5.4 HPgV-associated encephalitis features

Our group found that HPgV-associated encephalitis was associated with inflammatory changes including gliosis and leukocyte infiltration, principally defined by CD8 T-cells leading to white matter (leuko)-encephalitis. Magnetic resonance (MR) imaging of brain tissues in our study showed lesions in the white matter of HPgV-infected patients, and highlighted brainstem involvement[1]. MR imaging identified parenchymal changes that were consistent with meningoencephalitis in patient LE-2 from the report[137]. Other studies have failed to identify any signs of encephalitis or abnormalities using MR imaging[140]. Due to the significant presence of infiltrating macrophages and lymphocytes observed in the brain parenchyma, it is believed that infected leukocytes, either T cells, B cells, macrophages or natural killer (NK) cells, might penetrate the BBB as a 'Trojan horse', thereby carrying the virus into the brain under specific conditions, such as immune suppression[1,141]. Once in the brain parenchyma, it might be possible for the virus to spread to neighboring glial cells, leading to viral replication and subsequent spread within the CNS.

1.6 The relationship between HPgV and HIV-1 infection

1.6.1 Prevalence

Within the literature, the association with HPgV and HIV-1 co-infection is the most studied aspect of HPgV infection in patients, largely due to the lack of evidence that HPgV causes virulence. HPgV+/HIV-1+ co-infection is common, especially in at-risk

individuals, including those with other chronic viral infections which creates chronically dysregulated systemic antiviral immune responses[111]. Several studies reported that 20-45% of people infected with HIV-1 are co-infected with HPgV[142,143]. HPgV infection might exert beneficial effects in the setting of HIV-1 infection; in contrast, among HCV-infected individuals, HPgV co-infection is occasionally associated with worsened outcomes including slower HCV clearance[144].

In terms of CNS co-infection studies examining HPgV and HIV, only one study from 2016 exists, in which the authors hypothesized that HPgV may penetrate the BBB and colonize the CNS in HIV-infected patients, although the studies were limited to quantifying HIV-1 RNA in the CSF and the mechanism for viral interactions in the CNS was not discussed[136].

1.6.2 Clinical outcomes

In HPgV+/HIV+ co-infected patients, there is slower HIV-1 systemic disease progression, decreased HIV-1 transmission and increased survival; however there are several conflicting reports regarding the frequency of these improved outcomes[142]. In patients with existing HIV-1 infection, studies have shown that there is a reduced time in acquiring future HPgV co-infection, compared to those without an initial HIV-1 infection[144], potentially due to a higher-risk lifestyle (substance use, etc.). Further, it has been established that HIV-1-infected patients who are co-infected with HPgV have significantly lower viral loads, higher CD4+ counts and improved CD4+/CD8+ ratios[142].

An interesting retrospective study examined 197 HIV-1 infected patients, including subsets that were positive for HPgV RNA (n=26), positive for anti-HPgV E2 antibodies (n=90) or unexposed to HPgV (n=40). Survival curves were compared for each group and they found that the presence of HPgV RNA significantly increased the survival of these patients, as illustrated in Figure 1.1[145].

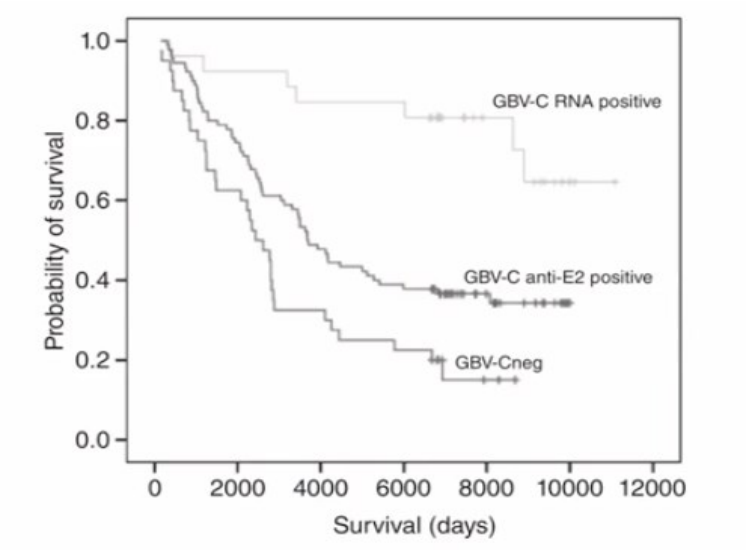

Figure 1.1: HPgV co-infection of HIV-1 individuals increases survival.

Kaplan-Meier survival curves illustrate the increased survival in patients with HPgV RNA or anti-HPgV E2 antibodies compared to those never co-infected with HPgV.

Adapted from Ernst et al. (2013). Impact of GB virus C viremia on clinical outcome in HIV-1-infected patients: a 20-year follow-up study. *HIV Medicine.* 15(4). 245-250.

Overall, the presence of HPgV within HIV-infected individuals is beneficial and is associated with increased patient longevity and a better quality of life.

1.6.3 HPgV and HIV-1 interactions within the host

There are several possible explanations as to why HPgV might be beneficial in patients with HIV-1 including down-regulation of HIV-1 co-receptors (C-C chemokine receptor (CCR) type 5 and C-X-C chemokine receptor (CXCR) type 4), activation of ISGs during chronic infection, reduction of T lymphocyte activation markers, and inhibition of HIV-1 replication, as shown in Figure 1.2[108].

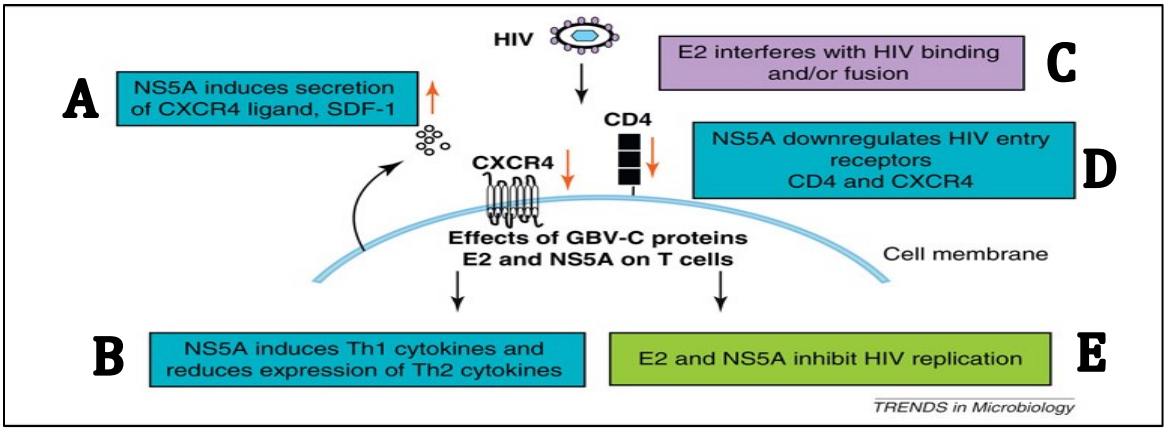

Figure 1.2: Selective effects of HPgV proteins on HIV-1 replication.

The HPgV envelope protein E2 and non-structural protein NS5A are known to have several effects on CD4+ T cells. The NS5A protein has been shown to induce secretion of SDF-1 [A], induce Th1 cytokines whilst reducing Th2 cytokines [B], and down-regulate the surface expression of CD4 and CXCR4 [C]. Both NS55A and E2 interact with different processes involved in HIV-1 replication [E] and E2 can also interfere with the binding and fusion of HIV-1 to T cells [C].

Adapted from: Bhattarai N, and Stapleton JT. (2012). GB virus C: the good boy virus?. *Trends in Microbiology.* 20(3), 124-130.

Several different HPgV/HIV-1 interactions within the host will be investigated below.

Chemokine expression

In vitro studies in PBMCs have shown that cytokine induction following HPgV infection reduces HIV-1 replication, in particular RANTES (CCL5), macrophage inflammatory protein (MIP)-1α, MIP-1β and stromal cell-derived factor (SDF)-1[146]. Individual HPgV proteins exert differential effects on the host immune response in the setting of HIV-1 co-infection.

Pertinent to the earlier discussion of HPgV *in vitro* studies showing the ability of HPgV E2 to inhibit IL-2 production in T cells, similar phenomena are observed in HPgV/HIV-1 co-infected individuals. In HPgV/HIV-1 co-infected individuals receiving IL-2 therapy, CD4+ expansion was significantly lower than in HIV-1 mono-infected individuals[147]. Therapeutically, this finding might underlie the observation that IL-2 therapy is ineffective in treating HIV-1-infected individuals, since HPgV was not typically screened in these individuals from several studies[148].

Lymphocyte profile and activation

As previously mentioned, PBMCs are inefficient in hosting HPgV replication for extended periods of time, thus posing the question of how HPgV alters HIV-1 replication and virulence in PBMC cultures. HPgV is known to reduce the expression

of activation markers on CD4+ and CD8+ cells in HPgV/HIV-1 co-infected individuals, suggesting that HPgV has paracrine effects on bystander cells that reduces the overall activation state of lymphocytes[108].

Within T cell populations, the T helper 1 (Th1) and T helper 2 (Th2) responses are well characterized within the HIV-1 literature. Th1 responses are more involved in producing cell-mediated immune responses and are typically considered to be more proinflammatory than Th2, which is characterized by more humoral responses[149]. Th1 cells typically produce cytokines such as IL-2, IFNγ and TNFα, while Th2 cells produce cytokines such as IL-4, IL-5, IL-6 and IL-10[149]. Immune responses mediated by Th1 cells are more involved during acute HIV-1 infection, although serum levels of Th1 cytokines tend to decrease over the course of chronic infection whereas Th2 cytokines increase[108]. Several studies investigating Th1 and Th2 profiles in HPgV/HIV-1 co-infected individuals illustrate that the presence of HPgV increases Th1 cytokines and reduces Th2 cytokines, suggesting they polarize the T cell profile towards a Th1 profile and thus may be beneficial in HIV-1 positive patients in fighting off the infection[108]. HPgV has also been shown to protect T cells from Fas-mediated apoptosis, reducing the CD4+ T cell death associated with HIV-1 infection[108].

HIV-1 entry

HIV-1 entry primarily depends on two co-receptors, CCR5 and CXCR4 as well as cluster of differentiation (CD)4 as the primary receptor. The combination of low expression of these receptors and high levels of their ligands (MIP-1α, MIP-1β, RANTES, and SDF-1) is known to slow HIV-1 progression[150]. As mentioned previously, HPgV induces the expression of these cytokines during infection and further, the HPgV NS5A protein reduces CXCR4 and CCR5 expression, increases SDF-1 expression (ligand for CXCR4) and leads to an overall reduction in HIV-1 replication[151,152]. The HPgV E2 glycoprotein also alters HIV-1 entry by enhancing the release of RANTES, which binds CCR5, as well as down-regulating CCR5 following HPgV E2 binding to CD81 on T-cells[153] *in vitro*.

1.7 Rationale and Thesis Objectives

Given the recent discovery of HPgV infection in the CNS that was associated with encephalitis and glial cell infection, it was imperative to investigate the cell tropism and accompanying neuropathogenic mechanisms of HPgV infection in the human CNS. My overarching hypothesis was:

HPgV productively infects CNS glial cells, resulting in immune activation that is differentially affected by a deletion in the HPgV NS2 gene.

Importantly, I wanted to determine whether HPgV productively infected specific types of neural cells and define the impact of the previously identified 87-nucleotide deletion[1] on viral infectivity and replication, as well as the associated host neuroimmune response(s). Moreover, I wanted to utilize our archived brain tissues to identify more patients with CNS HPgV infection, thus confirming and expanding upon the findings of our original case study. Building on this rationale and working hypothesis, I proposed the three major objectives for this thesis including:

Objective I.

Objective: Establish an *in vitro* model of human pegivirus infection in human glial cells and define the impact of the previously recognized HPgV *NS2* deletion on viral infection.

Hypothesis: Human pegivirus infects and replicates in human glial cells, which is enhanced by a deletion in the HPgV NS2 gene.

Within this objective, I first established a novel method for HPgV transfection in human astrocytoma cells using a molecular HPgV viral clone, followed by subsequent infection of human astrocytes with the isolated virions in cell supernatants. I then introduced an 87-nucleotide deletion into the molecular HPgV clone, recapitulating the deletion observed *in vivo* by our group[1]. We then compared the replication and tropism of HPgV wild type (WT) versus HPgV ΔNS2 to determine how the *NS2* deletion affected viral infection and replication in human glial cells *in vitro*.

Objective II

Objective: Define the host antiviral responses to HPgV WT and ΔNS2 infection in human astrocytes and microglia.

Hypothesis: HPgV WT and ΔNS2 viruses will elicit different host antiviral responses in human glia following infection.

Within this objective, I characterized the activation of inflammatory and antiviral pathways in glial cells following HPgV infection and assessed how these responses differed following infection with HPgV WT versus HPgV ΔNS2. I also explored the activation of cell death pathways in glial cells following HPgV WT versus HPgV ΔNS2 infection and assessed the impact of infection on glial cell viability.

Objective III

Objective: Examine HPgV neural cell tropism *in vivo* and associated immune responses in brain tissues from patients with detectable HPgV.

Hypothesis: HPgV infection in the CNS alters antiviral and immune-related gene expression.

Within this objective, I validated my *in vitro* findings by investigating HPgV infection of astrocytes in the human brain using immunofluorescent imaging of the HPgV NS5A antigen. I also established a cohort of seven patients who had HPgV RNA detected by ddPCR in post-mortem cortex samples. Within this cohort I examined the impact of HPgV infection of the CNS on several inflammatory and antiviral signaling pathways.

Chapter II: Methods

2.1 Ethics Statement

The use of autopsied brain tissues was approved (Pro0002291) by the University of Alberta Human Research Ethics Board (Biomedical) and written informed consent was received for all samples. Frontal cortex sections from HPgV+ and HPgV- patients were examined. Brain tissue from patients with and without HIV-1 or HPgV was obtained from the National Neuro-AIDS Tissue Consortium (NNTC) collection. Human fetal tissues were obtained from 15-22-week aborted fetuses that were collected with the written informed consent from the donor (Pro00027660), approved by the University of Alberta Human Research Ethics Board (Biomedical).

2.2 *In vitro* experiments

2.2.1 Cell culture

Primary fetal human microglia, astrocytes and neurons were isolated based on differential culture conditions, as previously described [64,66]. Fetal brain tissues from 15-22 week fetuses were dissected, meninges were removed, and a single cell suspension was prepared through enzymatic digestion for 1hr with 2.5% trypsin and 0.2 mg/ml DNAse I, followed by trituration through a 70-μm cell strainer. Cells were washed twice with fresh medium and plated in T-75 flasks. Cultures were maintained in MEM supplemented with 10% FBS, 2mM L-glutamine, 1mM sodium pyruvate, 1X MEM nonessential amino acids, 0.1% dextrose, 100 U/ml penicillin, 100 μg/ml streptomycin, 0.5 μg/ml amphotericin B, and 20 μg/ml gentamicin. For microglial cells,

mixed cultures were maintained for 1-2 weeks, at which point astrocytes and neurons formed an adherent cell layer with microglia loosely attached or floating in the medium. Cultures were gently rocked for 20-30 mins to re-suspend the weakly adhering microglia in medium, which were then decanted, washed, and plated. Astrocyte cultures were passaged once per week for 4–6 weeks until the neurons were eliminated. Human fetal neurons were cultured in medium containing cytosine arabinoside and used within 2 weeks of culture[154]. Purity of cultures was verified by immunofluorescent quantitation as previously reported by our group[64,66,154,155]. Mixed cultures were plated directly after the initial straining and wash steps and maintained for 1 week before undergoing infection. Astrocytoma U251 cell cultures (ATCC) were maintained in DMEM supplemented with 10% FBS and 100 U/ml penicillin, 100 µg/ml streptomycin. MO3.13 cell cultures (ATCC) were maintained in DMEM supplemented with 10% FBS and 100 U/ml penicillin, 100 µg/ml streptomycin. Before experimentation, cells were differentiated for 3 days using 50ng/mL Phorbol-12-myristate 13-acetate (PMA) in serum-free RPMI before media was removed, cells washed with PBS and fresh media (serum-free) was added for future experimentation. SK-N-SH cell cultures (ATCC) were maintained in DMEM (low glucose) supplemented with 10% FBS and, 1% Non-essential amino acids, 100 U/ml penicillin, 100 µg/ml streptomycin. Before experimentation, cells were differentiated for 3 days using dibutyral-cAMP (1mM).

2.2.2 Viral stock preparation and infection

For infectious virus, we obtained a clone of HPgV (NIH AIDS Reagent Program 9450), which was subsequently transformed into DH5α (library efficiency) cells (Invitrogen™) and plasmids were generated (geneJET Plasmid kit; Thermo Scientific™) as viral plasmid stocks for downstream applications. Several rounds of qPCR and Sanger sequencing were performed on the infectious clones to ensure in-house clones had not undergone mutagenesis during transformation. Mutant HPgV ΔNS2 virus was created from the HPgV clone listed above by targeting the 87-nucleotides in the HPgV *NS2* gene for site directed mutagenesis (New England Biolabs®). Primers for site directed mutagenesis were created using NEBaseChanger online software™. Both plasmids were subject to Sanger sequencing of various HPgV genes to ensure that no additional mutations were introduced during the mutagenesis. A similar protocol was used to create HPgV ΔNS5A and HPgV ΔNS2 ΔNS5A viruses. For the purposes of viral transfection, plasmids were linearized using the BcuI (SpeI) restriction enzyme (Fisher Scientific) and subjected to T7 RNA synthesis (New England Biolabs®)[112]. Newly transcribed RNA was quantified (Nanodrop™) and transfected (jetPRIME™ transfection reagent; Polyplus™ transfection) into the U251 astrocytoma-derived cell line (ATCC). Viral-infected supernatants were harvested at 7 and 10 days post-infection and RNA was prepared for viral quantitation (Viral RNA Mini Kit; Qiagen). Subsequent cDNA and droplet digital PCR (ddPCR) were used to quantify HPgV viral copies/mL of supernatant to determine the multiplicity of infection (MOI) for future infections. To assess infection of primary human neural cells, cells were plated for 24hrs and then infected with HPgV for 6 hours, at a MOI ranging from 0.1 to

1.0 depending on the sensitivity of the assay, before being thoroughly washed with PBS and incubated for the duration of the experiment; confirmation of infection in these cells was initially assessed by detection of increased HPgV copies in cell supernatants by ddPCR.

2.2.3 Real-time polymerase chain reaction (qRT-PCR)

8μL of prepared viral RNA (QIAamp Viral RNA Mini Kit, Qiagen) or 1μg of total cellular RNA (RNeasy Mini Kit, Qiagen) was prepared and used for first-strand cDNA using Superscript III reverse transcriptase (Invitrogen, Carlsbad CA, USA) and with random hexamer primers (Roche). Specific genes were quantified by real-time reverse transcriptase PCR (qRT-PCR) using the CFX 96 real-time system (Bio-Rad, Mississauga, ON, Canada). The specific primers used during qRT-PCR are provided in below [Table 2.1]. Semi-quantitative RT-PCR analysis was performed by monitoring, in real time, the increase of fluorescence of the SYBR Green dye (iQ™ SYBR Green Supermix, Bio-Rad) on the Bio-Rad detection system as previously reported[156], and was expressed as relative fold change (RFC) compared to uninfected cells and uninfected controls respectively.

2.2.4 Droplet-digital polymerase chain reaction (ddPCR)

Using 8μL of prepared viral RNA (QIAamp Viral RNA Mini Kit, Qiagen) or 1μg of total cellular RNA (RNeasy Mini Kit, Qiagen) was prepared and used for first-strand cDNA

using Superscript III reverse transcriptase (Invitrogen, Carlsbad CA, USA) and with random hexamer primers (Roche). ddPCR was performed using either the probe based or EvaGreen QX200™ droplet digital PCR system™ (Bio Rad) and analyzed with Quantasoft™ (Bio Rad). To calculate the number of HPgV copies per microgram of RNA, droplet numbers were first converted to the corresponding amount of cDNA (5μL used out of 150μL prepared), then to the amount of RNA generated from the tissue/cell cultures (8μL used out of 30μL prepared). This number was then used in future calculations to arrive at the final concentration of HPgV copies/mL of supernatant or HPgV copies/μg of RNA. The specific primers used during ddPCR reactions are provided below [Table 2.1]

Table 2.1: Human and viral primer sequences used

Gene Name	Species	Forward Sequence	Reverse Sequence
CASP1	human	5'-TCC AAT AAT GGA CAA GTC AAG CC-3'	5'-GCT GTA CCC CAG ATT TTG TAG CA-3'
IFNB	human	5'-CAT CTA GCA CTG GCT GGA ATG-3'	5'-ACT CCT TGG CCT TCA GGT AAT G-3'
IRF3	human	5'- GCA CAG CAG GAG GAT TTC G-3'	5'-AGC CGC TTC AGT GGG TTC-3'
MAVS	human	5'-CAG GAG CAG GAC ACA GAA C-3'	5'-AGG AGA CAG ATG GAG ACA CAG-3'
DDX58	human	5'-AAA CCA GAA TTA TCC CAA CCG A-3'	5'-TGA TCT GAG AAG GCA TTC CAC-3'
IL1B	human	5'-CCA AAG AAG AAG ATG GAA AAG C-3'	5'-GGT GCT GAT GTA CCA GTT GGG-3'
GAPDH	human	5'-AGC CTT CTC CAT GGT GGT GAA GAC-3'	5'-CGG AGT CAA CGG ATT TGG TCG -3'
NS3 [+]	HPgV	5'-CAG ATG GGG CAA CCT CGT T-3'	5'-GTC CAC GGC CTA GTG AAC C-3'
E2 [-]	HPgV	5'-GCC ACC GGA AAT ACA ACA CC-3'	5'-CTC GGT TGG TCC CGC TTA TC-3'

2.2.5 Cell culture immunofluorescence

Detection of cellular proteins was performed using immunofluorescence as described previously[154]. Cells were cultured on 180μm thick polymer coverslip 8 well plates (μ-Slide ibiTreat plates #80826) and treated. After 24hrs, cells were fixed using 4% formaldehyde. Cells were permeabilized using 0.1% Triton in PBS, blocked using Odyssey Blocking Buffer (LICOR; cat#927-40000), and incubated with primary antibody [Table 2.2] overnight at 4°C. Primary antibody binding was detected using species-matched secondary antibodies [Table 2.3]. Cells were stained with phalloidin (F-Actin) (ThermoFisher, #R37110) and DAPI and mounted using Prolong™ Gold antifade reagent (Invitrogen, #P36934). Slides were imaged using a Wave FX spinning disc confocal microscope (Zeiss) with Volocity 6.3 acquisition and analysis software (Perkin Elmer), and basic contrast enhancement performed using automatic black-point calculation. Composite z-stack images included 10 XY planes over a total vertical distance of 5-10 μm using the Improvision Focus Drive. All cells were imaged using a 20 or 40X oil immersion objective lens unless otherwise indicated.

2.2.6 Immunoblot analysis

Immunoblot analysis of tissue and cell lysates was performed as described previously[154,157]. Following protein extraction using RIPA buffer, samples were quantified using a DC Protein Assay Kit (Bio-Rad; cat# 5000112), then treated with Laemmli buffer (Bio-Rad; Cat#161-0747) and incubated at 95°C for 8-10mins. Samples were loaded onto 4-20% Precast SDS-PAGE gels (Bio-Rad; Cat# 456-1094)

and run for 1hr at 100-120V. Following electrophoresis, gels were transferred onto 0.2µm nitrocellulose (Bio-Rad; cat# 1620112) membranes using a BioRad Mini Trans-Blot Wet Transfer system for 55 minutes at 0.12A. Membranes were blocked for 1-4hrs with Odyssey Blocking Buffer (LICOR; cat#927-40000), followed by overnight incubation at room temperature with primary antibody [Table 2.2]. Membranes were then washed 3x5 minutes with PBS-T (1x PBS-0.05% Tween-20) and incubated with HRP-conjugated secondary antibody [Table 2.3] (Jackson ImmunoResearch) for 1 hour, followed by 3x5 minute washes. Membranes were developed with ECL reagent (Thermo Scientific; cat#32132) and imaged using an ImageQuant LAS4000 Biomolecular Imager (GE Life Sciences). Band intensity was quantified using ImageStudioLite and normalized to β-actin.

Table 2.2: Primary antibodies used

	Protein of Interest	Species	IF / IHC	Western Blot	Product Information
HPgV Antibodies	HPgV E2	Mouse	1:200	1:500	ThermoFisher UIE2-1
	HPgV NS5A	Rabbit	1:200	1:1000	Abcam ab1037
Human Antibodies	GFAP	Chicken	1:200	N/A	Abcam ab134436
		Mouse	1:200	N/A	BD Pharmingen 556330
	β-Actin	Mouse	N/A	1:10,000	Santa Cruz SC-47778

Table 2.3: Secondary antibodies used

	Antibody	Species	Ratio	Product Information
IF Secondary Antibodies	Alexa Fluor 488	Goat anti-mouse IgG Goat anti-rabbit IgG	1:500	Abcam
	AlexaFluor 647	Goat anti-mouse IgG Goat anti-rabbit IgG Goat anti-chicken IgG	1:500	Abcam
	AlexaFluor568	Goat anti-mouse IgG Goat anti-rabbit IgG	1:500	Abcam
Western Blot Secondary Antibodies	Goat anti-rabbit		1:10,000	Jackson Biolabs
	Goat anti-mouse		1:10,000	

2.2.7 Lactate dehydrogenase (LDH) assay

LDH activity in cell supernatants was assessed using the LDH-Cytotoxicity Assay Kit II (Abcam, ab65393) according to manufacturer's instructions. Astrocytes or microglia were plated in 96-well plates and cultured for 24 hours before infection or treatment. Supernatants were harvested and stored at -80°C prior to use.

2.2.8 Alamar Blue™ assay

Cell viability was assessed by Alamar Blue™ (Thermo Fisher, DAL1025) according to manufacturer's instructions. Astrocytes or microglia were plated in 96-well plates and

cultured for 24 hours before infection or treatment. Alamar Blue™ was then diluted in cell culture media (1/10) and placed on cells. Plates were read every 30 minutes for 4 hours to detect absorbance changes. Cell viability was measured by measuring the reducing power of viable cells in each condition.

2.2.9 Cytokine ELISA

IL-1β cytokine assays were performed on cell culture supernatants using the human IL-1β DuoSet ELISA kit (R&D Systems, DY201) according to the manufacturer's instructions. Nigericin (5μM; InvivoGen cat# tlrl-nig) was used as a positive inducer of cell death for a 4-hour treatment.

2.2.10 FAM-FLICA caspase assay

Astrocytes were initially plated and cultured in 96 well-plates (50,000/well) for 24hrs and then were infected with either HPgV WT or ΔNS2 viruses for either 4 or 7 days. Caspase-1 (Immunochemistry Technologies, #97), caspase-3/7 (ImmunoChemistry Technologies, #93), caspase-8 (Immunochemistry Technologies, #90) or caspase-9 (Immunochemistry Technologies, #912) activity was assessed according to manufacturer's instructions.

2.2.11 Viral sequences and phylogenetic tree generation

HPgV sequences were aligned using Mega-X software and phylogenetic trees were constructed using reported pegivirus and other related sequences by Clustal X N-J Bootstrap Method and evaluated with MEGA-X software with 10,000 replicates. Viral sequences were obtained from Genbank for the HPgV WT clone (Genbank: AF121950) and from a patient from our original case report, LE-1 (Genbank: MH179063) which represented HPgV ΔNS2.

2.3 *In vivo* experiments

2.3.1 Tissue Immunofluorescence

For human autopsy immunofluorescence studies, as described previously[157], tissue slides were de-paraffinized by incubation for 1hr at 60°C followed by one 10min and two 5min incubations in toluene baths through decreasing concentrations of ethanol to distilled water. Antigen retrieval was performed by boiling in 10mM sodium citrate (pH 6.0). Slides were blocked with Odyssey Blocking Buffer (LICOR; cat#927-40000) for 4hrs at room temperature. Slides were incubated with primary antibodies at 4°C overnight. Primary antibody was removed by PBS washes (5 min x3) and slides were incubated for 3min in 0.22μm filtered 1% (w/v) Sudan black in 70% ethanol and washed an additional three times in PBS. Slides were incubated in a mixture of 1:500 fluorescent secondary antibodies as appropriate for 2hrs, washed three times in PBS,

stained with DAPI for 10min, and mounted with Prolong Gold. Slides were imaged with an inverted Wave FX spinning disc confocal microscope (Zeiss).

To quantify the intracellular MFI of viral antigen in GFAP+ cells, the freehand tool in Volocity 6.3 was used to delineate each GFAP+ cell as a region of interest (ROI) and the MFI of viral antigen within that ROI was recorded. To quantify the number of immunopositive cells per FOV, a 'threshold' defined as 4x the background MFI was established separately for each FOV. FOVs were then individually contrast enhanced by setting the black point to the threshold value (4x background) calculated above. Each GFAP+ cell was then categorized as either immunopositive or immunonegative for viral antigen based upon whether the intracellular viral signal exceeded the 4x background threshold. Isotype secondary antibody controls were used to measure tissue auto-fluorescence.

2.4 Statistical Analyses

Comparisons between two or more groups were performed by unpaired Student's t-test or by ANOVA with Dunnett's post hoc tests, using GraphPad Instat 3.0 (GraphPad Software, San Diego, CA, USA). Comparisons between the proportions of two variables were performed by Fisher's exact test, using GraphPad Instat 3.0. Human patient data was analyzed with the Mann-Whitney test, using GraphPad Instat 3.0.

Chapter III: HPgV neurotropism *in vitro* and characterization of HPgV ΔNS2

3.1 Introduction

Chapter III Objective: *Establish an in vitro model of human pegivirus infection in human glial cells and define the impact of the previously recognized HPgV NS2 deletion on viral infection.*

Until recently, both the minimal association of HPgV infection with a disease phenotype and the lack of an effective *in vitro* model limited studies of viral tropism in the CNS and the periphery. Evidence for HPgV infection in the CNS was confined to the detection of viral RNA in the CSF and brain tissue[137,139,140], and no association with CNS pathology had been reported. However, our group recently identified viral antigen in astrocytes and verified active viral replication within the CNS in the context of severe leukoencephalitis[1]. Both of these original patients (hereafter referred to as "index patients", LE-1 and LE-2) were found to contain virus with an 87-nucleotide deletion in the *NS2* gene[1]. Following this initial report outlining an association of HPgV infection with encephalitis, we sought to establish an *in vitro* CNS model of infection to better understand HPgV neurotropism and viral propagation within the CNS.

Chapter III Hypothesis*: Human pegivirus infects and replicates in human glial cells which is enhanced by a deletion in the HPgV NS2 gene.*

Within this chapter, I established and optimized an *in vitro* model of HPgV infection in human astrocytes and have provided evidence that HPgV can infect and replicate

in both human astrocytes and microglia, but not in human neurons or an oligodendrocyte cell line. I delineated the effects of an 87-nucelotide deletion in the *NS2* gene of the virus, which appears to increase viral infectivity, replication and spread within glial populations. I also established a new technique to measure viral copy numbers in glial cultures as a method of quantifying both intracellular and extracellular HPgV RNA following infection. These results lay the foundation for later mechanistic studies to further understand virus-host interactions.

3.2 Results

3.2.1 Primary human astrocytes and the astrocytoma cell line U251 are both permissive to HPgV transfection

Previous studies by our group have detected HPgV antigen in glial cells, chiefly oligodendrocytes and astrocytes, at autopsy[1]. To model HPgV CNS infection *in vitro*, human fetal astrocytes (HFA) were selected because of their availability and their ability to be infected by other members of the *Flaviviridae* family[68,158,159]. To investigate HPgV tropism in human astrocytes, HPgV RNA derived from an HPgV molecular clone[112] was transfected into human astrocytes. Seven days post-transfection, HPgV NS5A antigen was detected [Figure 3.1A]. Although primary astrocytes were our cell type of interest, astrocytoma cell lines are widely known to have deficiencies in IFN signaling pathways that confer enhanced permissiveness to viral infection compared to primary astrocytes[160]. This property makes them highly

efficient for propagating large quantities of virus, and as such we utilized the astrocytoma cell line, U251, to propagate the virus [Figure 3.1B]. Supernatants from transfected cells were harvested and replaced 7 days post transfection, and fresh media was applied for 3 additional days. HPgV copies released into the supernatant were measured by droplet digital PCR (ddPCR) at the 7 day [Figure 3.1Ci] and 10 day time-points [Figure 3.1Cii] and compared to mock-transfected controls [Figure 3.1Ciii]. Copies of HPgV WT and ΔNS2 in cell supernatants [Figure 3.1Ci] were extrapolated to calculate viral stock copy numbers for future experimentation [Figure 3.1D]. To confirm that minimal cell death occurred during transfections, lactate dehydrogenase (LDH) activity was measured in U251 supernatants and was shown to be similar in transfected and mock-transfected cells [Figure 3.1E].

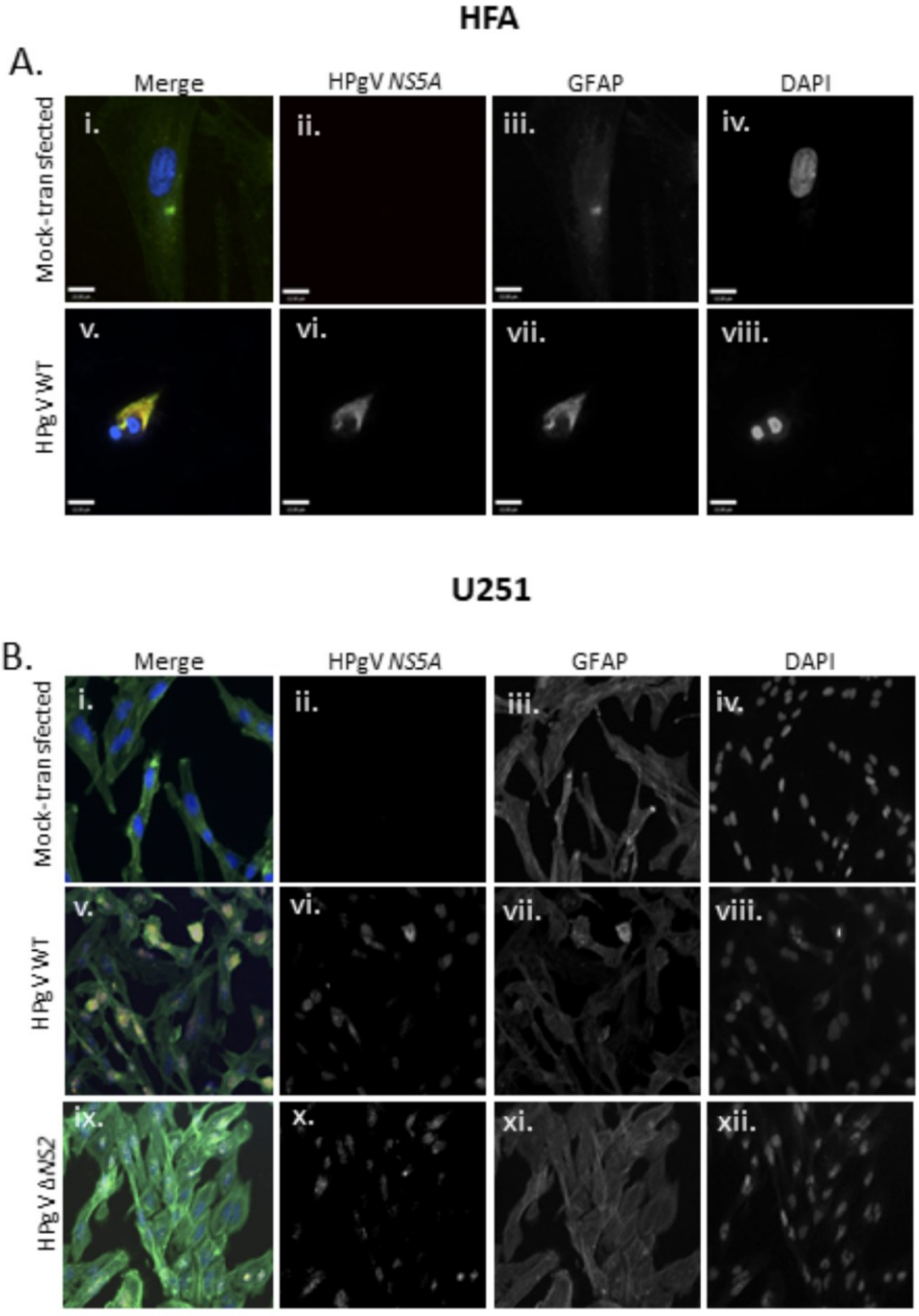
HFA
A.
Merge
HPgV NS5A
GFAP
DAPI
Mock-transfected
HPgV WT
i.
ii.
iii.
iv.
v.
vi.
vii.
viii.
U251
B.
Merge
HPgV NS5A
GFAP
DAPI
Mock-transfected
HPgV WT
HPgV ΔNS2
i.
ii.
iii.
iv.
v.
vi.
vii.
viii.
ix.
x.
xi.
xii.

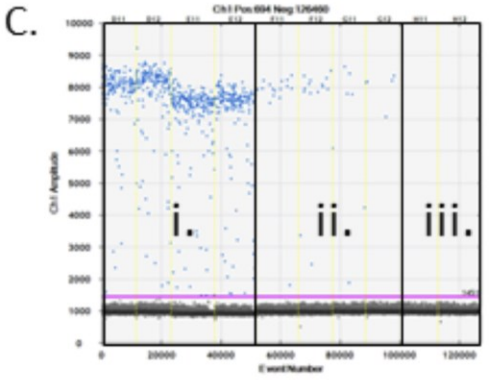
C.
i.
ii.
iii.

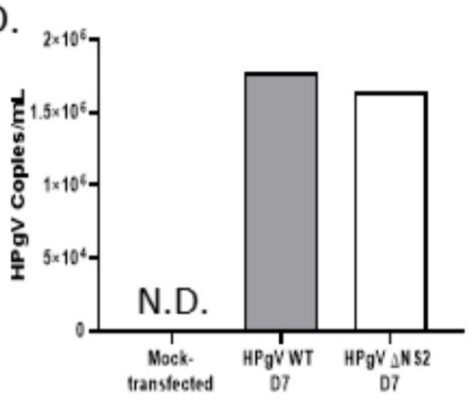
D.
HPgV Copies/mL
2×10^6
1.5×10^6
1×10^6
5×10^4
0
N.D.
Mock-transfected
HPgV WT D7
HPgV ΔNS2 D7

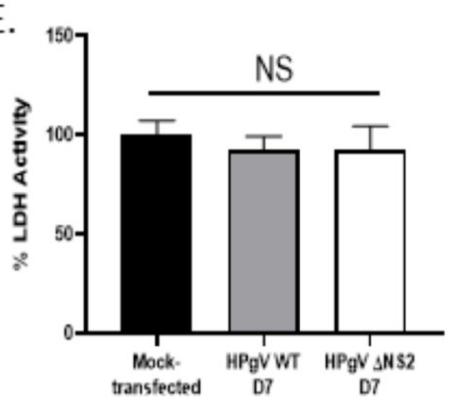
E.
% LDH Activity
150
100
50
0
NS
Mock-transfected
HPgV WT D7
HPgV ΔNS2 D7

Figure 3.1: The human astrocytoma U251 cell line and primary human astrocytes are permissive to HPgV transfection.

[Ai-Avii] Representative images showing HPgV+ HFAs following transfection with HPgV WT viral RNA (red), compared to mock-transfected cells 7 days post transfection. [Bi-Bvii] Representative images showing HPgV+ cells following transfection with HPgV WT [Bv-viii] and HPgV ΔNS2 [Bix-xii] viral RNA (yellow) in the human astrocytoma U251 cell line, compared to mock-transfected cells 7 days post transfection. [C, D] ddPCR thresholding and optimization of droplet amplitude was determined in U251 cells following 7 and 10 days of transfection. [D] Viral copies per milliliter of supernatant were determined following ddPCR quantitation for the 7-day time-point. [E] LDH activity in cell supernatants from both HPgV WT and ΔNS2 was measured following 7 days of transfection. (NS= Non-significant, One-way ANOVA).

3.2.2 HPgV infects and spreads in primary human astrocytes

Using HPgV WT viral stocks from above, human astrocyte cultures were infected at a MOI of 0.1 for 4, 7 and 14 days before cells were imaged for the presence of HPGV NS5A antigen using confocal microscopy [Figure 3.2A]. At each time point, the presence of NS5A antigen [Figure 3.2Avi, Ax, Axiv] was detected intracellularly, confirming successful viral infection. By quantifying the amount of intracellular HPgV NS5A antigen as determined by the mean fluorescence intensity (MFI) of each cell, intracellular HPgV was shown to be most abundant at 7 days post infection, significantly higher than both day 4 and day 14 levels [Figure 3.2B, $p<0.001$;$p<0.0001$]. To determine if the virus was replicating within astrocytes, supernatants were harvested at each time point, and viral RNA was extracted. Previous reports have used droplet digital PCR (ddPCR) analysis to detect HIV-1 in CNS tissues[65]. It is a highly sensitive assay that can quantify the precise number of viral copies present within a given sample. In my studies, ddPCR quantification of infected astrocyte supernatants showed a mean of 7577, 20434 and 4834 HPgV *NS3* viral RNA copies/mL were released at 4, 7 and 14 days post-infection, respectively from two independent experiments [Figure 3.2C, *$p<0.05$, **$p<0.01$]. This mimics the trend observed with intracellular viral immunodetection [Figure 3.2B], which showed that the increase in intracellular viral MFI is associated with an increase in replication of the virus. Further, to calculate the HPgV spread, astrocytes were quantified as either HPgV NS5A immunopositive or immunonegative in several fields of view (FOV) in each condition [Figure 3.2D, *$p<0.05$; **$p<0.01$]. Over time HPgV spread to a significantly greater number of astrocytes, with 49% of cells

immunopositive for HPgV by day 4, 65% at day 7 and 84% of cells by day 14, a significant increase relative to the previous two time-points. These data illustrate that HPgV is tropic for human astrocytes and can replicate and spread within astrocyte cultures.

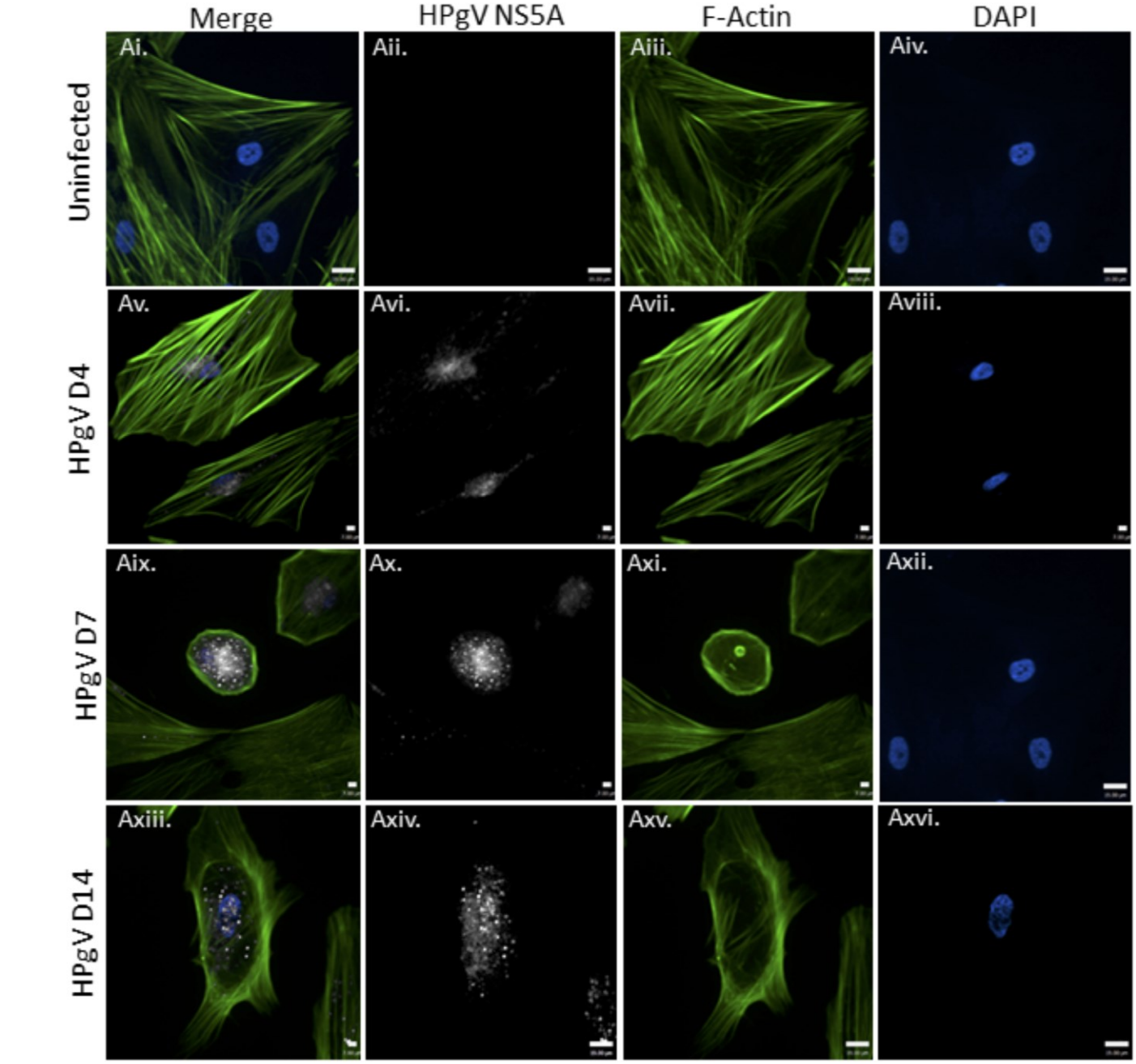
Merge
HPgV NS5A
F-Actin
DAPI
Uninfected
HPgV D4
HPgV D7
HPgV D14
Ai.
Aii.
Aiii.
Aiv.
Av.
Avi.
Avii.
Aviii.
Aix.
Ax.
Axi.
Axii.
Axiii.
Axiv.
Axv.
Axvi.

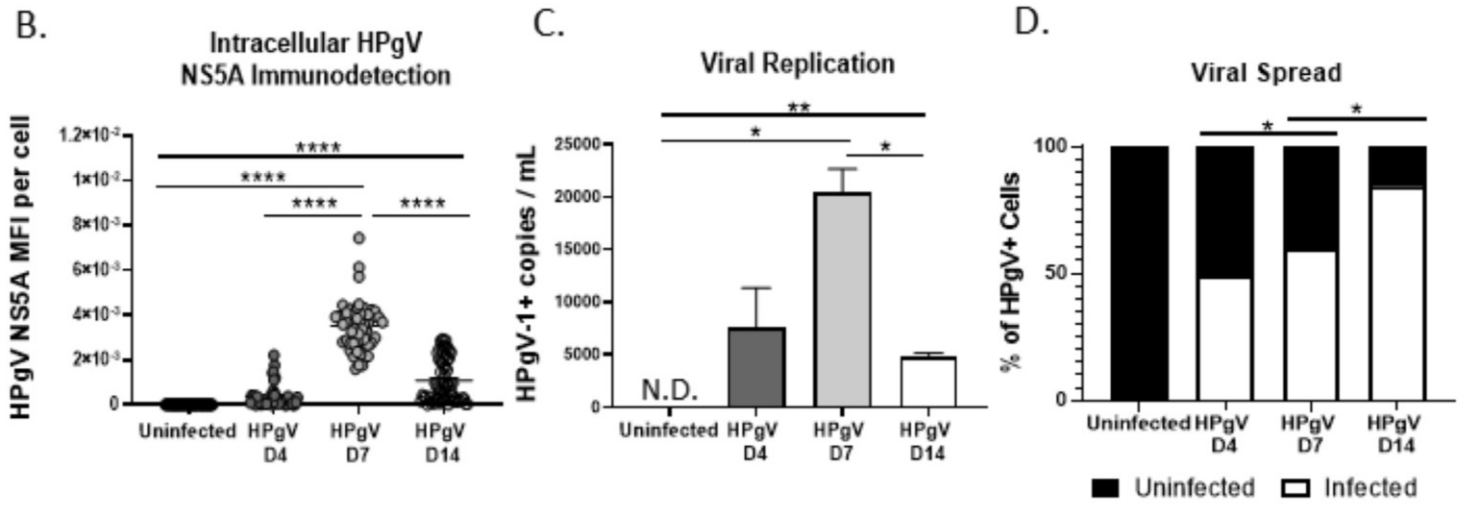
B.
Intracellular HPgV NS5A Immunodetection
HPgV NS5A MFI per cell
Uninfected
HPgV D4
HPgV D7
HPgV D14
C.
Viral Replication
HPgV-1+ copies / mL
N.D.
D.
Viral Spread
% of HPgV+ Cells
Uninfected
Infected

Figure 3.2: HPgV infects and spreads in human astrocytes *in vitro*.

Astrocytes were infected with HPgV WT (MOI = 0.1) for 4, 7 or 14 days after which cells were fixed and immunolabeled for HPgV NS5A antigen (white) and labeled with F-Actin (green) and DAPI (blue). Representative images are shown. To quantify viral infectivity, HPgV NS5A mean fluorescence intensity (MFI) per cell [B] was assessed for a minimum of n=50 astrocytes per condition using confocal microscopy and compared to uninfected cells [A]. [C] ddPCR of cell supernatants showed an increase in viral replication between D4 and D7, displayed by number of HPgV+ copies. (* $p<0.05$, ** $p<0.01$, Student's T-test). [D] Viral spread was determined by quantifying the number of HPgV+ cells per field of view (FoV) in each condition by immunofluorescence. Data shown represent data from two separate donors. (* $p<0.05$, ** $p<0.01$, *** $p<0.001$, **** $p<0.0001$, One-way ANOVA).

3.2.3 Characterizing the HPgV ΔNS2 mutation in relation to HPgV WT

The HPgV LE-1 and LE-2 genomes previously characterized by our group suggested the presence of both an 87-nucleotide deletion in the *NS2* gene and a 15-nucleotide insertion in the *NS5A* gene of the virus[1]. After optimizing HPgV infection of human astrocytes, I modified the HPgV WT plasmid by deleting an 87-nucleotide sequence in the *NS2* gene (genome position 2643-2730), to mimic our *in vivo* finding [Figure 3.3A]. The ΔNS2 plasmid was verified to have 87 nucleotides missing and the deletion was detected by gel electrophoresis [Figure 3.3B]. To confirm the plasmid did not undergo any off-site mutations within the viral genome, we sequenced the *E1* gene of both plasmids and found no differences between the WT and ΔNS2 viruses [Figure 3.3C]. This mutant virus RNA was then transfected into U251 cells [Figure 3.1B] to produce HPgV ΔNS2 viral stocks from released virus in the supernatant after 7 days.

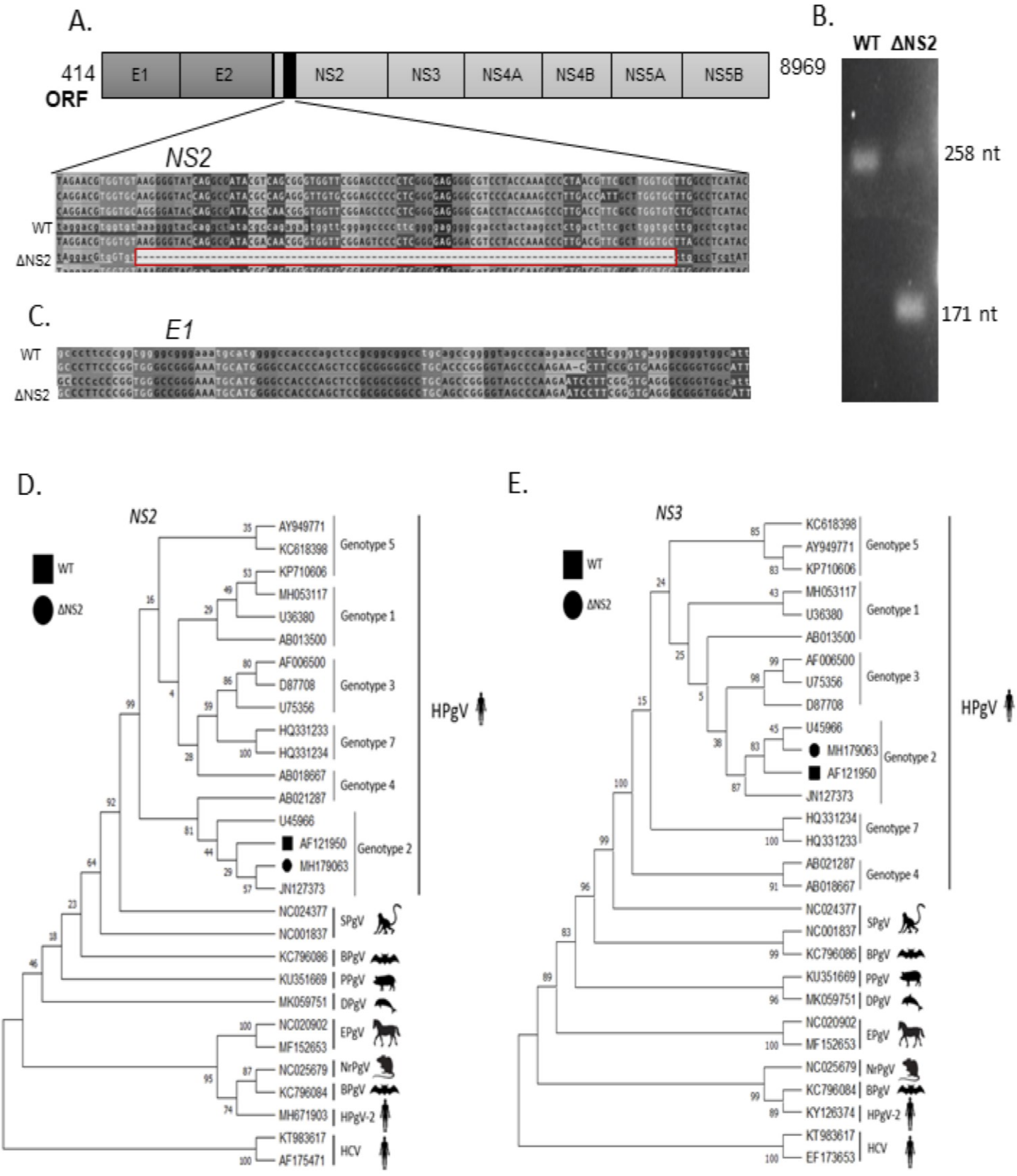
A.
414
ORF
E1
E2
NS2
NS3
NS4A
NS4B
NS5A
NS5B
8969
NS2
WT
ΔNS2
B.
WT ΔNS2
258 nt
171 nt
C.
E1
WT
ΔNS2
D.
NS2
WT
ΔNS2
AY949771
KC618398
KP710606
MH053117
U36380
AB013500
AF006500
D87708
U75356
HQ331233
HQ331234
AB018667
AB021287
U45966
AF121950
MH179063
JN127373
NC024377
NC001837
KC796086
KU351669
MK059751
NC020902
MF152653
NC025679
KC796084
MH671903
KT983617
AF175471
Genotype 5
Genotype 1
Genotype 3
Genotype 7
Genotype 4
Genotype 2
HPgV
SPgV
BPgV
PPgV
DPgV
EPgV
NrPgV
BPgV
HPgV-2
HCV
E.
NS3
WT
ΔNS2
KC618398
AY949771
KP710606
MH053117
U36380
AB013500
AF006500
U75356
D87708
U45966
MH179063
AF121950
JN127373
HQ331234
HQ331233
AB021287
AB018667
NC024377
NC001837
KC796086
KU351669
MK059751
NC020902
MF152653
NC025679
KC796084
KY126374
KT983617
EF173653
Genotype 5
Genotype 1
Genotype 3
Genotype 2
Genotype 7
Genotype 4
HPgV
SPgV
BPgV
PPgV
DPgV
EPgV
NrPgV
BPgV
HPgV-2
HCV

Figure 3.3: HPgV WT and ΔNS2 viruses can be differentiated by gel electrophoresis and sequences from both viruses cluster within genotype 2.

The HPgV ΔNS2 mutant is characterized by an 87-nucleotide deletion located in the *NS2* gene [A]. To verify the presence of a deletion, cDNA created from WT and ΔNS2 plasmids were by Sanger sequencing [A]. The presence of the *NS2* deletion in HPgV ΔNS2 is best observed by gel electrophoresis following qRT-PCR when compared to HPgV WT [B]. HPgV WT and ΔNS2 plasmids were also subject to Sanger Sequencing in the *E1* gene to ensure additional mutations were not introduced during mutagenesis [C]. Using HPgV WT (Genbank: AF121950) and ΔNS2 sequences from LE-1 (Genbank: MH179063), a phylogenetic tree was constructed for both the mutation site in *NS2* [D] and a region of the HPgV *NS3* gene [E]. All PgV, HPgV-2 and HCV sequences have corresponding Genbank accession numbers listed and HPgV sequences are grouped by genotype.

In addition to the creation of the HPgV ΔNS2 mutant [Figure 3.4B], further mutagenesis of the HPgV WT plasmid [Figure 3.4A] led to the creation of HPgV ΔNS5A [Figure 3.4C], which contained the 15-nucleotide insertion observed *in vivo* in our initial case, LE-1, and the HPgV ΔNS2 ΔNS5A virus [Figure 3.4D], which contained both mutations within the viral genome. Only HPgV ΔNS2 was utilized in this thesis, although the other clones are available for future experimentation.

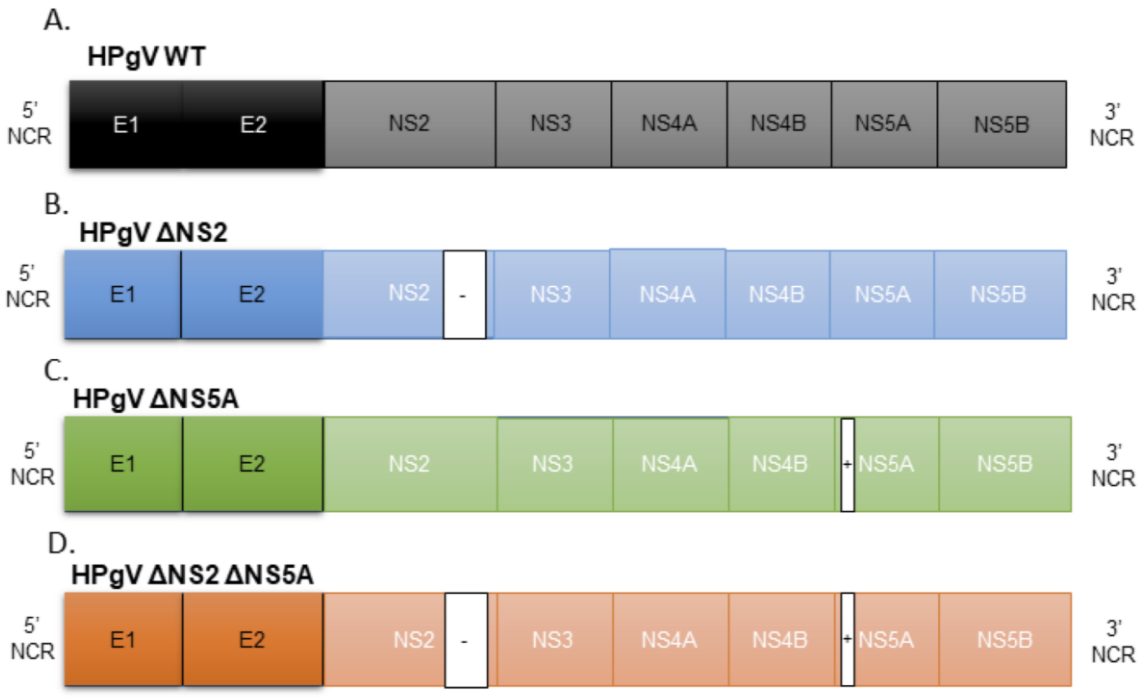

Figure 3.4: Multiple clones were generated to replicate mutations discovered in the HPgV genome.

Using sequences from our initial index case, patient LE-1 (Genbank: MH179063), three viral clones were produced following site-directed mutagenesis in our HPgV WT plasmid. The viral plasmid from HPgV WT [A] underwent mutagenesis using select primers directed to create an 87-nucleotide deletion in the *NS2* gene (HPgV ΔNS2) [B], a 15-nucleotide insertion in the *NS5A* gene (HPgV ΔNS5A) [C] or both mutations together in a single plasmid (HPgV ΔNS2 ΔNS5A) [D].

3.2.4 Phylogenetic analyses show that the HPgV WT and ΔNS2 viruses cluster together when compared with other pegiviruses

To understand HPgV phylogeny in the context of the HPgV WT and ΔNS2, I compared HPgV WT and ΔNS2 sequences to other pegiviruses. When investigating the *NS2* gene, HPgV WT (AF121950) and HPgV LE-1 (MH179063), a patient who had the *NS2* deletion from our original case report[1] both clustered as genotype 2 viruses, which are commonly found in North America (where the original clinical isolates originated from)[102] [Figure 3.3D]. A similar trend was also observed when investigating the HPgV *NS3* gene [Figure 3.3E]. In both genes, it appeared that the WT virus diverges before the HPgV ΔNS2 virus, indicating that the *NS2* deletion could represent a new strain that has recently been introduced. Of note, the other virus that clusters closely with both the WT and ΔNS2 viruses in genotype 2 (JN127373) is an HPgV isolate from the CNS of an individual with MS[107]. Within the *NS2* gene [Figure 3.3D], the three viruses cluster together more closely than the other genotype 2 virus (U45966) that was isolated from plasma, indicating potential mutations in the virus that increase the ability for HPgV to access the CNS.

3.2.5 HPgV proteins are detectable in lysates of human astrocytes following infection

To provide further evidence that HPgV is tropic for human astrocytes, we sought to detect HPgV antigens in lysates of human astrocytes following 7 days of infection. Both the E2 and NS5A proteins were detected in infected astrocytes [Figure 3.5A-C]. The presence of two HPgV proteins in cell lysate further supported our hypothesis that HPgV is tropic in human astrocytes. This immunoblot also provided validation of our antibodies by demonstrating that (i) minimal signal is detected in uninfected astrocytes, implying that cross-reactivity with host proteins is very limited, and (ii) signal is detected at the appropriate molecular weight for each viral protein, suggesting that the antibodies are detecting their intended target. This validation recapitulates our previous validation of the NS5A antibody[1].

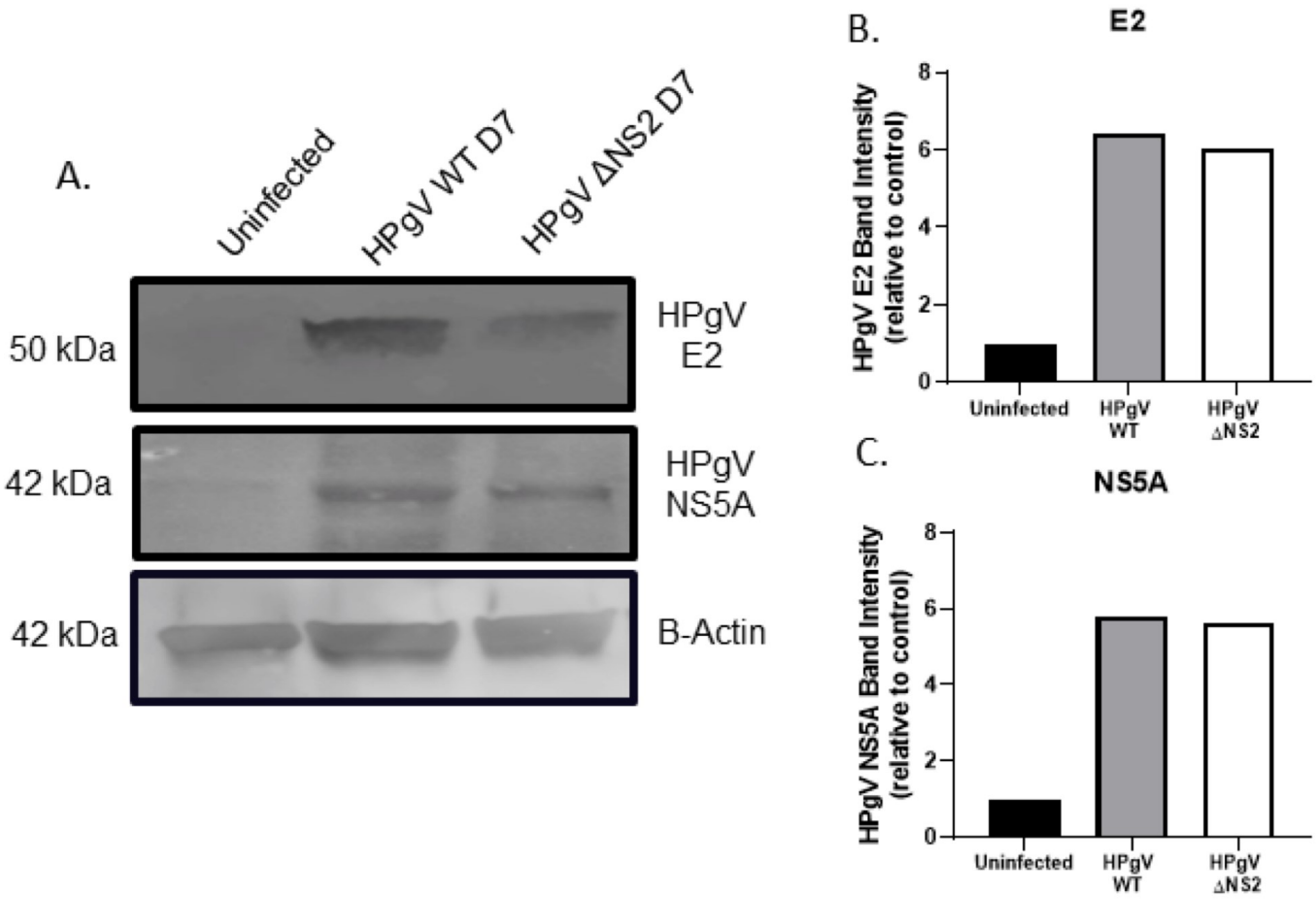

Figure 3.5: HPgV NS5A and E2 protein can be detected by immunoblot of HPgV-infected astrocytes.

[A-C] Astrocytes were infected with HPgV WT or ΔNS2 (MOI= 0.1) for 7 days before lysates were harvested and immunoblotted for HPgV NS5A and E2 as indicated. Data shown are HPgV NS5A [B] and E2 [C] band intensities normalized to beta-actin and expressed relative to the uninfected control. This experiment was repeated in two separate biological donors.

3.2.6 HPgV RNA is present in infected human glial cell cultures and the NS2 mutation confers greater replicative capacity

The above findings in human astrocytes prompted further examination of HPgV tropism in other CNS cell types. Following infection with HPgV WT and ΔNS2 for 12, 24, 48, 96, 196 (7 days), and 336 hours (14 days), only human astrocytes [Figure 3.6A, *p<0.05, **p<0.01, ***p<0.001] and microglia [Figure 3.6B] supported viral replication and release as measured by ddPCR; whereas human neurons [Figure 3.6C] and the human oligodendrocyte cell line (MO3.13) [Figure 3.6D] did not support HPgV replication. In human astrocytes, it appears that the ΔNS2 mutant does not have a 'lag phase' during infection and significantly greater copy numbers are detected beginning after 24 hours, compared to HPgV WT viral infection wherein virus is first detected in the supernatant after 48 hours. Infection of microglia showed a different time-course of infection when compared to human astrocytes, with viral presence in the supernatant peaking at 72 hours post-infection and decreasing rapidly over time.

To confirm that cells were indeed infected and HPgV WT and ΔNS2 were undergoing infection, cell lysates from day 14 post infected human astrocytes [Figure 3.6A] and microglia [Figure 3.6B] were harvested and analyzed by ddPCR to determine intracellular viral copy numbers for each condition [Figure 3.7A, *p<0.05, ***p<0.001, ****p<0.0001]. As expected, HPgV RNA (WT or ΔNS2) was not detected in uninfected cells. This prompted further investigation into the amount of

intracellular virus early during HPgV infection in human astrocytes. Following infection of human astrocytes with either HPgV WT or ΔNS2 viruses for 24, 48, 72 or 96 hours, cells were harvested and subject to the same ddPCR analysis as above [Figure 3.7B, *p<0.05].

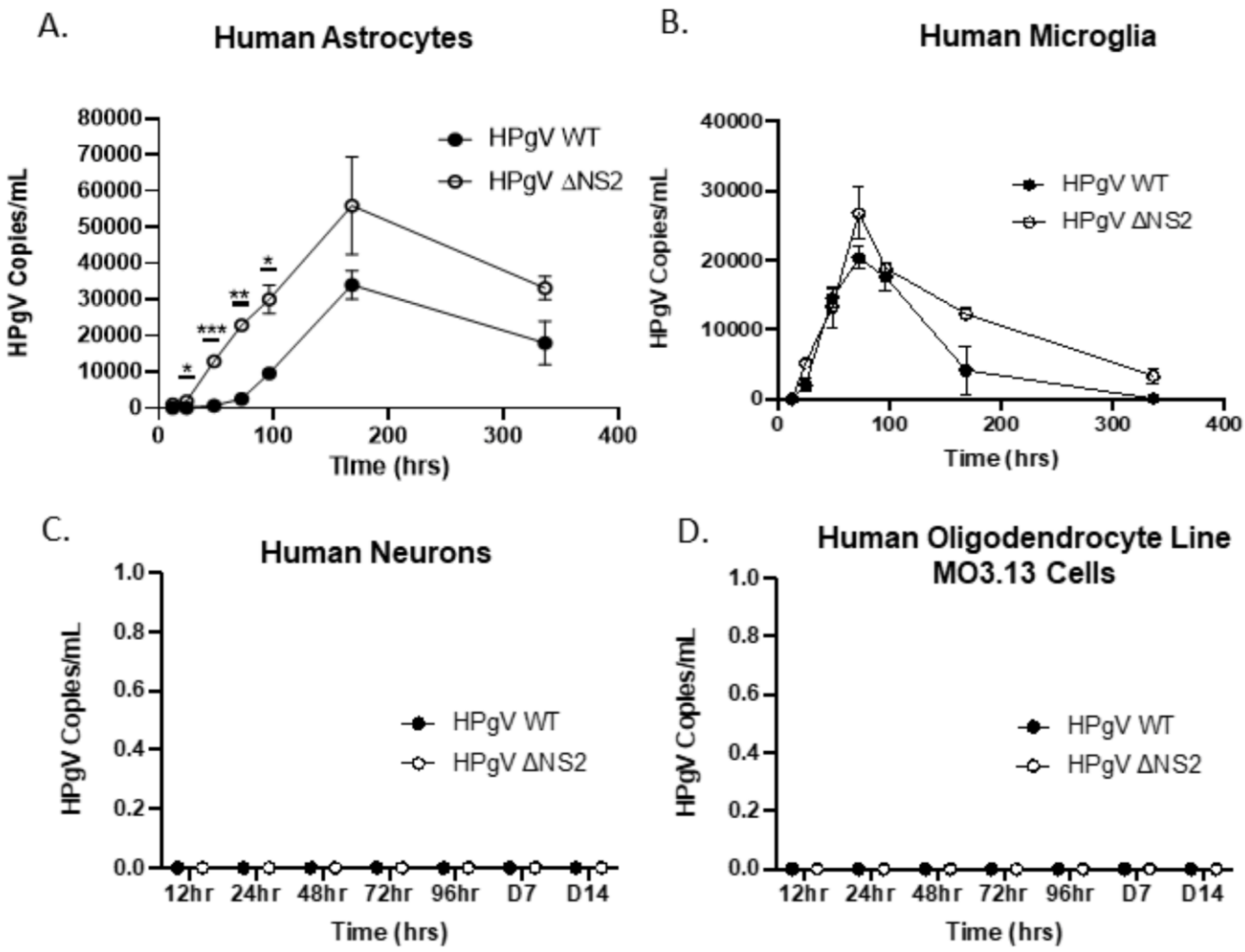

Figure 3.6: HPgV productively infects human astrocytes and microglia, with the ΔNS2 mutant virus displaying greater replication at multiple time points.

Human astrocytes [A], microglia [B], neurons [C] and a human oligodendrocyte cell line (MO3.13 cells) [D] were infected with HPgV WT or ΔNS2 (MOI=0.1) and supernatants were harvested after 12, 24, 48, 72, 96, 7 days or 14 days post-infection. Cell supernatants were then subjected to ddPCR analysis to determine the number of HPgV copies present in cell supernatants. (* p<0.05, ** p<0.01, *** p<0.001, Students T-test). n= 2 technical replicates were used.

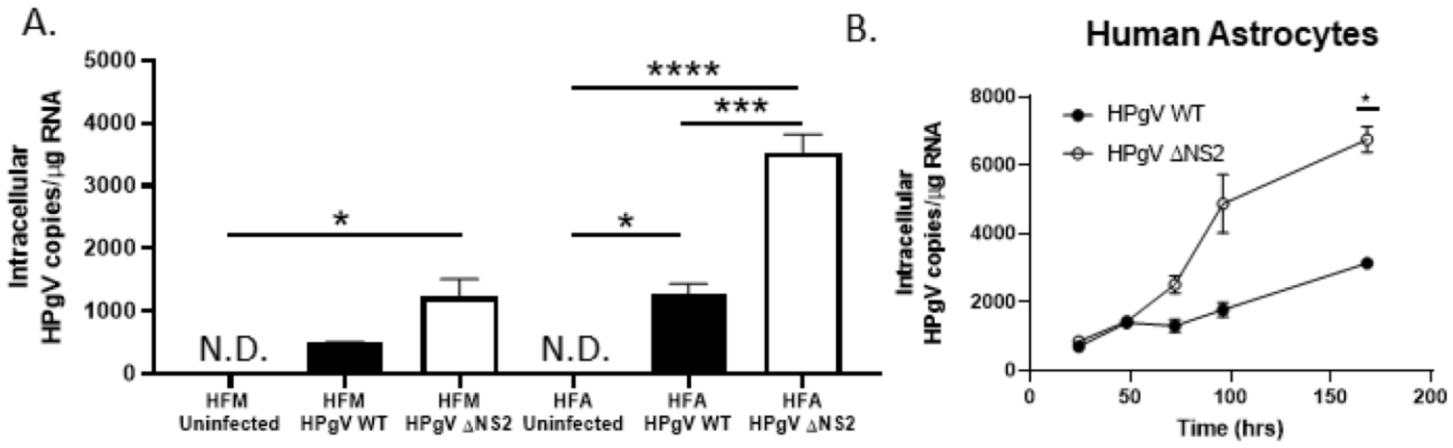

Figure 3.7: HPgV intracellular RNA detection in human astrocytes and microglia.

[A] Cell lysates from the human astrocytes and microglia in Figure 3.6 were harvested at day 14 for RNA and the number of intracellular HPgV copies was measured by ddPCR and normalized to the input of 1µg of cellular RNA. (* $p<0.05$, *** $p<0.001$, **** $p<0.0001$, One-way ANOVA). [B] Astrocytes were infected with either HPgV WT or ΔNS2 (MOI=0.1) for 24, 48, 72, 96 or 7 days. At each time-point post-infection, cells were harvested and RNA was collected. ddPCR analysis was completed using an input of 1µg of cellular RNA to determine the number of HPgV copies intracellularly at each time-point. (* $p<0.05$, Students T-test). n= 2 technical replicates were used.

These data clearly indicated that HPgV ΔNS2 is detected in significantly greater quantities intracellularly during infection and viral quantities increase rapidly in supernatants when compared to HPgV WT. The significantly greater quantities of the HPgV ΔNS2 virus in both cell lysates and cell supernatants when compared to HPgV WT suggested that the deletion in the *NS2* gene increases viral replicative capacity in astrocytes.

3.2.7 HPgV antigen detection in human microglial cultures

Based on the above finding that HPgV replicated in human microglia, I wanted to know if HPgV antigen can similarly be detected in microglial cultures. In our initial case report we did not identify any HPgV immunopositive microglia *in vivo* by immunofluorescence imaging[1]. Nevertheless, in microglia cultures infected with either HPgV WT or ΔNS2 viruses, I was able to detect HPgV NS5A antigen within F-actin stained cells following 7 days of infection [Figure 3.8A]. Further, HPgV NS5A protein was detected by immunoblot in HPgV WT infected cells in a similar experiment [Figure 3.8B,C]. Of interest, the peptide appears to be approximately 10kD lower than what is typically detected in astrocyte cultures, suggesting that the NS5A peptide may be processed differentially in these cells.

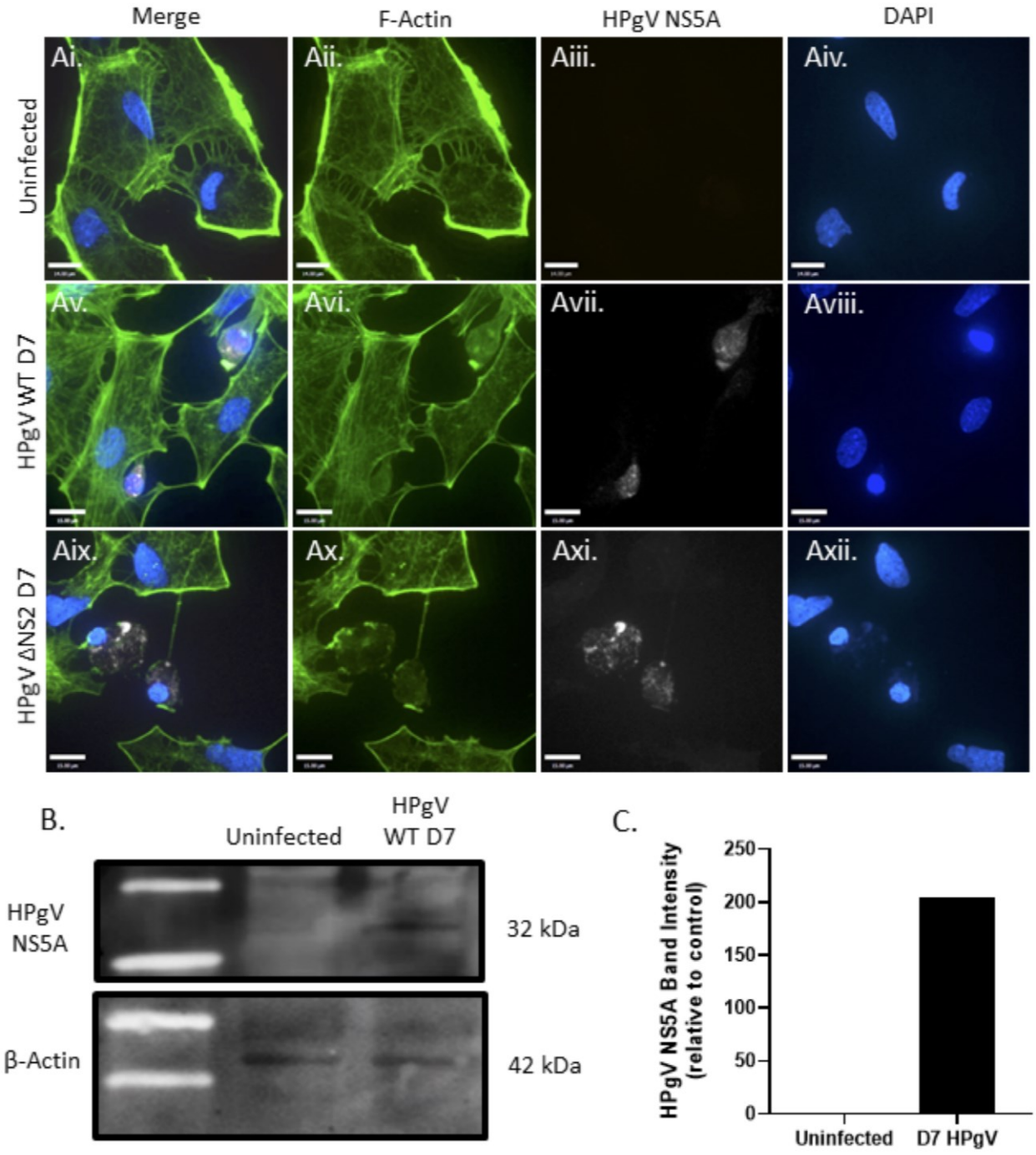

Figure 3.8: NS5A antigen detection in human microglia 7 days post-infection with HPgV WT and ΔNS2.

[A] Microglia were infected with HPgV WT and ΔNS2 (MOI=0.1) for 7 days, after which cells were fixed and immunolabeled for HPgV NS5A antigen (white) and labeled for F-actin (green) and DAPI (blue). [B,C] Microglia were infected with HPgV WT (MOI=0.1) or uninfected for 7 days before lysates were harvested and immunoblotted for HPgV NS5A. Data shown are HPgV NS5A band intensities normalized to beta-actin and expressed relative to the uninfected control.

3.2.8 Infectious HPgV is released from cells following infection in human astrocytes

The ability for viruses to spread to different cells is imperative for viral infection to persist and propagate within its host. In the context of CNS infection, I initially identified that HPgV WT spreads in human astrocytes [Figure 3.2D], although I did not delineate the differences in viral spread between HPgV WT and ΔNS2 viruses in astrocyte cultures. Based on my above results, I hypothesized the HPgV ΔNS2 virus would spread more efficiently in cell cultures, resulting in a greater proportion of astrocytes being immunopositive over time. When examining GFAP+ astrocytes infected with HPgV WT or ΔNS2 viruses, I saw that at 4 days post infection, 62% of astrocytes were infected in HPgV WT cultures and 83% of astrocytes were immunopositive in cultures infected with HPgV ΔNS2 [Figure 3.9A-G]. After quantifying astrocytes infected for 7 days, I saw these numbers rise significantly in HPgV WT infected cells to 71% and HPgV ΔNS2 infected cells to 90% [Figure 3.9A-G, $^{**}p<0.01$].

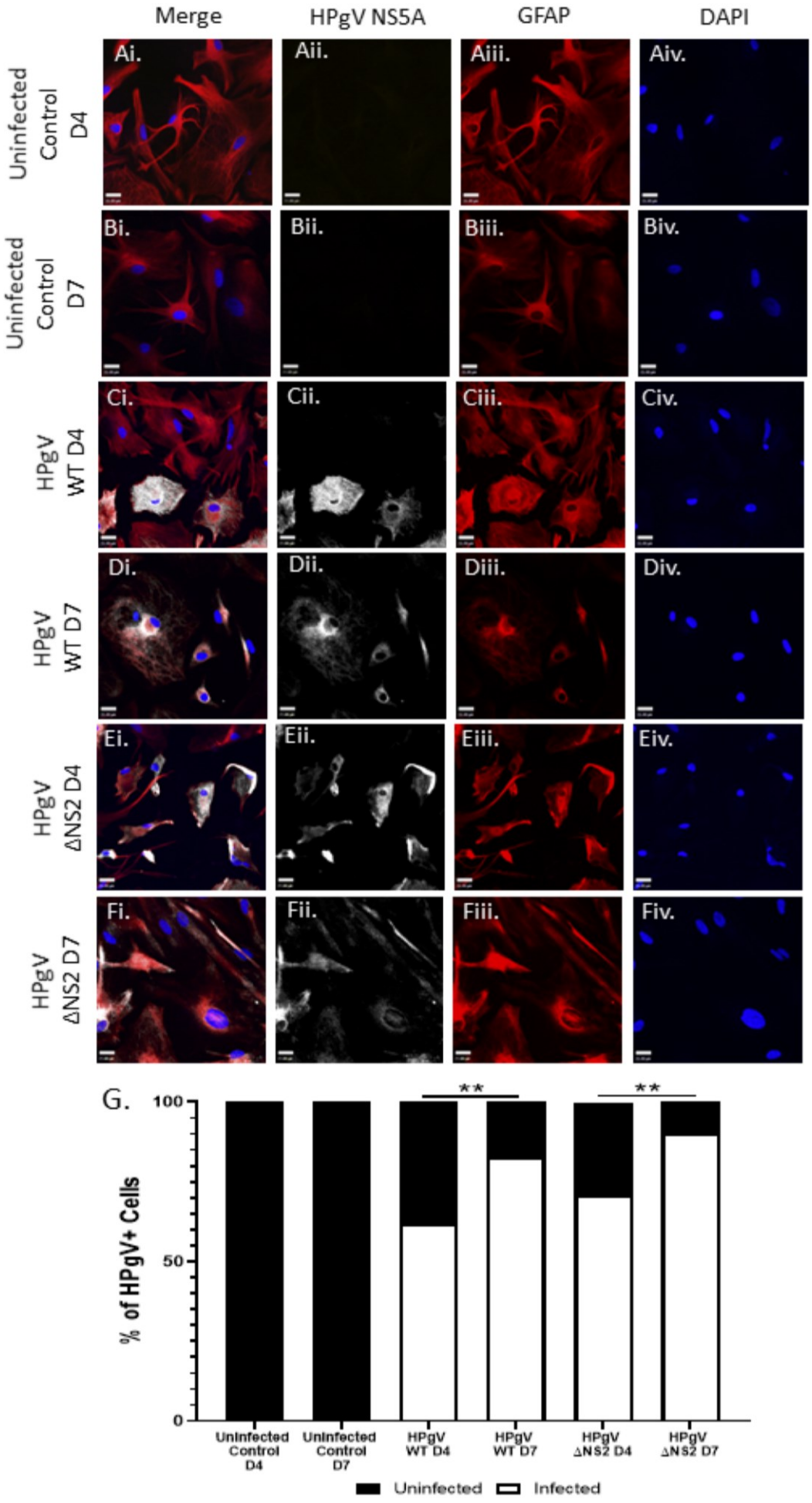
Merge
HPgV NS5A
GFAP
DAPI
Uninfected Control D4
Uninfected Control D7
HPgV WT D4
HPgV WT D7
HPgV ΔNS2 D4
HPgV ΔNS2 D7
Ai.
Aii.
Aiii.
Aiv.
Bi.
Bii.
Biii.
Biv.
Ci.
Cii.
Ciii.
Civ.
Di.
Dii.
Diii.
Div.
Ei.
Eii.
Eiii.
Eiv.
Fi.
Fii.
Fiii.
Fiv.
G.
% of HPgV+ Cells
100
50
0
**
**
Uninfected Control D4
Uninfected Control D7
HPgV WT D4
HPgV WT D7
HPgV ΔNS2 D4
HPgV ΔNS2 D7
Uninfected
Infected

Figure 3.9: HPgV WT and ΔNS2 infect and spread in human astrocytes.

[A-G] Astrocytes were infected with HPgV WT or ΔNS2 (MOI=0.1) and cells were subsequently harvested and immunolabeled for HPgV NS5A (white), GFAP (red) and labeled with DAPI at both 4 and 7 days post infection and imaged using confocal microscopy. Viral spread was determined by quantifying the number of HPgV+ cells per field of view (FoV) in each condition by immunofluorescence and the proportion of infected GFAP+ cells is shown [G]. (** $p<0.01$, Fisher's exact test).

3.2.9 Passaged HPgV shows similar spread in human astrocytes to virus derived from astrocytoma-generated viral stocks

My earlier findings indicated that after 4 days of HPgV infection, 30,000 copies of HPgV ΔNS2 and 9,555 copies of HPgV WT are found in cell supernatants which increases to 55,971 HPgV ΔNS2 and 34,001 HPgV WT viral copies at 7 days post-infection in astrocyte culture supernatants [Figure 3.6A]. The evidence of viral replication within a given astrocyte culture prompted me to investigate whether the viruses released from these astrocytes could in turn re-establish infection in a subsequent infection experiment. For this experiment, I chose supernatants from day 4 infected astrocytes, due to the steep positive slope of the viral replication curve illustrated in Figure 3.6A, indicating that virus at this point is still replication competent. Viral spread within cell culture, as indicated by the proportion of cells that are immunopositive for HPgV NS5A over time, was chosen as a readout. Astrocytes were exposed to an equal abundance of virus (MOI=0.1) from day 4 conditioned media from uninfected and infected astrocytes for either 4 or 7 days [Figure 3.10A-G]. Following exposure to HPgV+ supernatants for 4 days, 65% of astrocytes exposed to HPgV WT and 80% of astrocytes exposed to HPgV ΔNS2 virus were positive for HPgV NS5A antigen [Figure 3.10C, E, G, $*p<0.05$]. These numbers significantly increased to 76% and 91% by 7 days of exposure, respectively [Figure 3.10D, F, G, $**p<0.01$]. These results indicated that infected astrocytes release infectious viral particles that display comparable spread kinetics as U251-propogated stock virus when applied to fresh astrocyte cultures [Figure 3.9].

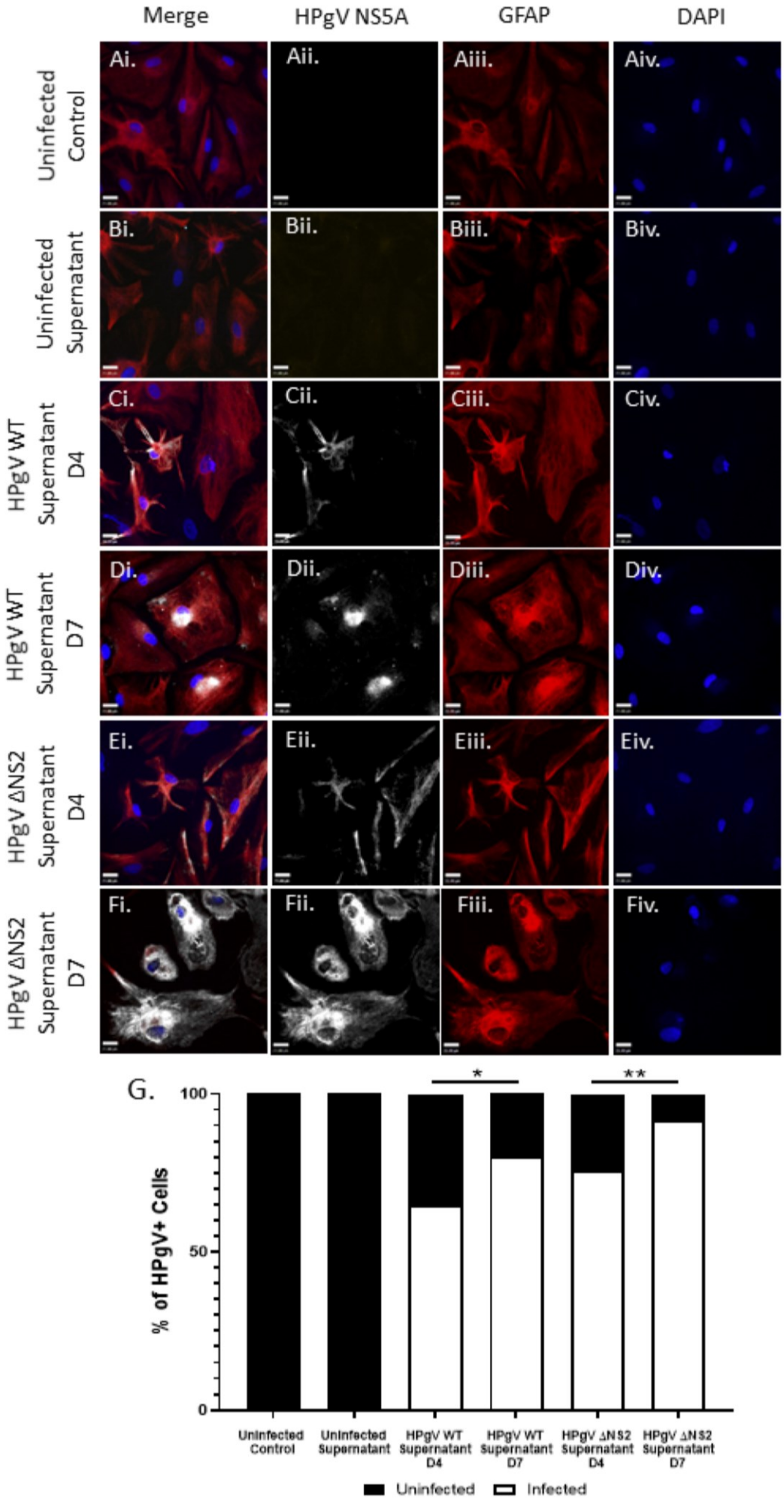
Merge
HPgV NS5A
GFAP
DAPI
Uninfected Control
Uninfected Supernatant
HPgV WT Supernatant D4
HPgV WT Supernatant D7
HPgV ΔNS2 Supernatant D4
HPgV ΔNS2 Supernatant D7
Ai.
Aii.
Aiii.
Aiv.
Bi.
Bii.
Biii.
Biv.
Ci.
Cii.
Ciii.
Civ.
Di.
Dii.
Diii.
Div.
Ei.
Eii.
Eiii.
Eiv.
Fi.
Fii.
Fiii.
Fiv.
G.
% of HPgV+ Cells
100
50
0
*
**
Uninfected Control
Uninfected Supernatant
HPgV WT Supernatant D4
HPgV WT Supernatant D7
HPgV ΔNS2 Supernatant D4
HPgV ΔNS2 Supernatant D7
Uninfected
Infected

Figure 3.10: HPgV WT and ΔNS2 viral particles released from infected astrocytes are infectious and spread in subsequent infection of human astrocytes.

[A-G] Astrocytes were exposed to supernatants from either HPgV WT (MOI=0.1), ΔNS2 (MOI=0.1) or uninfected supernatant. Cells were harvested and immunolabeled for HPgV NS5A (white), GFAP (red) and labeled with DAPI at both 4 and 7 days post infection and imaged using confocal microscopy. Viral spread was determined by quantifying the number of HPgV+ cells per field of view (FoV) in each condition by immunofluorescence and the relative proportion of infected GFAP+ cells is shown [G]. (*p<0.05, ** p<0.01, Fisher's exact test).

3.3 Summary

In this chapter, multiple experimental techniques were utilized to establish and optimize an *in vitro* model of HPgV infection in human glial cells. HPgV protein detection was completed by semi-quantitative confocal microscopy of the HPgV NS5A antigen and immunoblot detection of both the NS5A and E2 proteins in astrocyte cultures. Further, viral spread and replication within cultures over time could be determined by examining HPgV infection over time. HPgV viral RNA could also be detected both intracellularly and in cell supernatants by ddPCR analysis, a precise and quantitative novel method for investigating viral infection and replication. I was not only able to establish a robust and reproducible model of HPgV in human astrocytes, but also identified HPgV infection of human microglia, which has never been described previously.

Additionally, the construction and implementation of the HPgV ΔNS2 virus *in vitro* revealed that this mutant virus was replication competent and could spread and replicate at higher levels than HPgV WT in human glial cells. Taken together, the present observations confirmed HPgV neurotropism in human astrocytes, delineated the effect of a novel 87-nucleotide deletion in HPgV *NS2* on viral infectivity and replication and identified a new cell type that was permissive to HPgV infection.

Chapter IV: Host responses in HPgV-infected human astrocytes and microglia

4.1 Introduction

Chapter IV Objective: *Define the host antiviral responses to WT and ΔNS2 infection in human astrocytes and microglia.*

Human glia can mount robust immune responses to neurotropic flaviviruses, which can include engagement of antiviral, inflammatory and cell death signaling pathways[161]. Thus, members of the *Flaviviridae* family have in turn developed mechanisms to counteract these responses, including regulating apoptosis[56]. As the neurotropism of HPgV was only recently discovered in 2018[1], the interaction between HPgV and host antiviral, inflammatory and cell death signaling pathways in infected glia is unknown. Further, the effect of the 87 nucleotide deletion in the HPgV *NS2* gene (which was associated with encephalitis[1]) on the host immune response is uncharacterized. In the previous chapter, I demonstrated productive infection of HPgV in human astrocytes and microglia, which was enhanced by the deletion in the *NS2* gene. These initial findings prompted me to investigate immune responses as well as cell viability following infection of human astrocytes and microglia *in vitro*.

Chapter IV Hypothesis*: HPgV WT and ΔNS2 viruses will elicit different host antiviral responses in human glia following infection.*

Within this chapter, I have used several different techniques to investigate how HPgV infection affects astrocytes and microglia *in vitro*. I found that HPgV infection minimally affects host immune responses in human astrocytes unless combined with poly(I:C). HPgV infection of human microglia revealed that HPgV WT and ΔNS2 differentially affected transcription of several proinflammatory and antiviral genes *in vitro*. I have also provided evidence that HPgV infection did not result in (i) lytic cell death as measured through LDH activity in cell supernatants, (ii) the release of a proinflammatory cytokine (IL-1β) or (iii) a loss in viability in astrocyte cultures. Human astrocytes did however show a modest reduction in viability following high MOI (MOI of 1.0) infection with HPgV ΔNS2 and a greater loss in cell viability was also observed when there was a 'second-hit' with an inflammatory stimulus following infection with HPgV ΔNS2 at a MOI of 0.1.

4.2 Results

4.2.1 HPgV infection of human astrocytes does not alter the transcription of several antiviral and proinflammatory transcripts

To understand how HPgV modulates immune responses of astrocytes following infection, the transcript levels of several prototypic antiviral and proinflammatory genes were analyzed by qRT-PCR to determine if HPgV influenced host immune responses in infected versus uninfected cells. Following 2 and 7 days of HPgV WT or ΔNS2 infections, astrocytes were harvested for RNA and cDNA libraries were prepared. Multiple genes in several key antiviral and proinflammatory pathways were analyzed by qRT-PCR [Figure 4.1A-G]. After 2 days of infection, no transcript changes were observed other than a trend in *CASP1* induction [Figure 4.1F]. At 7 days post-infection, a trend towards a decrease in the transcription of *IFNB* [Figure 4.1A] was observed, together with slight reductions in both *CASP1* [Figure 4.1F] and *DDX58* [Figure 4.1D] expression. To visualize the transcriptional changes observed in these seven genes, a heat map was generated which further illustrated the overall similarities in gene expression profiles of HPgV WT and ΔNS2 infection [Figure 4.1G].

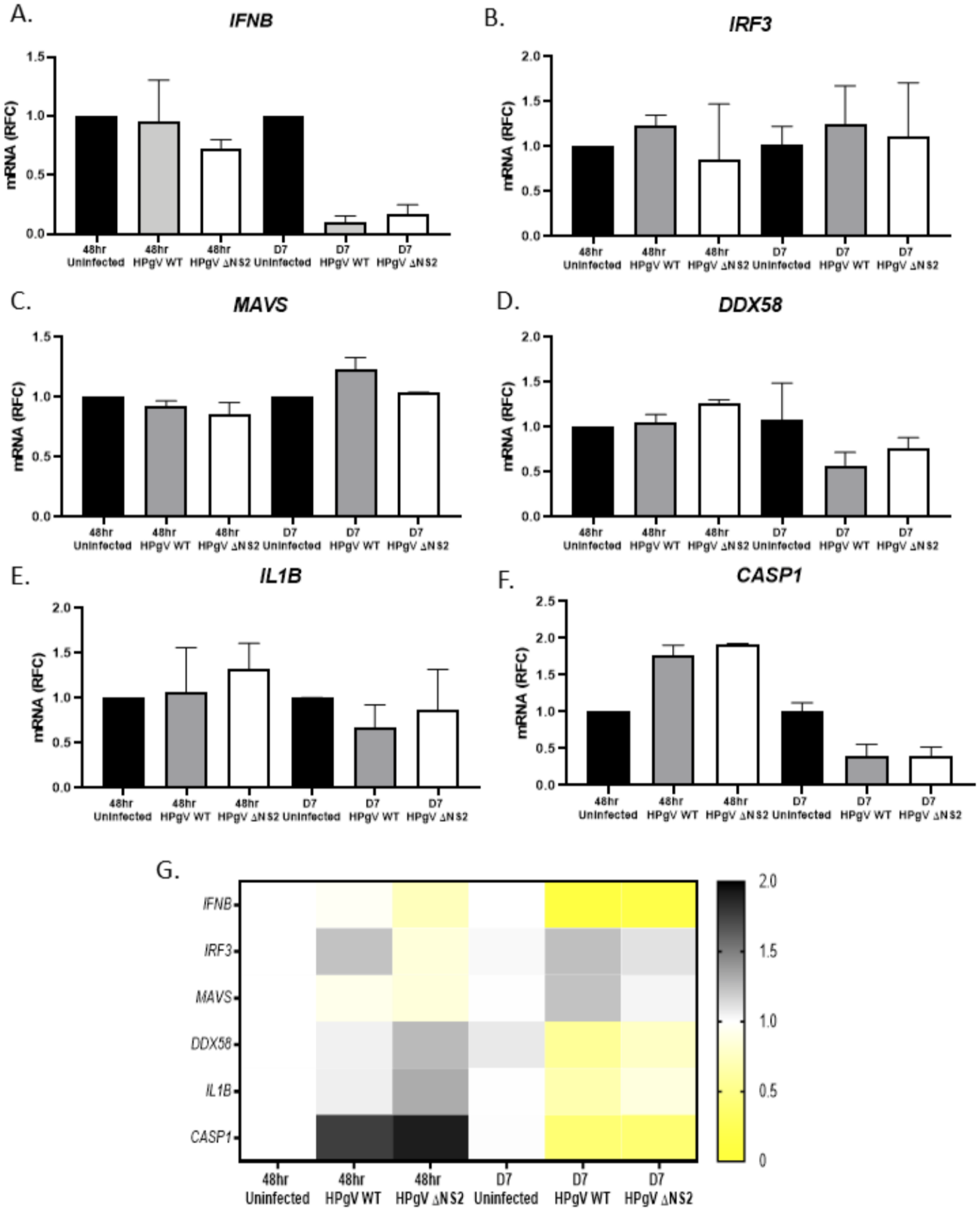
A.
IFNB
mRNA (RFC)
1.5
1.0
0.5
0.0
48hr Uninfected
48hr HPgV WT
48hr HPgV ΔNS2
D7 Uninfected
D7 HPgV WT
D7 HPgV ΔNS2
B.
IRF3
2.0
C.
MAVS
D.
DDX58
E.
IL1B
F.
CASP1
2.5
G.
IFNB
IRF3
MAVS
DDX58
IL1B
CASP1
2.0
1.5
1.0
0.5
0

Figure 4.1: HPgV infection does not alter host transcripts for several prominent antiviral and proinflammatory genes in human astrocytes.

Astrocytes were infected with HPgV WT or ΔNS2 (MOI=0.1) for either 2 or 7 days before cells were harvested for RNA and cDNA libraries were prepared. qRT-PCR analysis of *IFNB* [A], *IRF3* [B], *MAVS* [C], *DDX58* [D], *IL1B* [E], and *CASP1* [F] were completed and RFC ± SEM for each gene was compared to time-matched uninfected controls. A heat map [G] was generated to show the transcripts up-regulated (black) and down-regulated (yellow) following HPgV infection, compared to uninfected controls. n=2 technical replicates were used per condition.

4.2.2 Antiviral and proinflammatory transcripts are inducible following transfection of HPgV-infected astrocytes with poly(I:C)

Previous studies performed involving ZIKV infection of human epithelial cells reported that ZIKV inhibits the induction of interferon responses induced by poly(I:C) exposure[72]. Thus, it was important to understand if HPgV can inhibit the induction of interferon-associated responses, but also to ensure that astrocytes were capable of generating antiviral and proinflammatory response during infection. To investigate this issue, astrocytes were infected with HPgV WT or ΔNS2 for 6-hours and then transfected with poly(I:C). Cells were then harvested 42 hours later for cDNA library preparation and qRT-PCR analysis [Figure 4.2A-H, *p<0.05, **p<0.01]. As observed in Figure 4.1, HPgV WT or ΔNS2 infection alone did not induce gene expression at 48 hours post-infection, but the addition of poly(I:C) to astrocyte cultures induced transcript changes in genes associated with both the antiviral and proinflammatory immune response. Contrary to what was observed in ZIKV-infected epithelial cells, HPgV did not inhibit the induction of the IFN-associated responses, but rather further induced the transcription of *IFNB*. This was apparent when all three poly(I:C) conditions are internally normalized to the poly(I:C) control, in which it is apparent that pre-infection with HPgV further increased the trend of transcription when compared to poly(I:C) transfection alone [Figure 4.2G].

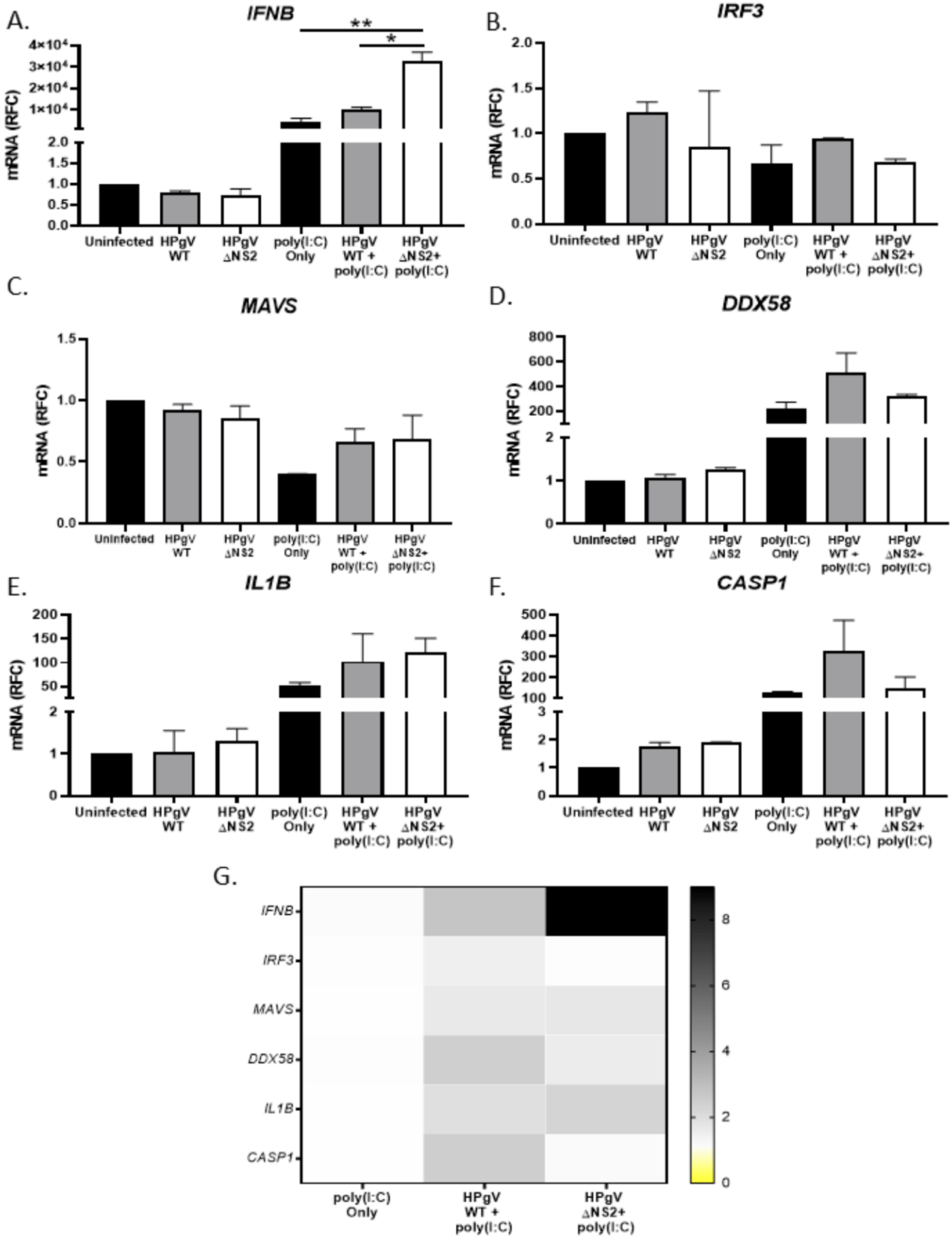
A.
IFNB
**
*
mRNA (RFC)
4×10⁴
3×10⁴
2×10⁴
1×10⁴
2.0
1.5
1.0
0.5
0.0
Uninfected
HPgV WT
HPgV ΔNS2
poly(I:C) Only
HPgV WT + poly(I:C)
HPgV ΔNS2+ poly(I:C)
B.
IRF3
mRNA (RFC)
2.0
1.5
1.0
0.5
0.0
Uninfected
HPgV WT
HPgV ΔNS2
poly(I:C) Only
HPgV WT + poly(I:C)
HPgV ΔNS2+ poly(I:C)
C.
MAVS
mRNA (RFC)
1.5
1.0
0.5
0.0
Uninfected
HPgV WT
HPgV ΔNS2
poly(I:C) Only
HPgV WT + poly(I:C)
HPgV ΔNS2+ poly(I:C)
D.
DDX58
mRNA (RFC)
800
600
400
200
2
1
0
Uninfected
HPgV WT
HPgV ΔNS2
poly(I:C) Only
HPgV WT + poly(I:C)
HPgV ΔNS2+ poly(I:C)
E.
IL1B
mRNA (RFC)
200
150
100
50
2
1
0
Uninfected
HPgV WT
HPgV ΔNS2
poly(I:C) Only
HPgV WT + poly(I:C)
HPgV ΔNS2+ poly(I:C)
F.
CASP1
mRNA (RFC)
500
400
300
200
100
3
2
1
0
Uninfected
HPgV WT
HPgV ΔNS2
poly(I:C) Only
HPgV WT + poly(I:C)
HPgV ΔNS2+ poly(I:C)
G.
IFNB
IRF3
MAVS
DDX58
IL1B
CASP1
8
6
4
2
0
poly(I:C) Only
HPgV WT + poly(I:C)
HPgV ΔNS2+ poly(I:C)

Figure 4.2: HPgV infection does not inhibit the induction of IFN responses.

Astrocytes were infected with HPgV WT or ΔNS2 (MOI=0.1) or mock-infected for 6 hours and then transfected with poly(I:C) for 42 hours. After a total of 48 hours, cells were harvested for RNA and cDNA libraries were prepared. qRT-PCR analysis of *IFNB* [A], *IRF3* [B], *MAVS* [C], *DDX58* [D], *IL1B* [E], and *CASP1* [F] were completed and RFC ± SEM for each gene was compared to time-matched uninfected controls. A heat map [G] was generated to show the transcripts up-regulated (black) and down-regulated (yellow) following poly(I:C) transfected, with and without prior HPgV infection. n=2 technical replicates were used per condition. (* $p<0.05$, ** $p<0.01$, One-way ANOVA).

4.2.3 An apoptotic nuclear phenotype is observed in a subset of HPgV infected astrocytes

Given the recognition of neurovirulence within the *Flaviviridae* family, along with the putative association of HPgV with encephalitis[1], it was important to investigate if HPgV infection of human astrocytes caused cell death. To address this question, I infected human astrocytes with HPgV WT or ΔNS2 viruses and imaged the cells at 7 days post infection for HPgV NS5A immunodetection, and screened the cells for morphological indicators of cell death (e.g. retraction of astrocytic processes, changes in nuclear morphology) [Figure 4.3]. As demonstrated in Chapter III, I observed glial fibrillary acidic protein GFAP immunopositive cells that contained abundant HPgV NS5A immunoreactivity. Morphologically, these cells displayed a rounded appearance in both HPgV WT- [Figure 4.3Avii] and HPgV ΔNS2-[Figure 4.3xi] infected cultures when compared to uninfected cultures [Figure 4.3Aiii]. Further, I also identified a small population of cells with aberrant nuclei in both HPgV WT [Figure 4.3Aviii] and HPgV ΔNS2 [Figure 4.3xii] infected cells, suggestive of karyorrhexis (fragmentation of the nucleus) that occurs during apoptosis[52]. These observations implied a small population of cells might be undergoing apoptosis following HPgV infection of human astrocytes.

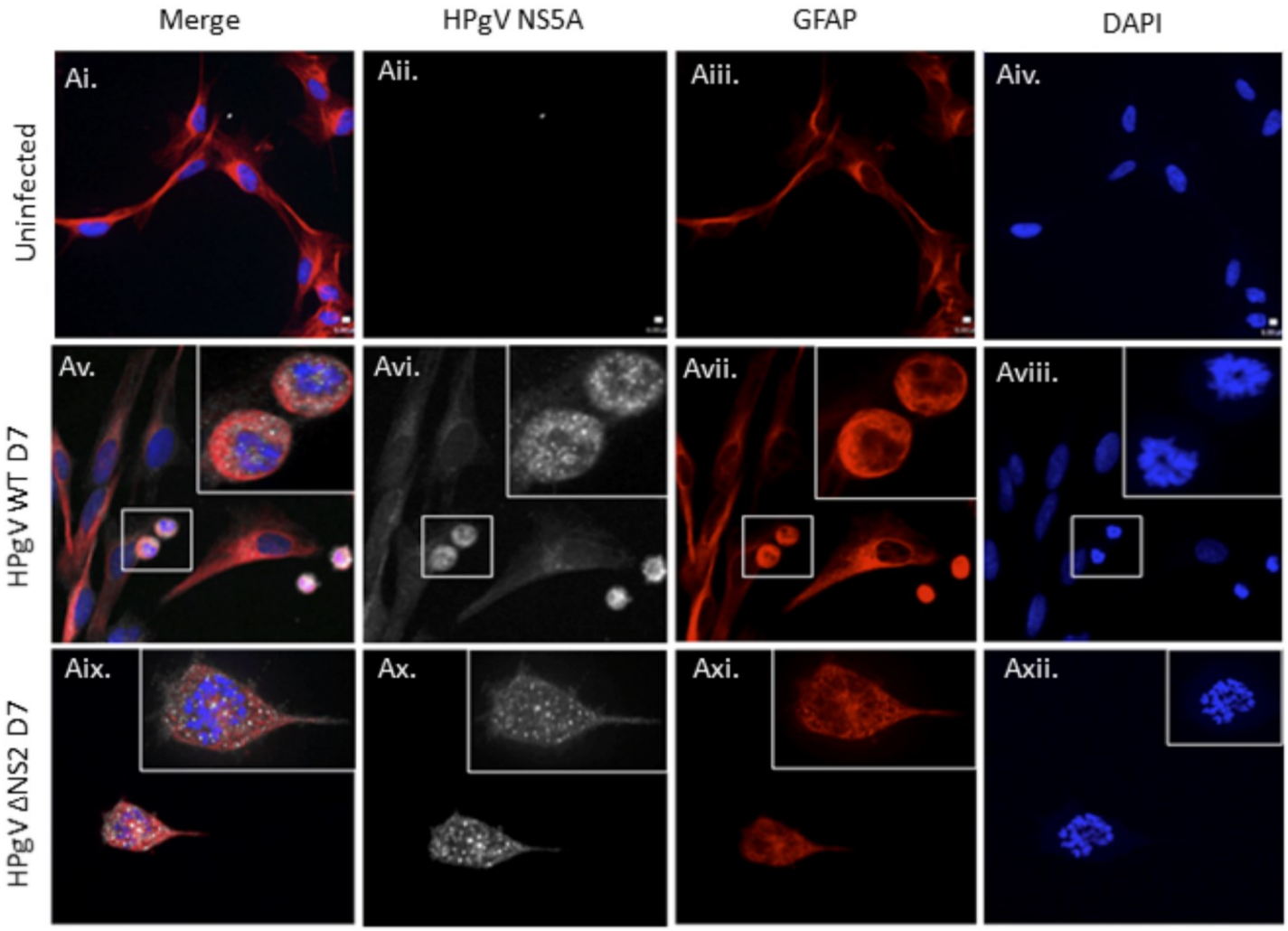

Figure 4.3: HPgV-infection in astrocytes causes nuclear disruption in a small population of infected astrocytes.

[Ai-Axii] Astrocytes were infected with HPgV WT or ΔNS2 (MOI= 0.1) for 7 days. Cells were then fixed and immunolabeled for HPgV NS5A (white) and GFAP (red) and labeled with DAPI (blue) and imaged using confocal microscopy (20x; insets shot at 40x) Representative images are shown.

4.2.4 There is minimal caspase activation following HPgV infection in human astrocytes

The activation of caspases, in particular caspase-3/7 is a hallmark of apoptosis following cellular stress[52]. Since viral infection is a major cause of cell stress, I investigated (i) if caspase activation was present in human astrocytes following infection by HPgV and (ii) whether this activation differed between the two viruses. Following infection with HPgV WT or ΔNS2 viruses for 24, 48, 72, 96 and 168 hours, intracellular caspase activation was measured by activity-dependent fluorescent probes (FAM-FLICA™ assays) for caspase-1 [Figure 4.4A, $*p<0.05$], caspase-3/7 [Figure 4.4B], caspase-8 [Figure 4.4C, $*p<0.05$, $***p<0.001$] and caspase-9 [Figure 4.4D]. Caspase-1, -3/7 and -9 activation appeared to follow a similar trend over time following infection with either HPgV WT or ΔNS2 viruses. Of interest, caspase-8 activation shows a significant increase following 48 and 168 hours of HPgV ΔNS2 infection compared to infection with WT virus [Figure 4.4C] and uninfected controls. Although caspase-8 activation was observed, there is no subsequent HPgV ΔNS2-specific activation of the executioner caspases -1 and -3/-7, suggesting that the cell might not be undergoing cell death following the transient activation of caspase-8.

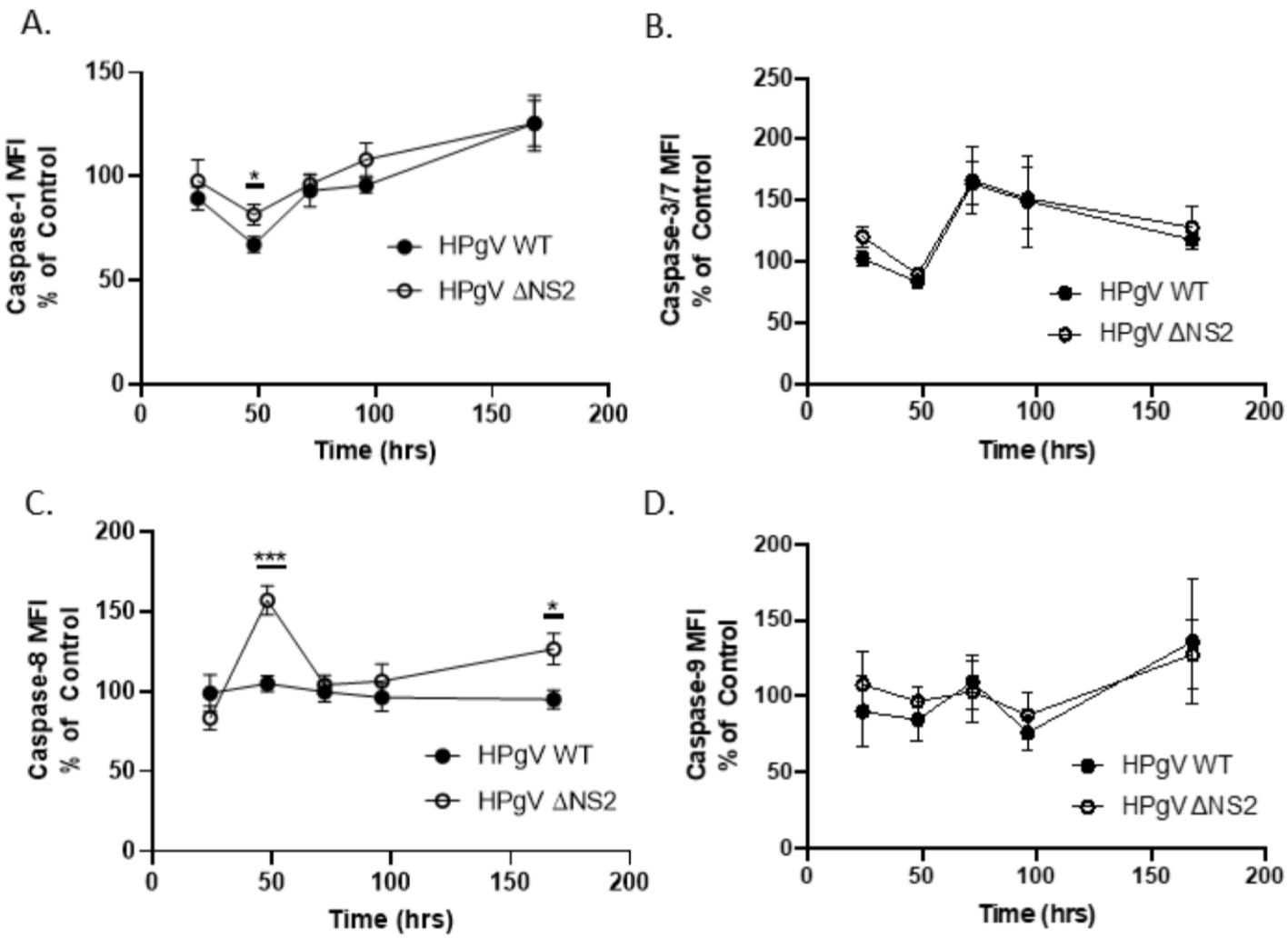

Figure 4.4: Select caspases are modestly activated following infection with HPgV WT and ΔNS2 in human astrocytes.

[A-D] Astrocytes were infected with HPgV WT or ΔNS2 (MOI=0.1) for 24, 48, 72, 96 or 168 hours (7 days). Intracellular caspase-1 [A], -3/7 [B], -8 [C] and -9 [D] activity was then assessed using activity-dependent caspase fluorescent probes for each condition and normalized to DAPI at each time-point. Uninfected controls were set to 100% as baseline. (* $p<0.05$, *** $p<0.001$, Students T-test). n=6 technical replicates were used per condition and the experiment was repeated in two separate biological donors.

4.2.5 HPgV infection of human astrocytes is not associated with cell lysis, cytokine release or reduced viability

To analyze the cellular response to HPgV infections further, cell viability in human astrocytes was measured using the Alamar Blue™ assay to determine if loss of cell viability occurred following HPgV infection. For both HPgV WT and ΔNS2 viral infections, no loss in astrocyte viability [Figure 4.5A] was seen following 24, 48, 72, 96 or 168 hours of infection when compared to uninfected astrocyte controls. LDH activity (a measure of lytic cell death) was also measured in cell supernatants from human astrocytes following 24, 48, 72, 96 and 168 hours of infection with either HPgV WT or ΔNS2 infection. Increased LDH activity [Figure 4.5B] was not detected in cell supernatants from human astrocytes following infection, suggesting that these cells were not undergoing cell lysis. Additionally, IL-1β, a well-characterized proinflammatory cytokine, was measured in cell supernatants from human astrocytes. IL-1β levels did not exceed 5pg/mL of IL-1β in HPgV-infected astrocyte supernatants, compared to 74pg/mL in the positive control (human microglia exposed to 5μM of nigericin) [Figure 4.5C]. Together these data provided evidence that HPgV-infected astrocytes did not undergo cell lysis, nor did they release large quantities of a proinflammatory cytokine into their environment, despite modest intracellular caspase activation. A preliminary experiment also showed that supernatants from day 4 HPgV-infected astrocytes do not cause the loss of viability of neuronal (SK-N-SH) or oligodendrocyte (MO3.13) cell lines, suggesting that HPgV does not induce the release of neurotoxic factors [Figure A.1]. These data, along with the above findings suggest that human astrocytes did not undergo cell death

following HPgV infection and human astrocytes do not produce the proinflammatory cytokine IL-1β following infection.

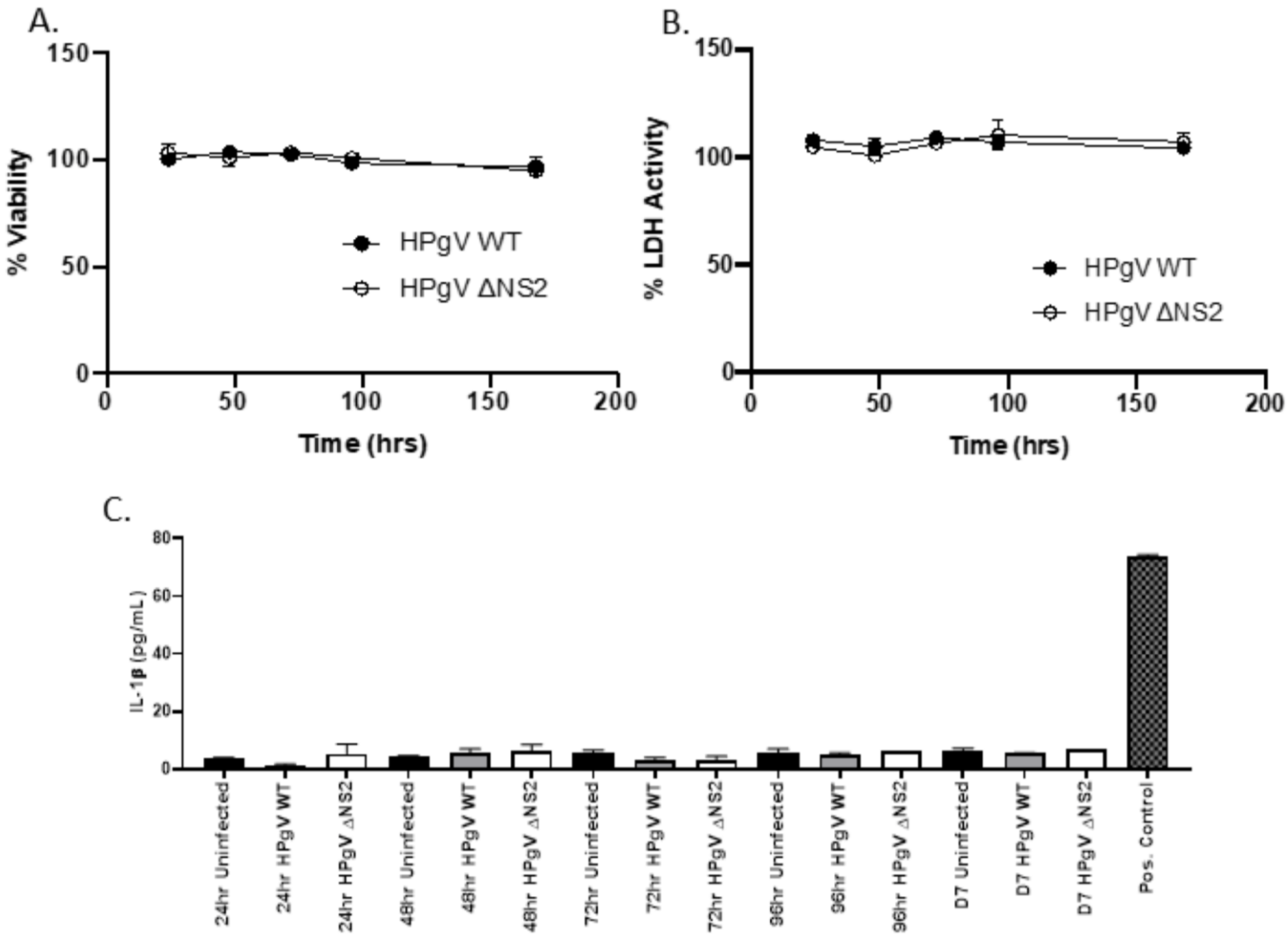

Figure 4.5: HPgV WT and ΔNS2 infection in human astrocytes does not cause a loss in cell viability.

[A] Astrocytes were infected with HPgV WT or ΔNS2 (MOI=0.1) for 24, 48, 72 96 and 168 hours and cell viability was measured using Alamar Blue™. Uninfected controls were set to 100% and n=6 technical replicates were used in each assay per condition and the experiment was repeated in two separate biological donors. [B] Astrocytes or were infected with HPgV WT or ΔNS2 (MOI=0.1) and cell supernatants were measured for LDH activity at 24, 48, 72, 96 and 168 hours post infection and normalized to uninfected controls set at 100%. n=6 technical replicates were used per condition and the experiment was repeated using two biological donors. [C] ELISA was performed on the cell supernatants from [B] to assess IL-1β release from infected astrocytes. The positive control used for the IL-1β ELISA was human microglia exposed to 5μM of nigericin (a bacterial pore-forming toxin). n=2 technical replicates were used per condition and the experiment was repeated in two separate biological donors.

4.2.6 Increasing the input titer of HPgV ΔNS2 reduced astrocyte viability following infection

An obvious explanation for the absence of cell death observed following HPgV infection was that viral infection with a MOI of 0.1 was insufficient to cause cell death. To address this question, human astrocytes were infected with HPgV WT and ΔNS2 viruses at a MOI of 1.0 for 24, 48 and 96 hours. Cells were examined for viability using the Alamar Blue™ viability assay [Figure 4.6A, *p<0.05] and cell supernatants were examined for LDH activity, suggestive of lytic cell death [Figure 4.6B, *p<0.05, ****p<0.0001]. A high input titer of HPgV ΔNS2 significantly reduced cell viability compared to HPgV WT and uninfected cells at 48-hours post infection (84% compared to 92%, relative to uninfected cells) and significantly increased LDH activity to 116% (relative to uninfected cells), compared to HPgV WT infected cells (101%, relative to uninfected cells) and uninfected cells. Nonetheless, it is worth noting that even at high MOIs, the effect on cell viability was modest, suggesting that pathogenicity of these viruses in the clinical setting is unlikely to be driven solely by virus-induced cell death within the astrocyte population.

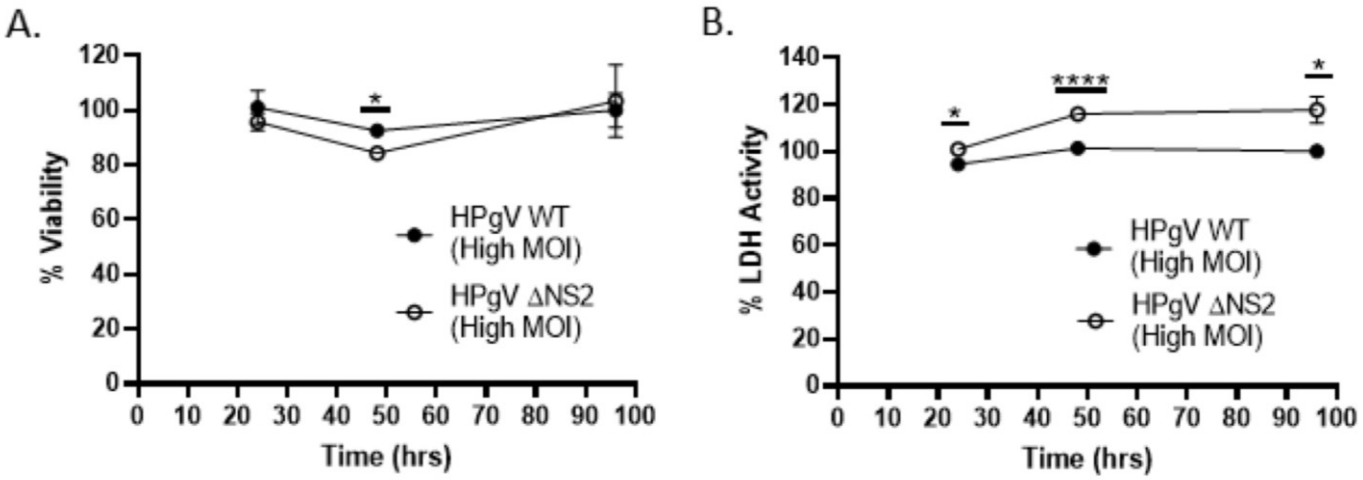

Figure 4.6: Increasing the input titer of HPgV ΔNS2 leads to a modest reduction of human astrocyte viability following infection.

Astrocytes were infected with HPgV WT or ΔNS2 (MOI=1) for 24, 48, 72 96 and 168 hours and cell viability was measured using Alamar Blue™ [A]. In a similar experiment as in [A], LDH activity was measured at each time-point post-infection [B]. For both [A,B] uninfected controls were set to 100% and n=6 technical replicates were used in each assay per condition. (* $p<0.05$, **** $p<0.0001$, Students T-test).

4.2.7 TNFα exposure after HPgV infection reduced cell viability following HPgV ΔNS2 infection

As HPgV infection alone was insufficient to reduce cell viability in human astrocytes, I initiated a 'double hit' model wherein human astrocytes were infected with HPgV WT and ΔNS2 for 48 and 96 hours, and the inflammatory cytokine, TNFα (200ng/mL), was added 12-hours post-infection in both conditions. Cells were then analyzed for viability by Alamar Blue™ from which it was apparent that while TNFα alone was not cytotoxic, TNFα exposure caused a significant decrease in astrocyte viability following HPgV ΔNS2 infection at both 48 (17% reduction compared to uninfected controls) and 96 hours (33% reduction compared to uninfected controls) post-infection when compared to all other conditions [Figure 4.7A, $*p<0.05$]. No change in LDH activity was measured in cell supernatants and therefore the loss in cell viability was likely not a result of lytic cell death following HPgV infection along with TNFα exposure [Figure 4.7B]. These data suggested that the dying cells observed in the combined TNFα + HPgV ΔNS2 conditions were undergoing a non-lytic form of cell death, such as apoptosis. These data supported the notion that a two-hit model of viral infection with inflammatory cytokine exposure might be sufficient to cause astrocyte cell death.

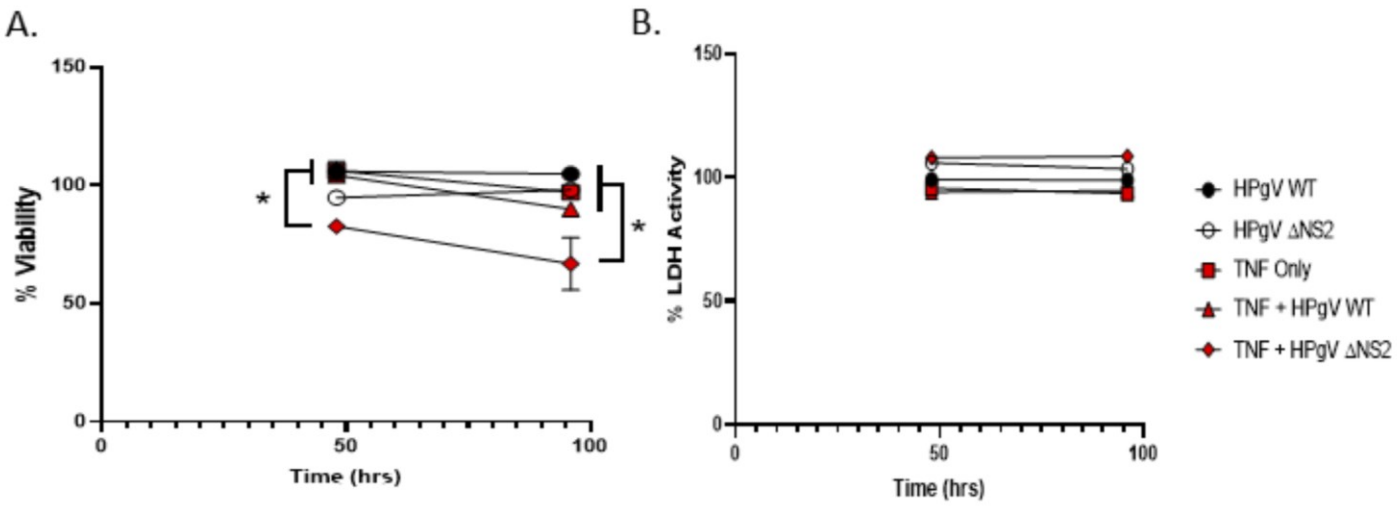

Figure 4.7: TNFα exposure after HPgV ΔNS2 infection causes reduced cell viability in human astrocytes.

Astrocytes were infected with HPgV WT or ΔNS2 (MOI=0.1) for 12 hours before media was changed and TNFα (200ng/mL) was added to HPgV infected or uninfected cultures. Cells were then harvested at 48 or 96 hours post infection and cell viability was analyzed using Alamar Blue™ [A]. Supernatants from above were measured for LDH activity [B]. For both [A,B] uninfected controls were set to 100% and n=6 technical replicates were used in each assay per condition. (* $p<0.05$, One-Way ANOVA of HPgV ΔNS2 relative to other conditions).

4.2.8 Antiviral and proinflammatory genes are differentially induced by HPgV WT and ΔNS2 viruses in human microglia.

To investigate transcriptional changes following HPgV infection, microglia were infected with HPgV WT or ΔNS2 for 2 days before cells were harvested for RNA and cDNA preparation. Pilot studies using qRT-PCR analyses showed that several genes associated with antiviral and proinflammatory responses were differentially affected by HPgV infection. Infection with HPgV ΔNS2 suppressed several genes when compared to HPgV WT and uninfected cells including *IFNB* [Figure 4.8A], *IRF3* [Figure 4.8B], *MAVS* [Figure 4.8C], and *CASP1* [Figure 4.8F]. Conversely, HPgV ΔNS2 significantly increased the transcription of *IL1B* [Figure 4.8D, ***$p<0.001$] in human microglia when compared to uninfected or HPgV WT cells, an observation that had not been observed in astrocytes. These transcript level changes in human microglia following HPgV infection represented potential differences in the host immune response to HPgV WT versus ΔNS2 infections.

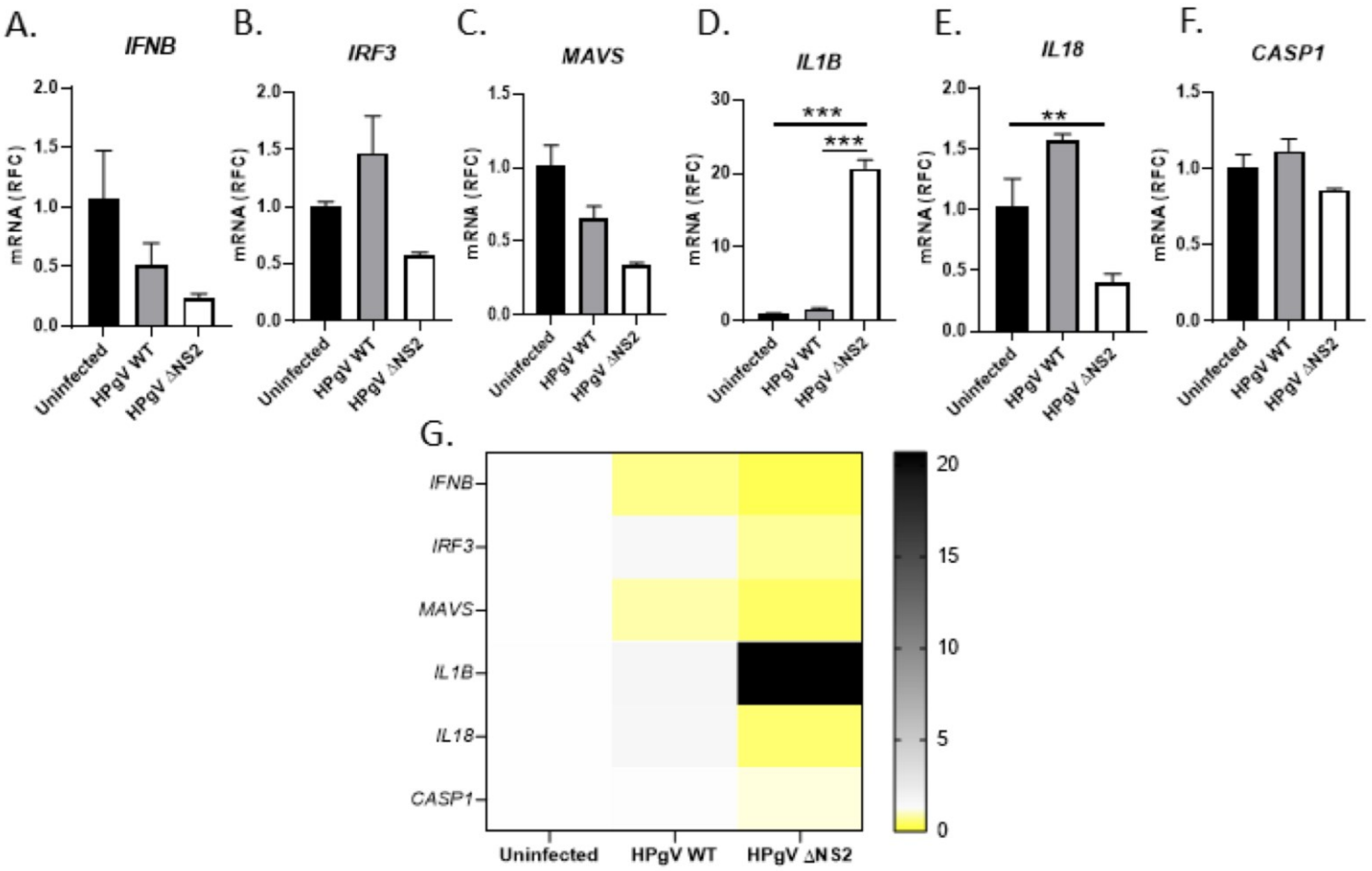

Figure 4.8: HPgV WT ΔNS2 infection causes differential transcript activation in human microglia.

Microglia were infected with HPgV WT or ΔNS2 (MOI=0.1) for 2 days before cells were harvested for RNA and cDNA libraries were prepared. qRT-PCR analysis of *IFNB* [A], *IRF3* [B], *MAVS* [C], *IL1B* [D], *IL18* [E], and *CASP1* [F], were completed and RFC ± SEM for each gene was compared to time-matched uninfected controls. A heat map [G] was generated to show the transcripts up-regulated (black) and down-regulated (yellow) following HPgV infection, compared to uninfected controls. n=2 technical replicates were used per condition. (* $p<0.05$, ** $p<0.01$, *** $p<0.001$, One-way ANOVA).

4.2.9 HPgV infection of human microglia does not cause cell lysis or cytokine release

As described in Chapter 3, human microglia are permissive to HPgV infection *in vitro* and thus, I wanted to characterize cellular changes following HPgV infection of microglia. LDH activity [Figure 4.9A] and supernatant IL-1β levels [Figure 4.9B] were measured in cell supernatants from human microglia following 24, 48, 72, 96 and 168 hours of infection with either HPgV WT or ΔNS2 infection. Both assays failed to show release of LDH or IL-1β in microglial supernatants, thus recapitulating the above findings in HPgV-infected human astrocytes [Figure 4.5B,C].

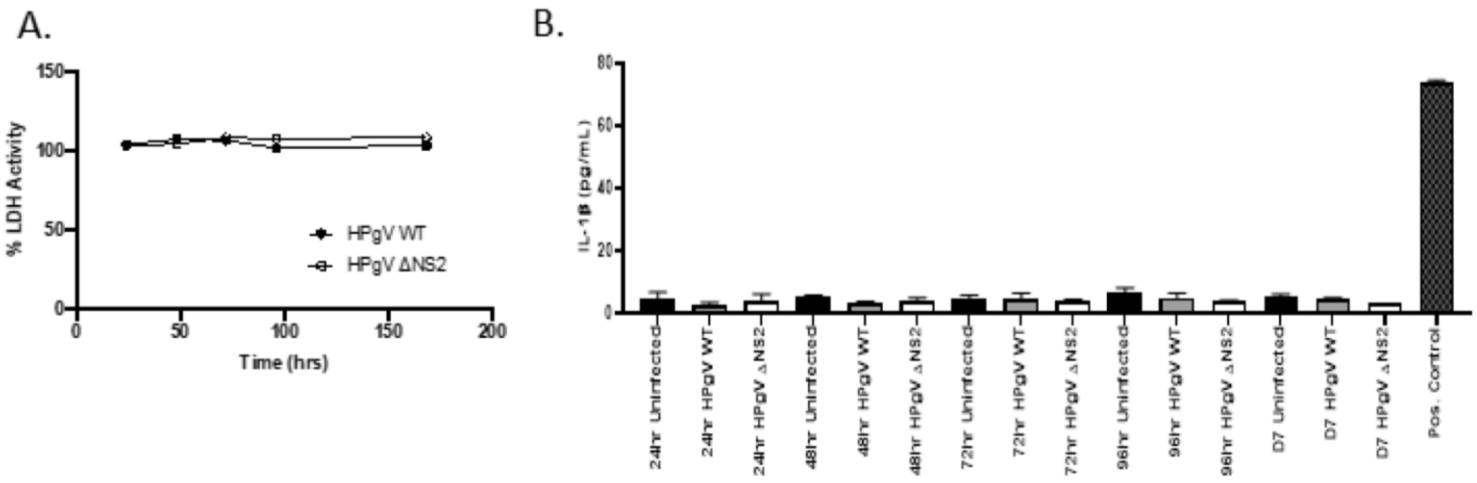

Figure 4.9: Human microglia show no LDH release or IL-1β release following HPgV infection.

[A] Microglia were infected with HPgV WT or ΔNS2 (MOI=0.1) and cell supernatants were measured for LDH activity at 24, 48, 72, 96 and 168 hours post infection and normalized to uninfected controls set at 100%. n=6 technical replicates were used per condition and repeated using two biological donors. [B] ELISA was performed on the cell supernatants from [A] to assess the presence of released IL-1β in supernatants of infected microglia. The positive control used for the IL-1β ELISA was human microglia exposed to 5μM of nigericin (a bacterial pore-forming toxin). n=2 technical replicates were used per condition and the experiment was repeated in two separate biological donors.

4.3 Summary

Within this chapter, I characterized host antiviral and proinflammatory transcript changes in human astrocytes following HPgV infection. Using two time points, there were only modest alterations in the host responses to HPgV infection of human astrocytes for both viruses. The addition of poly(I:C) showed that astrocytes could mount robust antiviral and proinflammatory responses, and that HPgV accentuated these responses, rather than inhibiting them. A different finding was evident in human microglia, as HPgV ΔNS2 infection induced significantly different antiviral and proinflammatory responses compared with that of HPgV WT after 2 days of HPgV infection.

My observation of a small population of infected astrocytes that displayed a morphological phenotype suggestive of apoptosis, including nuclear disruption and rounding of astrocytes[52], prompted me to examine several aspects of cell death, beginning with caspase activation in HPgV infected cells. Although a modest induction of caspase-8 was seen following HPgV ΔNS2 compared to HPgV WT infection, the discrepancy between both viruses initially suggested that an apoptotic mechanism might be initiated activated by HPgV ΔNS2 infection. However, follow-up studies revealed no detectable changes in overall astrocyte viability following infection with either virus, suggesting that apoptosis as a result of viral infection may be an extremely rare event. Additional analysis of LDH activity, IL-1β release and cell viability all verified that HPgV infections did not induce proinflammatory

cytokines nor reduce cell viability. The same absence of inflammatory cytokine release and loss in cell viability was observed in HPgV-infected human microglia. When a higher input titer of HPgV was used to infect astrocytes, HPgV ΔNS2 appeared to reduce cell viability and increase LDH activity, with significant differences observed compared to HPgV WT infected cells. In an attempt to mimic an inflammatory model of encephalitis, TNFα was applied to HPgV infected astrocyte cultures following infection, wherein HPgV ΔNS2 reduced cell viability in a proinflammatory environment. By using several techniques, I have provided evidence that HPgV infection with HPgV WT or ΔNS2 alone did not induce cell death in astrocyte or microglial cultures unless another inflammatory stimulus was present.

Chapter V: *In Vivo* HPgV Infection of the CNS

5.1 Introduction

Chapter V Objective: *Examine HPgV neural cell tropism and associated immune responses in brain tissues from patients with detectable HPgV.*

Although several groups have identified HPgV within the CNS by qPCR detection of viral RNA[1,137,139,140], the detection of HPgV antigen within the CNS has only been reported once previously, in the case report by our group[1]. This latter study identified HPgV NS5A antigen in multiple glial cell types (most prominently oligodendrocytes and astrocytes) as well as infiltrating CD3+ T cells[1]. These observations prompted the experiments detailed within the previous chapters of my thesis, wherein I developed and characterized an *in* vitro model of HPgV infection in primary human astrocytes. In this chapter, I sought to expand upon the results of our original clinical case study, through a quantitative characterization of the two HPgV encephalitis index cases along with newly identified HPgV+ neurologically normal cases. As there had been no previous studies investigating the host immune responses to HPgV infection in the CNS, I utilized ddPCR to quantify HPgV copies within the CNS and explored host immune responses to HPgV infection of the CNS.

Chapter V Hypothesis: *HPgV infection in the CNS alters antiviral and immune-related gene expression.*

Within this chapter I have developed and optimized ddPCR as a technique to detect HPgV positive and negative strand copies in human brain tissues. I have provided evidence that active HPgV replication was evident in the CNS and that, except for the LE-1 HPgV index case with an extremely high viral load, these patients generally have suppressed proinflammatory and antiviral immune responses in the CNS. Using RNA-seq, several host immune pathways were identified that were suppressed in the CNS of individuals with low-levels of HPgV infection. In the HPgV encephalitis index cases (LE-1 and LE-2), I also found widespread HPgV infection of GFAP+ astrocytes, which recapitulates our findings in Chapter III regarding viral spread in human astrocyte cultures.

5.2 Results

5.2.1 HPgV viral load can be quantified using ddPCR of patient cortex samples

As shown in Chapter 3, ddPCR can be used to accurately quantify viral RNA copy number within human samples and has been used previously for these purposes[65,162]. In Chapter 3, I demonstrated that this technique could be effectively used to quantify viral copy number in cell lysates and culture supernatants. To establish ddPCR as a quantitative method to determine HPgV viral load in clinical human CNS cortical samples, I first needed to optimize the methodologies using positive and negative controls from our group's previous case report[1]. Using several annealing temperatures, the number of positive HPgV *NS3* copies was detected in tissue from our index case (positive control/LE-1) [Figure 5.1 A-C]. At lower temperatures (52°C and 50°C), our negative control did have some amplification of non-specific product as seen by the presence of droplets at these temperatures. However, this phenomenon was not observed at higher temperatures, suggesting higher temperatures were required for optimizing assay specificity. By converting the number of identified droplets/copies detected per reaction (20μL) I could identify the original number of copies found in 1μg of RNA, which in this run was 5880 HPgV *NS3* copies/μg of RNA in our positive control at the 60°C annealing temperature [Figure 5.1C].

A.

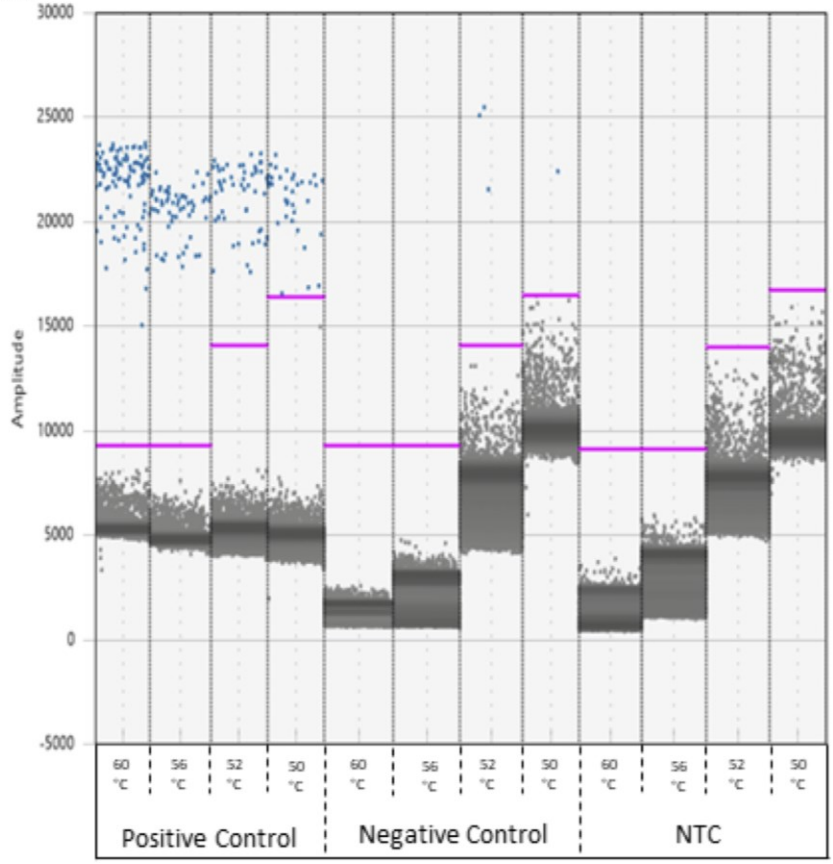

B.

Temp.	Copies / 20 µL Reaction		
	Positive Control	Negative Control	NTC
60°C	196	N.D.	N.D.
56°C	98	N.D.	N.D.
52°C	96	5	N.D.
50°C	67	2	N.D.

C.

Temp.	Copies / µg RNA (tissue)		
	Positive Control	Negative Control	NTC
60°C	5880	N.D.	N.D.
56°C	2952	N.D.	N.D.
52°C	2871	144	N.D.
50°C	2019	53	N.D.

Figure 5.1: Optimizing droplet digital PCR (ddPCR) HPgV detection in human clinical samples.

Using a positive and negative control sample from our initial case report[1], droplet digital PCR (ddPCR) analysis was completed on prepared cDNA at several different annealing temperatures (60°C, 56°C, 52°C, 50°C) to optimize sample amplification for HPgV *NS3* [A]. The threshold of detection for each sample was held consistent at each annealing temperature and the number of detected PCR copies was detected per sample [B]. These copy numbers were normalized to 1µg of RNA isolated from tissue [C] to determine HPgV+ copies present.

5.2.2 Both positive and negative strand HPgV sequences were detected in all HPgV+ patients

ddPCR analysis was used as a tool to identify the presence of HPgV in post-mortem cortex samples from several individuals. For the purposes of this thesis, 45 human brain samples were screened for HPgV RNA detection and seven individuals were identified as being HPgV-positive (HPgV+) [Table 5.1]. There were an additional six patients with detectable HPgV RNA, although these patients were excluded from our analysis because of HIV-1 co-infection. Nonetheless, six age- and sex-matched controls (HPgV-) were selected and the first neuroHPgV cohort was established and used for host immune response investigations, along with HPgV LE-1 and LE-2 from our initial case study for comparative purposes. Within this cohort outlined in Table 5.1, there are HPgV-infected (+) patients (n=7) and age- and sex-matched HPgV uninfected (-) other-disease controls (ODC) (n=6), along with data from our index cases, LE-1 and LE-2, that were described in our previous study[1].

Table 5.1: Clinical and demographic features of HPgV+ and HPgV- (ODC) patients.

	CNS HPgV- (ODC) (n=6)	**CNS HPgV+ (n=7)**	**CNS HPgV+ LE (n=2)**
Age	49.5 (±6.2)	48 (±10.9)	56 (±7.1)
Sex	5M / 1F	6M / 1F	2F
NS2 Deletion	N/A	0	2

The number of HPgV copies (*NS3* gene) present in cortical samples from each patient was quantified per microgram of RNA used per reaction [Figure 5.2A]. Similarly, I was interested in detecting negative strand RNA within the tissue, which suggests active viral replication due to the RNA dependent RNA polymerase. Again utilizing ddPCR, HPgV [-]*E2* was detected in each of our six HPgV+ patients, along with both of our index cases, verifying previous results[1] [Figure 5.2B]. Within the HPgV+ patients, the number of negative strand HPgV copies varied, with some individuals having as little as 15.36 copies per microgram of RNA. For the majority of patients, the number of positive strand copies correlated with an increased number of negative strand copies [Figure 5.2C].

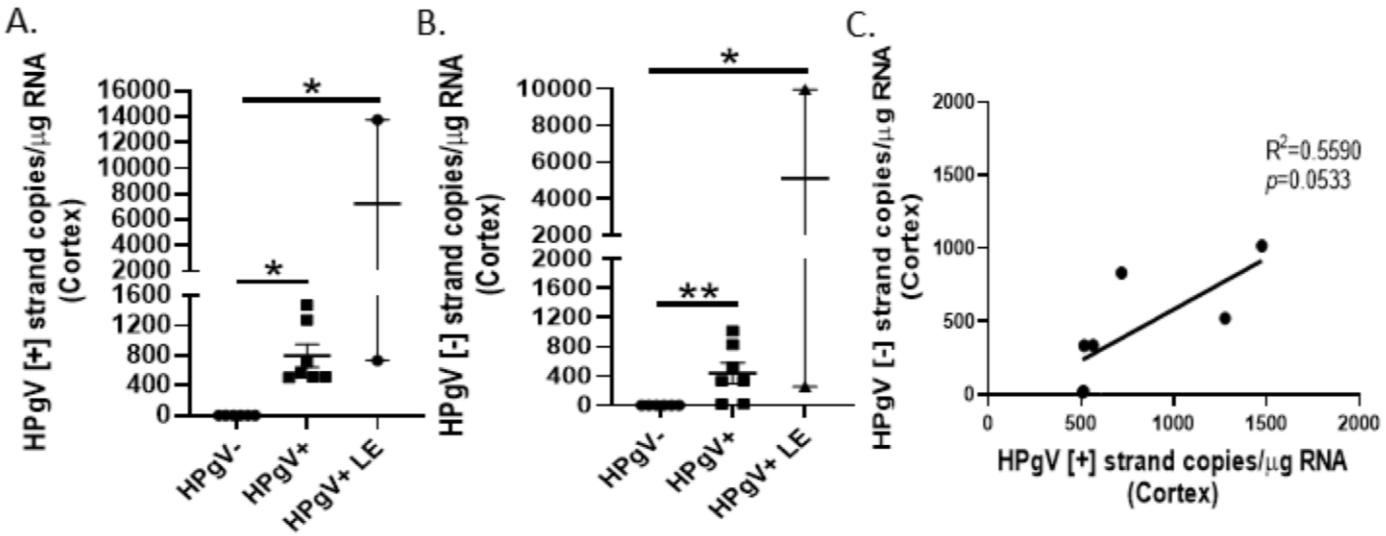

Figure 5.2: In human cortex samples, HPgV+ patients had detectable positive and negative strand RNA.

Using ddPCR analysis, HPgV [+]*NS3* copies were detected in HPgV+ (n=7) and HPgV+ LE (n=2) cortex samples but not in HPgV- (n=6) cortex samples [A]. Similarly HPgV [-]*E2* copies were detected in the same samples as above in HPgV+ (n=7) and HPgV+ LE (n=2) groups, and was not detected in HPgV- (n=6) samples [B]. Using data from the HPgV+ group only from [A] and [B], linear regression analysis was performed comparing the number of HPgV [+] and [-] strand copies per patient [C]. The R^2 value is included for reference. (* $p<0.05$, ** $p<0.01$, One-way ANOVA).

5.2.3 *In vivo* HPgV NS5A antigen is abundant in human astrocytes

Based on our initial case study[1], I was interested in quantifying both the frequency of HPgV+ astrocytes in the affected brain regions of our two HPgV encephalitis index cases and the relative intracellular levels of HPgV antigen in those infected astrocytes. The mean fluorescence intensity of HPgV NS5A antigen was quantified per cell in both of our original case report patients[1], along with a negative control patient [Figure 5.3A-C]. The intracellular MFI of HPgV NS5A for each GFAP+ cell was quantified using representative images from the affected brain regions in both patients. These analyses demonstrated a significantly higher mean HPgV NS5A MFI detected in LE-1 and LE-2 compared to a HPgV- control patient [Figure 5.3D, ****p<0.0001]. There was also a significantly higher mean HPgV NS5A MFI in LE-1 compared to LE-2, indicative of more abundant HPgV NS5A antigen present in each infected cell.

To determine the frequency of HPgV+ astrocytes, the number of GFAP+ astrocytes that were immunopositive for HPgV NS5A antigen were counted per patient using representative images from the affected brain regions. In a similar trend to Figure 5.3D, patient LE-1 had a significantly higher number of HPgV infected astrocytes (88%) compared to both patient LE-2 (66%) and the HPgV- control [Figure 5.3E, ***p<0.001, ****p<0.0001].

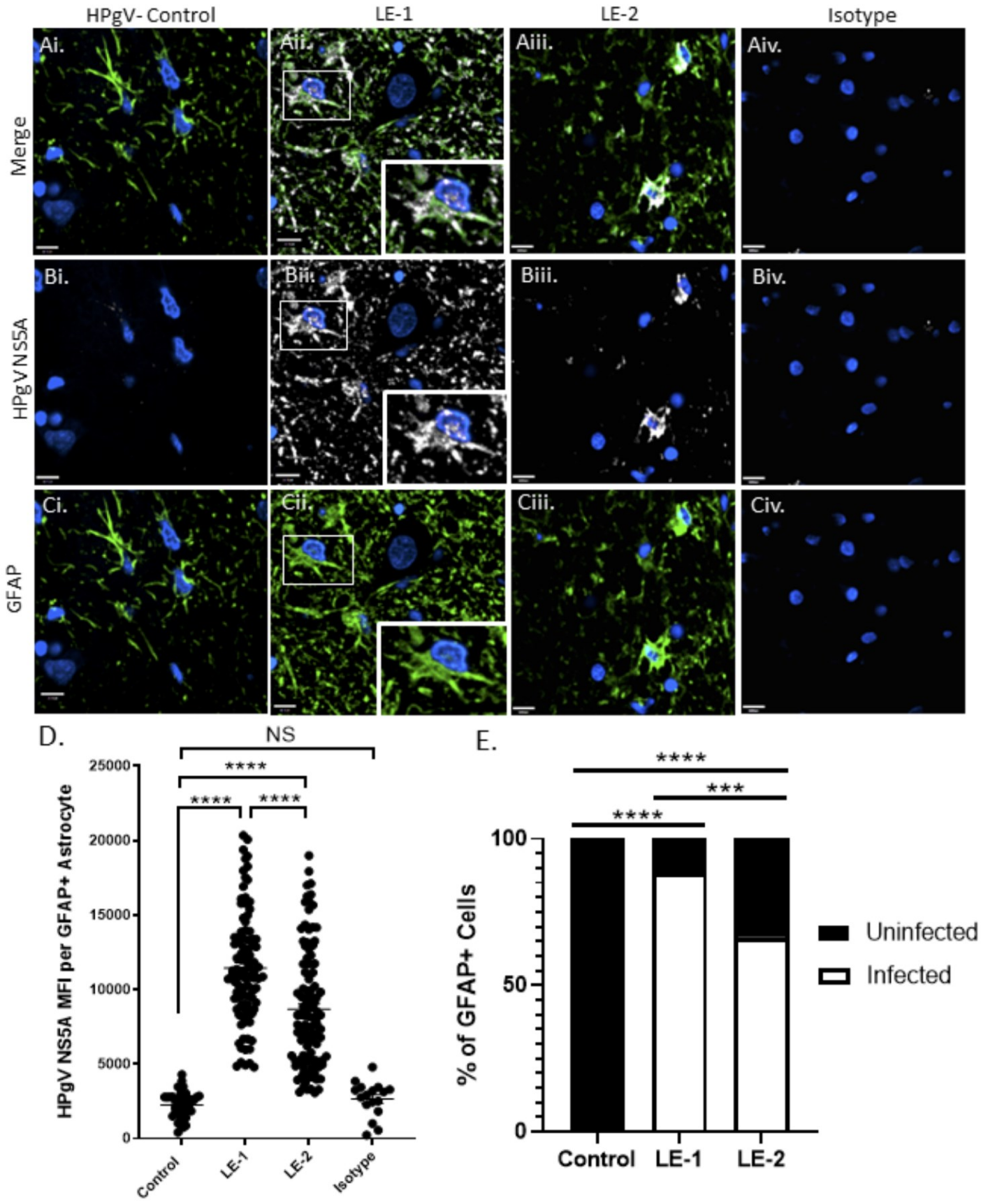
HPgV- Control
LE-1
LE-2
Isotype
Merge
HPgV NS5A
GFAP
Ai.
Aii.
Aiii.
Aiv.
Bi.
Bii.
Biii.
Biv.
Ci.
Cii.
Ciii.
Civ.
D.
NS
****
****
****
HPgV NS5A MFI per GFAP+ Astrocyte
25000
20000
15000
10000
5000
0
Control
LE-1
LE-2
Isotype
E.
****
***
****
100
50
0
% of GFAP+ Cells
Control
LE-1
LE-2
Uninfected
Infected

Figure 5.3: HPgV infection of human astrocytes is abundant in both of our index cases.

[Ai-Civ] Human patient tissue slides from our two index cases, LE-1 and LE-2, along with a HPgV- control patient were immunolabeled for HPgV NS5A (white) and GFAP (green) and labeled with DAPI (blue) and imaged using confocal microscopy. Intracellular MFI of HPgV NS5A was quantified per cell for at least n=40 cells per patient [D]. An isotype control with secondary only is provided to show tissue autofluorescence levels. (**** $p<0.0001$, One-way ANOVA). [E] The proportion of HPgV NS5A immunopositive astrocytes was also quantified per patient using representative images. To calculate the number of HPgV-positive astrocytes, n=18 FOVs were used for patient LE-1, n=10 FOVs were used for patient LE-2, and n=11 FOVs were used for the negative control. (*** $p<0.001$, **** $p<0.0001$, Fisher's exact Test).

5.2.4 HPgV infection of the CNS alters host immune responses

Next, I wanted to examine the full cohort of ODCs and HPgV+ patients to see if immune response data was similar to what was observed *in vitro* in Chapter IV. In general there was an overall suppression in transcription of several proinflammatory genes in HPgV+ patients [Figure 5.4A-F, * $p<0.05$, ** $p<0.01$, *** $p<0.001$, **** $p<0.0001$] with significant reductions in *IRF3*, *DDX58*, and *IL1B*. When displayed as a heat map, it was apparent that the HPgV+ patients' samples showed an overall suppression in inflammatory gene transcripts compared to uninfected ODC patients [Figure 5.4G]. In addition, the two index cases were also assessed (LE-1 and LE-2)[1], wherein it appears that viral load (red) is associated with the immune response differences observed in LE-1 versus the other patients. Each of the HPgV+ patients and LE-2 shared a similar transcriptional profile and were in the same range of HPgV viral load in the CNS (507-1473 copies/μg of RNA). This is in comparison to patient LE-1, who had a greater abundance of HPgV RNA present in the CNS (13770 copies/μg RNA) and showed a much different transcriptional profile than the other patients [Figure 5.4G].

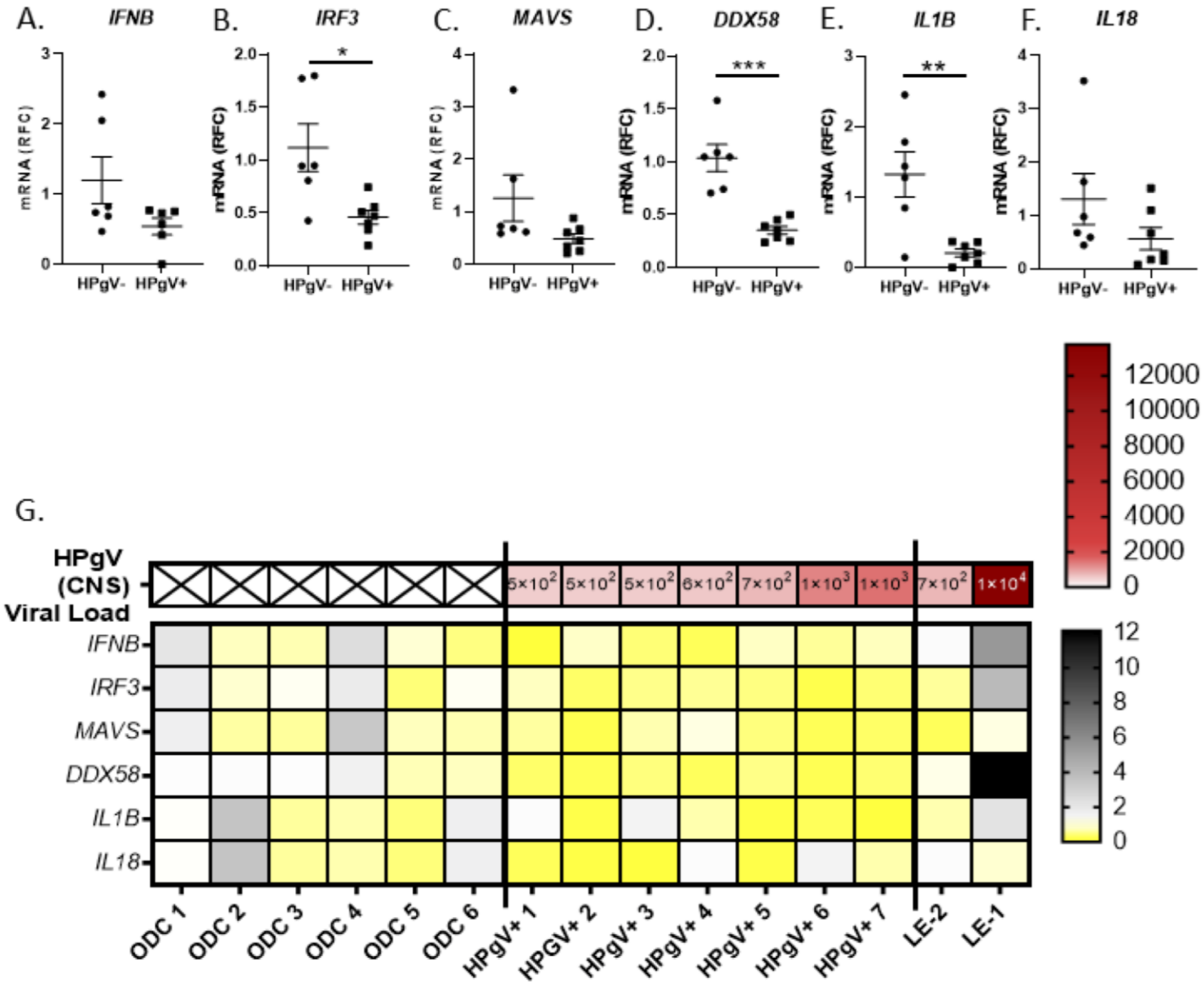

Figure 5.4: Several proinflammatory and antiviral transcripts are suppressed in the cortex of individuals with HPgV compared to uninfected controls.

Post-mortem cortex samples were collected from HPgV- (n=6) and HPgV+ (n=7) individuals and harvested for RNA and cDNA libraries. qRT-PCR analysis of *IFNB* [A], *IRF3* [B], *MAVS* [C], *DDX58* [D], *IL1B* [E], and *IL18* [F] were completed and relative fold change (RFC) ± SEM for HPgV+ individuals is shown compared to HPgV- controls. A heat map [G] was generated to show the transcripts up-regulated (black) and down-regulated (yellow) in HPgV+ individuals, compared to HPgV- controls. Transcript changes from HPgV LE-1 and LE-2 (n=2) from Table 5.1 were also included and the HPgV viral load associated with each patient shown at the top of the heat map (HPgV copies/µg RNA) (red). (* $p<0.05$, ** $p<0.01$, *** $p<0.001$, **** $p<0.0001$, Students T-Test).

5.2.5 RNA-Seq of human cortical tissue from HPgV-infected patients discloses a unique neuroinflammatory response profile

Using a subset of ODC (n=2) and HPgV+ (n=3) patients, RNA deep sequencing (RNA-seq) was performed on human cortex samples to examine transcript changes in HPgV-infected individuals in a broad unbiased manner. The genes with the largest positive and negative fold changes [Figure 5.5] were identified and Ingenuity™ analysis was performed on these genes.

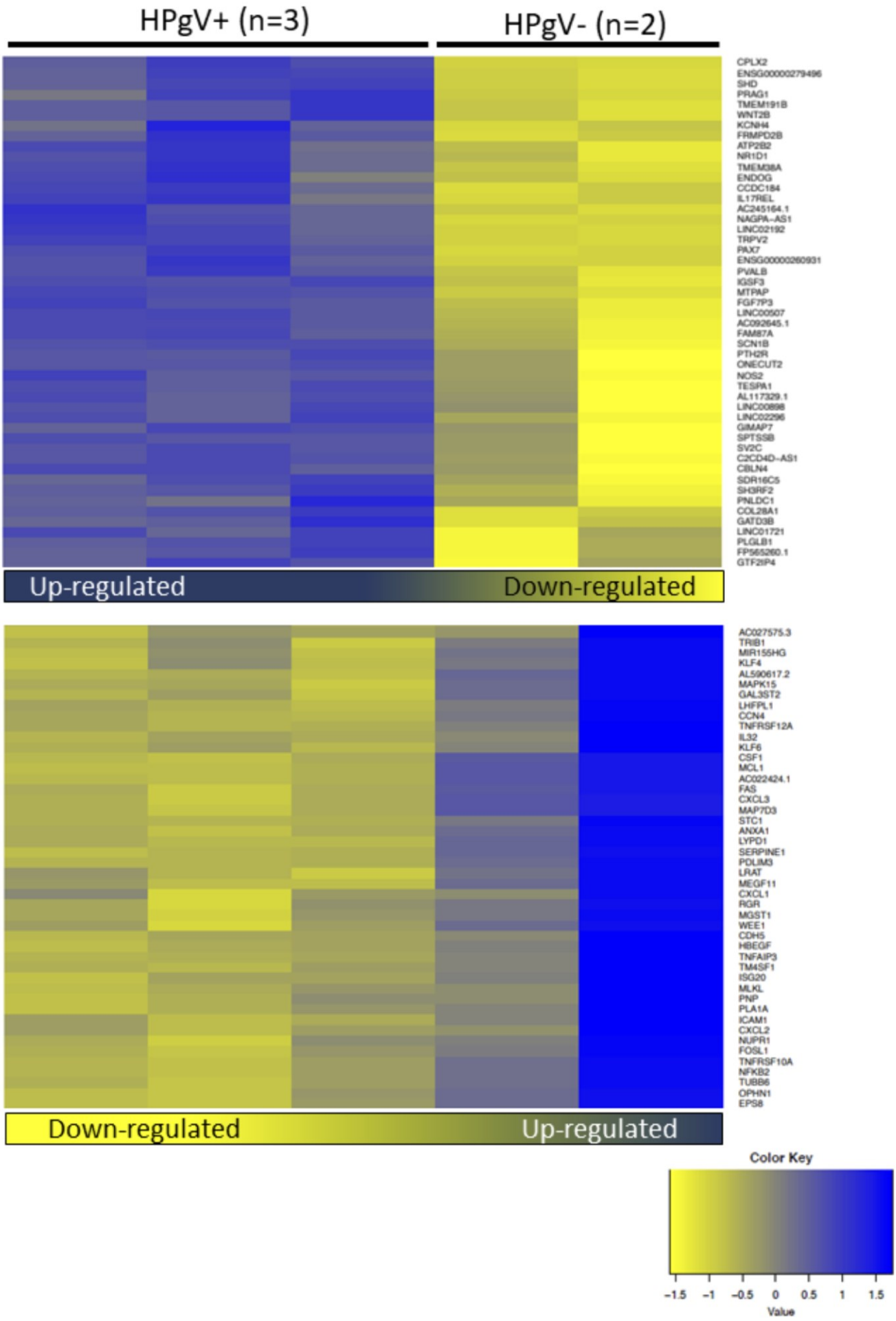
HPgV+ (n=3)
HPgV- (n=2)
CPLX2
ENSG00000279496
SHD
PRAG1
TMEM191B
WNT2B
KCNH4
FRMPD2B
ATP2B2
NR1D1
TMEM38A
ENDOG
CCDC184
IL17REL
AC245164.1
NAGPA-AS1
LINC02192
TRPV2
PAX7
ENSG00000260931
PVALB
IGSF3
MTPAP
FGF7P3
LINC00507
AC092645.1
FAM87A
SCN1B
PTH2R
ONECUT2
NOS2
TESPA1
AL117329.1
LINC00898
LINC02296
GIMAP7
SPTSSB
SV2C
C2CD4D-AS1
CBLN4
SDR16C5
SH3RF2
PNLDC1
COL28A1
GATD3B
LINC01721
PLGLB1
FP565260.1
GTF2IP4
Up-regulated
Down-regulated
AC027575.3
TRIB1
MIR155HG
KLF4
AL590617.2
MAPK15
GAL3ST2
LHFPL1
CCN4
TNFRSF12A
IL32
KLF6
CSF1
MCL1
AC022424.1
FAS
CXCL3
MAP7D3
STC1
ANXA1
LYPD1
SERPINE1
PDLIM3
LRAT
MEGF11
CXCL1
RGR
MGST1
WEE1
CDH5
HBEGF
TNFAIP3
TM4SF1
ISG20
MLKL
PNP
PLA1A
ICAM1
CXCL2
NUPR1
FOSL1
TNFRSF10A
NFKB2
TUBB6
OPHN1
EPS8
Down-regulated
Up-regulated
Color Key
−1.5
−1
−0.5
0
0.5
1
1.5
Value

Figure 5.5: Transcriptional analysis of HPgV-positive and uninfected patients identified numerous differences in gene expression.

RNA deep sequencing (RNA-Seq) was completed on a subset of HPgV- (n=2) and HPgV+ (n=3) patients from Table 5.1. Numerous transcripts were identified that were significantly up-regulated (blue) and down-regulated (yellow) in HPgV-positive patients compared to uninfected patients.

Subsequent analysis was performed to classify the differentially expressed genes identified above in Figure 5.5 into several different signaling pathways. This analysis revealed that certain genes associated with neuroinflammation were amongst the up-regulated transcripts. [Figure 5.6].

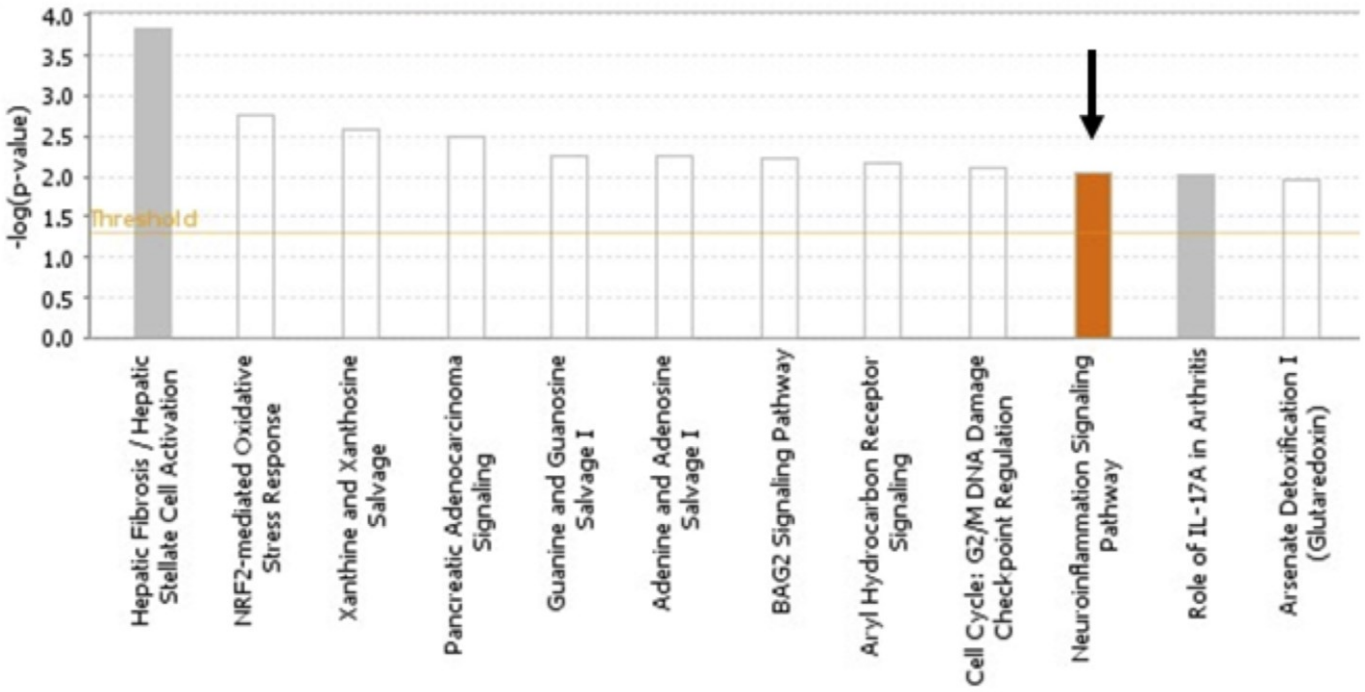

Figure 5.6: RNA-Seq pathway analysis identifies an association between HPgV infection and neuroinflammatory signaling.

RNA deep sequencing (RNA-Seq) was completed on a subset of HPgV- (n=2) and HPgV+ (n=3) patients from Table 5.1. Ingenuity™ analysis identified several pathways that contained genes significantly different between HPgV-positive and HPgV-negative patients. Positive associations are represented in orange and the arrow (black) indicates the pathway of interest.

Although a subset of upregulated transcripts were classified as belonging to the "neuroinflammation signaling pathway" [Figure 5.6], further analysis also revealed somewhat paradoxically that an array of specific genes related to the proinflammatory NF-κB transcription factor family were significantly reduced (red) in HPgV+ individuals [Figure 5.7]. However, significant induction (green) of *NOS2* was observed [Figure 5.7]. This particular isoform of NOS is inducible in human astrocytes and microglia following immune activation and under normal circumstances, acting as an enzyme to produce nitric oxide (NO)[35]. The induction of iNOS in the CNS following viral infection has been shown previously during HIV-1 infection and seems to be involved in virus-induced cytotoxicity rather than viral clearance in this context[35].

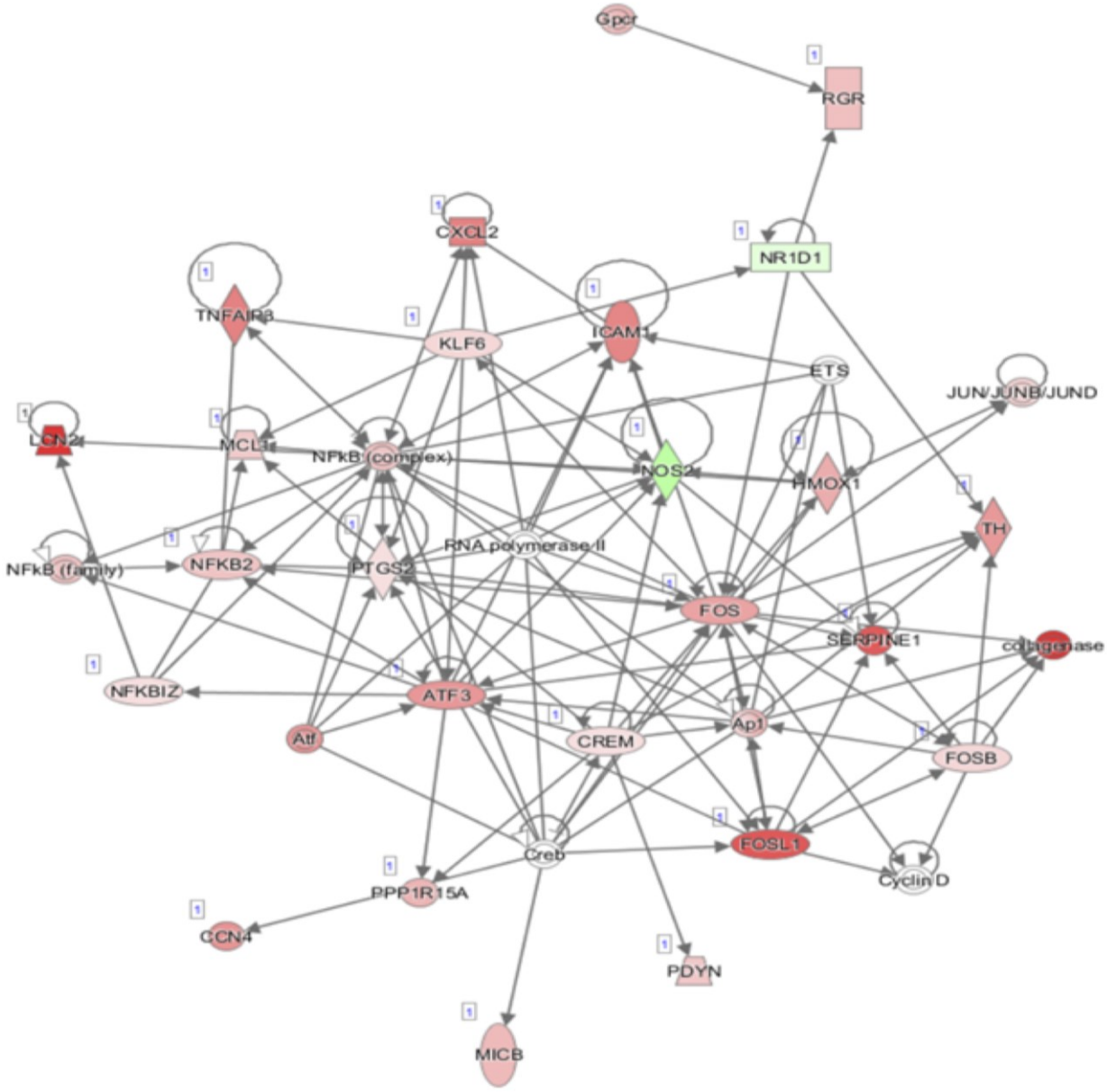

Figure 5.7: Proinflammatory transcripts are differentially affected in HPgV-positive individuals.

RNA deep sequencing (RNA-Seq) was performed on a subset of HPgV- (n=2) and HPgV+ (n=3) patients from Table 5.1. Ingenuity™ analysis identified numerous genes with significantly reduced transcripts (red) including members of the NF-κB family along with several cytokines and adhesion molecules. Meanwhile an induction of certain genes (green) was identified, including a significant upregulation of *NOS2*.

5.3 Summary

Within this chapter I have illustrated important parallels between our *in vitro* astrocyte infection model (Chapters III and IV) and the clinical data contained herein. I have shown that HPgV does indeed infect upwards of 88% of human astrocytes in the affected brain region of LE-1 using immunodetection of the HPgV NS5A antigen in GFAP+ astrocytes. A significant difference was seen between LE-1 and LE-2 in terms of fluorescence intensity of intracellular HPgV NS5A antigen and in the proportion of HPgV NS5A immunopositive astrocytes per FOV. These data recapitulate the ddPCR data, which had indicated that LE-1 had a higher HPgV viral load than LE-2.

After identifying a new cohort of HPgV+ individuals (n=7) we were able to ask additional questions about infected patients who, to our knowledge, did not have any neurological manifestations of infection (e.g. encephalitis). Within these new patients, an overall suppression in the transcription of several prominent antiviral and proinflammatory transcripts were observed. Using a subset of these patients for RNA-sequencing and subsequent Ingenuity™ analysis, several genes associated with neuroinflammatory signaling were up-regulated. *NOS2* was identified as a gene that was up-regulated in the CNS of HPgV-positive individuals. Nonetheless, many other antiviral pathways, including members of the NF-κB family, were shown to be suppressed with HPgV infection, recapitulating both the qRT-PCR data and the *in vitro* data from Chapter IV that indicated a suppression of proinflammatory

signaling following viral infection. Taken together, these data illustrate that HPgV has a very specific neuroimmune response, which requires further investigation to be elucidated.

Chapter VI: Discussion

6.1 Overall Summary

In this thesis I have provided evidence for HPgV infection and replication in human astrocytes and microglia, investigated how an 87-nucleotide deletion in the *NS2* gene impacts viral tropism, characterized the host responses following HPgV infection in human astrocytes and microglia, and elucidated the host responses to HPgV infection in human brain tissue.

Prior to this thesis, our group was the first to detect HPgV antigen in the brain associated with fatal encephalitis in two index cases and the first to confirm active viral replication by detecting negative strand HPgV RNA within brain tissue[1]. Further, we identified a novel 87-nucleotide deletion within the *NS2* gene in both encephalitis cases. Although a pivotal series of observations, this report left several unanswered questions including: (i) could HPgV successfully infect and replicate productively in human glial cells *in vitro* and what was the cellular response profile following infection? (ii) how did the *NS2* deletion affect parameters such as viral replication and spread and would this deletion also affect host antiviral responses? (iii) could HPgV RNA and antigen be detected in the brains of neurologically normal patients and if so, what differentiated these patients from those with fatal HPgV-associated encephalitis?

The overarching purpose of this thesis was to address these questions using a two-pronged approach that involved first creating an *in vitro* model of HPgV infection that could be utilized to characterize both HPgV WT and ΔNS2 viruses in human glial cells (Chapter III and IV), and second, building a neuroHPgV cohort of patients with HPgV infection in the CNS, permitting analyses of viral burden and associated host responses following HPgV infection (Chapter V).

Using these two platforms, I was able to provide several novel insights regarding the nature of HPgV infection in the CNS. First, in my model of HPgV infection *in vitro*, I confirmed HPgV tropism in human astrocytes and identified a new cell type (i.e. microglia) that was permissive to HPgV infection and replication. I also determined that the NS2 deletion exerted a significant effect on parameters such as viral replication and spread. This suggested that the mutation was advantageous in terms of viral fitness and provided the first evidence for functional differences between the two viruses.

While the differences in viral replication were clear, the effect of the ΔNS2 deletion on host responses was less obvious, as both HPgV WT and ΔNS2 viruses failed to elicit conventional antiviral responses such as activation of the interferon pathway. Similarly, a trend towards the suppression of inflammatory signaling pathways, including *IFNB* gene expression, was observed for following infection of human astrocytes with both HPgV WT and ΔNS2 viruses. Nonetheless, in the context of a

'second-hit', differential host immune responses in human astrocytes emerged between the two viruses at the transcript level (e.g. *IFNB*).

To advance the clinical understanding of the virus, I also assembled an HPgV cohort consisting of seven neurologically normal HPgV+ patients with matched uninfected controls, in addition to the two HPgV encephalitis index cases (LE-1 and LE-2). This cohort represented the first neuroHPgV cohort to be described in the literature and will be essential in further characterization of the virus. Verifying my *in vitro* observations, I observed suppression of antiviral and proinflammatory signaling at the transcript levels in neurologically normal HPgV+ samples both by qRT-PCR and RNA-seq. Interestingly, RNA-seq also identified a subset of neuroinflammatory genes that were up-regulated during non-encephalitic infection including *NOS2*, a gene that encodes an inducible enzyme (iNOS) important in the production of NO under stress. Depending on the context, iNOS may propagate inflammation or may serve as a central signaling hub to down-regulate antiviral signaling[163]. Thus, my observation that *NOS2* was induced during HPgV infection *in vivo* positions iNOS as a potential target for future investigation and highlights the concordance between my clinical and *in vitro* model systems.

6.2 Discussion of Objective 1

Objective 1:

Establish an in vitro model of human pegivirus infection in human glial cells and define the impact of the previously recognized HPgV NS2 deletion on viral infection.

Within this objective, I created and optimized the first *in vitro* HPgV model of infection in human fetal astrocyte cells using a HPgV viral clone to establish viral cultures [Figure 3.1-3.2]. Establishing a model to detect HPgV infection, replication and spread within human astrocyte cultures was imperative because of the lack of *in vitro* or *ex vivo* models to study HPgV infection and replication in CNS cell types. Prior to my studies, HPgV had only been shown to replicate in B and T lymphocytes, the spleen and the bone marrow[121]. Not only did I discover that HPgV could replicate in human astrocytes [Figure 3.2, 3.6A, 3.7], but I also identified that microglia were permissive to HPgV infection and supported viral replication [Figure 3.6B, 3.7] by measuring HPgV RNA levels in cell supernatants and lysates using ddPCR quantitation. The identification of primary human microglia as permissive to HPgV infection is a novel set of observations, although the literature suggests this is not surprising. A previous study found that THP-1 cells, a monocytic cell line that once differentiated become macrophage-like cells[164], were permissive to HPgV infection and transfection, and subsequent infectious HPgV was released[165]. This suggested that macrophage-like cells were susceptible to HPgV infection, although

my studies represent the first evidence that primary human microglia are permissive to HPgV and can support HPgV replication. Compared to human astrocytes, HPgV infection in microglia had a faster growth phase, with peak virus production detected in the supernatant at 2 days post infection [Figure 3.6B], compared to 7 days in human astrocytes [Figure 3.6A]. Human microglia are less permissive to HPgV, as evidenced by the relatively low abundance of virus found in the cell lysates and cell supernatants compared with HPgV infection of human astrocytes at matched time points [Figure 3.6, 3.7].

ddPCR analyses has previously been used for quantification of viral RNA including HIV-1 and influenza[65,166]. A similar technique, named real-time digital PCR (RT-dPCR) uses a microfluidic chip to separate nucleic acid molecules during PCR reactions, thus allowing individual molecules to be counted[165]. Earlier studies have utilized this approach to detect HPgV in the supernatants of several cell types, including PBMC's, Jurkat cells (a T cell line) and THP-1 cells (a monocytic cell line)[165]. Although similar, ddPCR is more sensitive than RT-dPCR because ddPCR can measure over 20,000 droplets per sample, compared to 770 reactions per sample in RT-dPCR, thus providing higher sensitivity to each reaction[165,167]. This makes it possible to detect low abundance transcripts, such as viruses within the human CNS, with a high degree of accuracy. For example, one study comparing detection methods of Hepatitis B Virus (HBV) found that qPCR required at least 50 nanograms (ng) of HBV DNA present in the sample for accurate detection,

meanwhile as little as 1ng of template DNA was needed when using ddPCR for accurate detection[168].

The characterization of an 87-nucleotide deletion in the *NS2* gene of HPgV that was identified in our original report[1] was another area I wanted to investigate. Since this deletion had only been observed from HPgV sequences isolated from the brain, it suggested that this mutation might confer neurotropism of the virus. For this reason, I constructed the HPgV ΔNS2 [Figure 3.4B]. I demonstrated that although the ΔNS2 virus had enhanced viral replication in glial cells, the WT virus could still sustain a robust infection in astrocytes [Figure 3.6A, 3.7]. This observation was important because of the outstanding question from our original report of whether the NS2 deletion was necessary for viral replication in human CNS cells. The results shown in Chapter III support the hypothesis that while the NS2 deletion may confer enhanced viral tropism of astrocytes, WT virus can still infect and replicate in CNS cell types and thus the mutation is not strictly required for glial cell tropism.

The HPgV NS2 protein is believed to function as a viral NS2-NS3 autoprotease, similar to its role in HCV[106]. Although little amino acid homology exists between the two viruses, two residues are common within the NS2 domain (His952 and Cys993)[169]. Other than amino acid sequence identity, little is known about how the NS2 protein functions during HPgV infection. If the protein functions in a similar manner to HCV's NS2 then we can might be able to determine how the 87 nucleotide

deletion in the *NS2* gene alters HPgV infectivity and replication, as seen in Chapter III, at a more mechanistic level in the future. The deletion that we observed is closer to the N-terminus of the NS2 protein, but it may still affect the viral protease's activity by altering the binding region of the protease and thus affecting the affinity of the protease for new or pre-existing substrates. Additionally, the NS2-NS3 cleavage during the HCV life cycle is also necessary for genome replication wherein the NS2 contributes in viral particle morphogenesis and hyperphosphorylation of the NS5A protein, which is required for efficient viral replication[170,171]. If a similar process occurs during the HPgV life cycle, the mutations detected in our studies in the HPgV *NS2* and *NS5A* genes could be linked and together lead to increased viral replication and potentially enhanced neurotropism. For the purposes of our study, both of the above findings in the HCV life cycle allow us to hypothesize that HPgV NS2 functions in a similar fashion and the deletion enhances protease activity and the hyperphosphorylation of NS5A, leading to greater viral replication within our astrocyte and microglia cultures.

It was unclear from our initial study whether the *NS2* deletion arose spontaneously within the two HPgV encephalitis patients as a result of random viral mutations that happened to confer enhanced neurotropism, or whether HPgV ΔNS2 represents a different viral strain with enhanced neurotropism circulating in the population. Unfortunately, patient-matched serum was unavailable for LE-1 and LE-2 from our original case report; future studies of patients with both brain- and blood-derived

HPgV virus should be sequenced to determine the prevalence of the *NS2* deletion. The course of infection for both HPgV WT and ΔNS2 in astrocytes is different from that observed in other flaviviruses. For example, in our model, both HPgV WT and ΔNS2 RNA levels in cell lysates peak around 7 days post infection in human astrocytes [Figure 3.7B]. In comparison, ZIKV infection of human fetal astrocytes showed that ZIKV RNA peaks after 2 to 3 days post-infection, albeit with a higher input titer of virus (MOI=3.0)[158].

The ability for HPgV to spread in astrocyte cultures, especially HPgV ΔNS2, [Figure 3.9, 3.10] is not commonly observed in the flavivirus literature. In my model, upwards of 90% of human astrocytes *in vitro* were HPgV NS5A immunopositive following infection with HPgV ΔNS2. Similarly, in our index case LE-1, 88% of GFAP+ astrocytes were positive for HPgV NS5A antigen in the affected brain region [Figure 5.3]. Comparing this data to ZIKV infected cells, ~20% of human fetal astrocytes were ZIKV immunopositive 5 days post-infection[158]. TBEV infection of primary human brain cortical astrocytes (HBCAs) also resulted in detectable infection of only 14% of HBCAs after 7 days[159]. One explanation for these discrepant findings is that although caspases are modestly activated following HPgV infection of human astrocytes [Figure 4.4], no loss in cell viability is observed without the additional of a proinflammatory cytokine [Figure 4.5A] and no immune response is initiated during infection [Figure 4.1]. This suggested that HPgV infection is uncontrolled in astrocyte cultures allowing it to spread between cells without immune regulation of

viral replication. In contrast, approximately 50% of ZIKV infected cells were positive for activated caspase-3 positive following 5 days of infection and approximately 30% loss in cell viability was also observed at this timepoint[159].

6.3 Discussion of 2nd Objective

Objective 2:

Define the host antiviral responses to WT and ΔNS2 infection in human astrocytes and microglia.

Given the association of the *NS2* deletion with HPgV encephalitis, we wanted to determine whether the mutant virus generated an enhanced inflammatory response in CNS cells compared to the WT virus. To address this question, several antiviral pathways were investigated following HPgV infection of both astrocytes and microglia. In human astrocytes, neither HPgV WT nor ΔNS2 viruses showed significant induction of interferon [Figure 4.1A-D] or other proinflammatory transcripts [Figure 4.1E,F] suggesting that HPgV infection, even with the deletion in the *NS2* gene, does not generate substantial antiviral or inflammatory responses. This finding is dissimilar to what is seen during ZIKV and WNV infection in which several interferon and inflammatory genes are induced following infection, including *IFNB* and *IL1B*[68]. Nonetheless, there is precedent in the literature whereby ZIKV actively inhibits antiviral signalling[72]. However, unlike ZIKV, HPgV cannot

actively down-regulate the response induced by a different inflammatory signal such as poly(I:C) [Figure 4.2]. This latter finding suggested that the virus potentially escapes intracellular detection, although the mechanisms by which this phenomenon occurs are unknown. The flavivirus literature suggests several possibilities for how this might happen, including delaying PRR detection of the virus, inhibition of interferon gene expression, or evasion of recognition by the complement network[172]. For example, TBEV infection delays PRR detection through accumulation of viral dsRNA in intracellular vesicles and thus delaying the interferon response for at least 24 hours while the virus can replicate[173]. To regulate the complement function of the host, both DENV and WNV NS1 proteins have been shown to interfere with the classical and lectin pathways of the complement pathway, specifically complement 4[172].

Conceptually, the fact that a virus clinically associated with encephalitis could fail to elicit a proinflammatory immune response in CNS cells is interesting and highlights that alternative mechanisms may be involved in triggering encephalitis. One possible example is in the form of molecular mimicry, where a virus has a cross-reactive epitope with host proteins and thus host antibodies will begin targeting those host proteins[174]. An example of this has been shown in HBV-infected rabbits, wherein the HBV polymerase shared 6 consecutive amino acids with the an encephalitogenic site of rabbit myelin basic protein (MBP)[175]. Following peripheral injection of HBV polymerase into the rabbits, the animals developed encephalitis

and PBMCs isolated from the rabbits proliferated when incubated with MBP *ex vivo*[175].

I was particularly curious to know if HPgV ΔNS2 could elicit a distinct innate immune response that distinguished it from HPgV WT, given the clinical association with encephalitis and the detection of the 87-nucleotide deletion in the *NS2* gene. However, the intracellular immune responses were similar between the two viruses in human astrocytes, indicating the deletion in HPgV *NS2* does not interfere with the virus' ability to evade immune detection in human astrocytes [Figure 4.1]. However, preliminary transcript data from microglia suggested that HPgV WT and ΔNS2 viruses caused differential transcriptional induction in several antiviral and proinflammatory genes, including the extremely proinflammatory molecule IL-1β. [Figure 4.3]. The successful induction of innate immune responses in human microglia may have facilitated viral clearance by the adaptive immune response, a possible explanation as to why HPgV NS5A antigen was not detected in microglia in our report[1].

As part of the clinical association with encephalitis, I was interested in whether HPgV ΔNS2 could effectively kill host cells. Abundant viral-induced cell death would provide a simple explanation for why this virus might elicit a strong immune response in the clinical setting. However, despite transient activation of some caspase family members by HPgV infection [Figure 4.4], little evidence of cell death

was observed, including no loss in cell viability [Figure 4.5A] and an increase in supernatant LDH activity [Figure 4.5B] in human astrocytes. To attempt to elicit cell death in infected cells, I infected astrocytes at a higher MOI (MOI =1.0), resulting in a modest reduction in cell viability and increased supernatant LDH activity after 48 and 96 hours post-infection [Figure 4.6]. Nonetheless, these effects were limited, especially when compared to the increased immune responses (i.e. cytokine induction, cell death) observed in other flaviviruses such as ZIKV and WNV, following infection of human astrocytes[68]. Taken together, this suggests that direct HPgV-induced glial cell death was unlikely to be the primary cause of pathology in the infected CNS.

To further elucidate how HPgV WT and ΔNS2 differentially affected the innate immune response in human astrocytes and microglia, future studies should investigate how viral infection by either HPgV WT or ΔNS2 affect gene transcripts by RNA-seq analysis in human astrocytes and microglia with qPCR validation. This would also validate RNA-seq data derived from human cortical tissue that was completed in Chapter V of this thesis.

6.4 Discussion of 3rd Objective

Objective 3:

Examine HPgV neural cell tropism in vivo and associated immune responses in brain tissues from patients with detectable HPgV.

In our original case report, I screened 66 additional patient brain tissue samples (other than LE-1 and LE-2) for the presence of HPgV. These patients represented a variety of neurologically normal or diseased brains (i.e. NeuroHIV, MS, and stroke) and all were negative for HPgV RNA[1]. To follow up on these observations, I optimized a ddPCR screening technique for HPgV RNA detection in human cortical samples [Figure 5.1]. Within the cohort both HPgV positive and negative strand RNA was detected in each HPgV+ patient (n=7) and the numbers of positive and negative strands were positively correlated with one another [Figure 5.2C]. When analyzing the HPgV+ LE group, patient LE-1 from our original case report had a markedly higher number of viral copies than LE-2 and the HPgV+ cohort, similar to what was observed in the original study[1].

The host immune response was investigated in these patients using qRT-PCR analysis of several antiviral and proinflammatory genes that were examined in Chapter IV. In patient cortical samples, these genes were suppressed in the HPgV+ group, suggesting that HPgV infection suppressed both the interferon and

proinflammatory responses that are typically induced following viral infection [Figure 5.4]. Within our cohort, low-level HPgV infection is associated with immune suppression, but very high levels of inflammation were observed in the one patient with significantly higher HPgV viral load (LE-1) compared with all other patients in the cohort, including patient LE-2. Similar results have been reported in an animal model of HBV infection wherein inoculation of the mice with different input titers led to different immune responses in the mice[176]. Similarly, a higher input titer of feline immunodeficiency virus (FIV) in cats increased the severity of neurovirulence in this animal model[177]. The magnitude of differences between patient LE-1 and other HPgV-infected patients, including LE-2, in terms of viral quantity appears to modulate the immune response in these patients. A caveat to this is that we are unsure if the neuroimmune gene suppression was caused by virus infection of the CNS or if these patients were already immunosuppressed, thus creating an environment for HPgV to infiltrate and infect CNS cells. Further investigation into which comes first is warranted.

Interestingly, despite having abundant HPgV antigen in the brain [Figure 5.3], and a fatal leukoencephalitis, the transcriptional profile of LE-2 resembled the non-encephalitic patients [Figure 5.4]. The primary reason for this finding was that I examined cortical samples for all the individuals in the cohort, while patient LE-2 showed focal HPgV infection in the white matter (WM) of the brainstem. Cortical samples were used for analysis because these anatomic-specific samples were

available for the entire HPgV+ cohort and thus for consistency, cortical samples were used for both LE-1 and LE-2. For this reason, I assume that the transcriptional profile would be similar to LE-1 if brain regions with a greater abundance of virus were interrogated by qRT-PCR. This assumption is based on the results of IF imaging from patient LE-2 [Figure 5.3] wherein HPgV NS5A was detected in 66% of astrocytes in WM tissue from LE-2. There is precedent for differential immune activation in different brain regions in the literature; for example clearance of rabies virus causes significantly higher immune activation in the cerebellum than the cerebral cortex in animal models of the disease[178]. As we develop our neuroHPgV cohort, it would thus be important to collect and compare different brain regions from infected individuals.

Another outstanding question from my results in Chapter III is whether microglia are infected *in vivo*. Since HPgV infection of microglia is relatively transient *in vitro*, it remains to be determined whether microglial infection occurs to a convincing degree in the infected human CNS. Further, since microglia are the primary phagocytes of the brain, it will be necessary to verify whether any HPgV antigen detected in microglia truly represents infection or merely phagocytosis of particulate from infected astrocytes. These experiments are currently in progress.

The analysis of a subset of non-encephalitis HPgV+ (n=3) and HPgV- (n=2) patients by RNA-seq allowed me to generate new hypotheses regarding how HPgV infection

modulates the host neuroimmune response. Numerous genes were identified that were either significantly increased or decreased in the CNS of HPgV-infected patients versus uninfected patients [Figure 5.5]. The associated Ingenuity™ analyses showed that specific genes classified as "neuroinflammatory signaling pathways" were associated with HPgV infection [Figure 5.6] and that expression of NF-κB-associated genes was significantly decreased at the transcript level in HPgV-infected patients [Figure 5.7]. These findings supported my qRT-PCR analysis showing the suppression of several important antiviral genes. However, an interesting finding was made from these analyses in the form of *NOS2* transcription induction [Figure 5.7]. NOS2, or inducible NOS, is an inducible form of NOS in human astrocytes and microglia that is expressed following immune activation and under normal circumstances, and acts as an enzyme to produce nitric oxide (NO)[35]. iNOS can be inflammatory or immunomodulatory and several examples exist in the literature describing its role within the CNS. Generally, the overproduction of NO by iNOS leads to an enhanced inflammatory response, often resulting in tissue damage in the CNS[179]. Indeed, iNOS$^{-/-}$ mice are hypersusceptible to inflammatory diseases such as experimental autoimmune encephalomyelitis (EAE) suggesting that iNOS exerts a regulatory effect during CNS inflammation[179]. How iNOS affects the antiviral response in the CNS remains uncertain, although several studies have examined the interplay between iNOS and specific viruses. For example, the induction of *iNOS* in the CNS following HIV-1 viral infection has been shown previously and seems to be involved in virus-induced cytotoxicity rather than viral clearance in this context[35].

Further investigation is necessary to elucidate how iNOS is important in the context of HPgV infection of the CNS.

Taken together, two important conclusions from studies of this cohort include: (i) low levels of replicating HPgV in the CNS do not cause encephalitis and are instead associated with neuroimmune gene suppression, and (ii) the *NS2* deletion is neither necessary nor sufficient for neurotropism of the virus, since none of the non-encephalitis HPgV patients' HPgV sequences contained the deletion in the *NS2* gene, despite the detection of both HPgV-encoded positive and negative ssRNA in all cases. To determine the circumstances under which HPgV does cause encephalitis, a larger cohort of HPgV encephalitis patients will be essential. Until then, we will continue to build our neuroHPgV cohort, which will be assisted by more routine screening for HPgV in cases of suspected viral encephalitis. This will enable us to perform RNA-seq on HPgV encephalitis versus non-encephalitis cases. Only when these experiments are performed will we be able to elucidate the factors that transform HPgV from an immunologically quiescent and non-pathogenic CNS infection to a fatal leukoencephalitis.

6.5 Future Directions

Based upon the findings of this thesis and the preliminary work I have initiated within several new areas of HPgV neurotropism, I propose the following 4 aims that I believe will advance our understanding of how HPgV acts within the CNS:

Aim 1: Investigate other mutations in the HPgV genome and how they affect viral infectivity, replication, and host responses in glial cells

As seen in our report[1], sequences from patient LE-1 and LE-2 shared a 91% similarity with other viruses from HPgV genotype 2[1]. This finding was further investigated within my thesis wherein I found that HPgV sequences from the WT and ΔNS2 plasmid (which is identical to sequences isolated from LE-1 and LE-2), cluster in genotype 2 [Figure 3.3D,E]. Although this 87-nucleotide deletion in the *NS2* gene that I investigated throughout this thesis explains some variability, other mutations were identified in the viral genome in our original case study. This included a number of point mutations, along with a 15-nucleotide insertion in the *NS5A* gene of the virus[1]. Due to the size of this mutation, I constructed a mutant viral clone containing this insertion in the *NS5A* gene [Figure 3.4C], and also combined the *NS2* deletion and *NS5A* insertion mutations into one viral clone [Figure 3.4D]. The analyses of these viral clones in future experiments might advance the understanding of how these mutations could interact to cause disease and what the role of the *NS5A* mutation is in viral infectivity, replication or eliciting a host

immune response. I propose that these new viral clones could be used in similar experiments to those I performed in Chapter III, including side-by-side infections with HPgV WT and ΔNS2 viruses to determine how each viral clone differs in its ability to infect glial cells.

Aim 2: Determine how iNOS and similar enzymes participate in HPgV infection of the CNS

As discussed above, the identification of *NOS2* induction at the transcript level in HPgV-positive patients raises new hypotheses regarding how HPgV interacts with the neuroimmune response. To investigate the effects of iNOS, several experiments are necessary including: (i) screen HPgV-infected astrocytes and microglia to determine how *NOS2* transcription changes in both HPgV WT and HPgV ΔNS2 infected cultures, (ii) validate the up-regulation of iNOS in human astrocytes and human microglia following HPgV infection at the protein level using western blot analysis, (iii) analyze a functional readout of iNOS in human microglia and astrocytes, using reagents such as the nitric oxide kit (Abcam™) to quantify NO production following infection, and (iv) using small-interfering RNA (siRNA) to knock-down *NOS2* expression in human astrocytes and microglia and investigate how this affects HPgV infection, replication and the immune response following infection by ddPCR and qRT-PCR analysis.

Aim 3: Investigate how HPgV and HIV-1 co-infection impacts the CNS pathogenesis

Within this aim, HIV-1-infected patients with and without brain disease would be screened for the presence of HPgV RNA in the CNS using ddPCR, as done previously in Chapter V. As discussed, HPgV co-infection is beneficial in HIV-1 patients because of the increased survival, increased CD4+ counts and lower delayed progression to AIDS[108]. The identification of six additional HPgV+ patients, all of whom are HIV-1 infected, creates a unique opportunity to investigate how HPgV+/HIV-1+ co-infection alters viral replication in the CNS. Within this aim it would be essential to: (i) investigate the HPgV and HIV-1 viral loads in the brain and compare those data to mono-infected individuals, (ii) assess the host immune responses and how co-infection changes both the HPgV only and HIV-1-only patient neuroimmune transcriptional profiles, and (iii) utilize RNA-sequencing to discover how co-infection alters the overall immune response compared to mono-infected patients. To confirm the *in vivo* findings, it would be helpful to utilize my established *in vitro* model in human astrocytes and microglia to co-infect cells in the following 3 ways: (i) infection with HPgV followed by HIV-1 infection, (ii) infection with HIV-1 followed by HPgV infection, and (iii) co-infection of both HPgV and HIV-1 at the same time. To analyze how HPgV affects HIV-1 infection, subsequent p24 analysis would be utilized to measure HIV-1 replication. ddPCR analysis would also be used to test HPgV and HIV-1 present in cell supernatants following infection. A similar

setup has been done using PBMC cells, wherein PBMCs previously exposed to HPgV before HIV-1 infection showed no HIV-1 viral replication[180].

Aim 4: Develop an *in vivo* model of HPgV infection

To understand the mechanisms underlying viral encephalitis, many animal models have been created to investigate how viral infection in the CNS elicits immune responses and subsequent encephalitis. A variety of mouse models exist for viruses including ZIKV, WNV, and DENV, which examine how these viruses cause encephalitis[181]. After answering several of the above questions regarding viral infectivity and the associated host responses that HPgV might elicit following infection of glial cells, the utilization of an animal model is essential to test several of the generated hypotheses. One challenge to establishing model is the lack of existing knowledge about HPgV host specificity and whether HPgV can infect and replicate in host cells of a different species. Therefore, preliminary studies testing HPgV infection of mouse astrocytes *in vitro* are essential. The use of immune suppressed animal models, including RAG-$1^{-/-}$ mice, which lack mature B and T lymphocytes[182], might be necessary first step to allow HPgV to avoid immune recognition in *in vivo* models. The one caveat to using a model such as RAG-$1^{-/-}$ mice is that the virus would have to be implanted directly into the CNS, since the virus would be unable to utilize B and T lymphocytes for primary infection and subsequent CNS infiltration if the virus was injected in the periphery.

References

1 Balcom, E. F. *et al.* Human pegivirus-1 associated leukoencephalitis: Clinical and molecular features. *Ann Neurol* **84**, 781-787, doi:10.1002/ana.25343 (2018).

2 Halperin, J. J. Diagnosis and management of acute encephalitis. *Handb Clin Neurol* **140**, 337-347, doi:10.1016/B978-0-444-63600-3.00018-0 (2017).

3 Jmor, F., Emsley, H. C., Fischer, M., Solomon, T. & Lewthwaite, P. The incidence of acute encephalitis syndrome in Western industrialised and tropical countries. *Virol J* **5**, 134, doi:10.1186/1743-422X-5-134 (2008).

4 Swanson, P. A., 2nd & McGavern, D. B. Viral diseases of the central nervous system. *Curr Opin Virol* **11**, 44-54, doi:10.1016/j.coviro.2014.12.009 (2015).

5 Saylor, D., Thakur, K. & Venkatesan, A. Acute encephalitis in the immunocompromised individual. *Curr Opin Infect Dis* **28**, 330-336, doi:10.1097/QCO.0000000000000175 (2015).

6 Tyler, K. L. Acute Viral Encephalitis. *N Engl J Med* **379**, 557-566, doi:10.1056/NEJMra1708714 (2018).

7 Messacar, K., Fischer, M., Dominguez, S. R., Tyler, K. L. & Abzug, M. J. Encephalitis in US Children. *Infect Dis Clin North Am* **32**, 145-162, doi:10.1016/j.idc.2017.10.007 (2018).

8 Ellul, M. & Solomon, T. Acute encephalitis - diagnosis and management. *Clin Med (Lond)* **18**, 155-159, doi:10.7861/clinmedicine.18-2-155 (2018).

9 Venkatesan, A. *et al.* Case definitions, diagnostic algorithms, and priorities in encephalitis: consensus statement of the international encephalitis consortium. *Clin Infect Dis* **57**, 1114-1128, doi:10.1093/cid/cit458 (2013).

10 Terry, R. L. *et al.* Inflammatory monocytes and the pathogenesis of viral encephalitis. *J Neuroinflammation* **9**, 270, doi:10.1186/1742-2094-9-270 (2012).

11 Soung, A. & Klein, R. S. Viral Encephalitis and Neurologic Diseases: Focus on Astrocytes. *Trends Mol Med* **24**, 950-962, doi:10.1016/j.molmed.2018.09.001 (2018).

12 Bauer, J. & Bien, C. G. Neuropathology of autoimmune encephalitides. *Handb Clin Neurol* **133**, 107-120, doi:10.1016/B978-0-444-63432-0.00007-4 (2016).

13 Turtle, L., Griffiths, M. J. & Solomon, T. Encephalitis caused by flaviviruses. *QJM* **105**, 219-223, doi:10.1093/qjmed/hcs013 (2012).

14 Michael, B. D. *et al.* The Interleukin-1 Balance During Encephalitis Is Associated With Clinical Severity, Blood-Brain Barrier Permeability, Neuroimaging Changes, and Disease Outcome. *J Infect Dis* **213**, 1651-1660, doi:10.1093/infdis/jiv771 (2016).

15 Thompson, C., Kneen, R., Riordan, A., Kelly, D. & Pollard, A. J. Encephalitis in children. *Arch Dis Child* **97**, 150-161, doi:10.1136/archdischild-2011-300100 (2012).

16 Venkatesan, A. & Murphy, O. C. Viral Encephalitis. *Neurol Clin* **36**, 705-724, doi:10.1016/j.ncl.2018.07.001 (2018).

17 Kelley, B. P. *et al.* Autoimmune Encephalitis: Pathophysiology and Imaging Review of an Overlooked Diagnosis. *AJNR Am J Neuroradiol* **38**, 1070-1078, doi:10.3174/ajnr.A5086 (2017).

18 Lancaster, E. The Diagnosis and Treatment of Autoimmune Encephalitis. *J Clin Neurol* **12**, 1-13, doi:10.3988/jcn.2016.12.1.1 (2016).

19 Dalmau, J. & Rosenfeld, M. R. Autoimmune encephalitis update. *Neuro Oncol* **16**, 771-778, doi:10.1093/neuonc/nou030 (2014).

20 Newman, M. P. *et al.* Autoimmune encephalitis. *Intern Med J* **46**, 148-157, doi:10.1111/imj.12974 (2016).

21 Roos, K. L. Encephalitis. *Handb Clin Neurol* **121**, 1377-1381, doi:10.1016/B978-0-7020-4088-7.00094-8 (2014).
22 Weingarten, L., Enarson, P. & Klassen, T. Encephalitis. *Pediatr Emerg Care* **29**, 235-241; quiz 242-234, doi:10.1097/PEC.0b013e318280d7f3 (2013).
23 Waisman, A., Liblau, R. S. & Becher, B. Innate and adaptive immune responses in the CNS. *Lancet Neurol* **14**, 945-955, doi:10.1016/S1474-4422(15)00141-6 (2015).
24 Gadani, S. P., Walsh, J. T., Lukens, J. R. & Kipnis, J. Dealing with Danger in the CNS: The Response of the Immune System to Injury. *Neuron* **87**, 47-62, doi:10.1016/j.neuron.2015.05.019 (2015).
25 Takeuchi, O. & Akira, S. Pattern recognition receptors and inflammation. *Cell* **140**, 805-820, doi:10.1016/j.cell.2010.01.022 (2010).
26 Paul, S., Ricour, C., Sommereyns, C., Sorgeloos, F. & Michiels, T. Type I interferon response in the central nervous system. *Biochimie* **89**, 770-778, doi:10.1016/j.biochi.2007.02.009 (2007).
27 Becher, B., Spath, S. & Goverman, J. Cytokine networks in neuroinflammation. *Nat Rev Immunol* **17**, 49-59, doi:10.1038/nri.2016.123 (2017).
28 Bonaventura, P., Lamboux, A., Albarede, F. & Miossec, P. Differential effects of TNF-alpha and IL-1beta on the control of metal metabolism and cadmium-induced cell death in chronic inflammation. *PLoS One* **13**, e0196285, doi:10.1371/journal.pone.0196285 (2018).
29 Minagar, A. & Alexander, J. S. Blood-brain barrier disruption in multiple sclerosis. *Mult Scler* **9**, 540-549, doi:10.1191/1352458503ms965oa (2003).
30 Kuang, Y., Lackay, S. N., Zhao, L. & Fu, Z. F. Role of chemokines in the enhancement of BBB permeability and inflammatory infiltration after rabies virus infection. *Virus Res* **144**, 18-26, doi:10.1016/j.virusres.2009.03.014 (2009).
31 Hu, S., Sheng, W. S., Schachtele, S. J. & Lokensgard, J. R. Reactive oxygen species drive herpes simplex virus (HSV)-1-induced proinflammatory cytokine production by murine microglia. *J Neuroinflammation* **8**, 123, doi:10.1186/1742-2094-8-123 (2011).
32 Singh, A., Kukreti, R., Saso, L. & Kukreti, S. Oxidative Stress: A Key Modulator in Neurodegenerative Diseases. *Molecules* **24**, doi:10.3390/molecules24081583 (2019).
33 Reiss, C. S., Chesler, D. A., Hodges, J., Ireland, D. D. & Chen, N. Innate immune responses in viral encephalitis. *Curr Top Microbiol Immunol* **265**, 63-94, doi:10.1007/978-3-662-09525-6_4 (2002).
34 Saha, R. N. & Pahan, K. Regulation of inducible nitric oxide synthase gene in glial cells. *Antioxid Redox Signal* **8**, 929-947, doi:10.1089/ars.2006.8.929 (2006).
35 Akaike, T. & Maeda, H. Nitric oxide and virus infection. *Immunology* **101**, 300-308, doi:10.1046/j.1365-2567.2000.00142.x (2000).
36 Yuste, J. E., Tarragon, E., Campuzano, C. M. & Ros-Bernal, F. Implications of glial nitric oxide in neurodegenerative diseases. *Front Cell Neurosci* **9**, 322, doi:10.3389/fncel.2015.00322 (2015).
37 Jesus, L. B. *et al.* IDO, COX and iNOS have an important role in the proliferation of Neospora caninum in neuron/glia co-cultures. *Vet Parasitol* **266**, 96-102, doi:10.1016/j.vetpar.2019.01.003 (2019).
38 Boon, J., Scholten, P. C., Oldenhave, A. & Heintz, A. P. Continuous intrauterine compared with cyclic oral progestin administration in perimenopausal HRT. *Maturitas* **46**, 69-77, doi:10.1016/s0378-5122(03)00163-4 (2003).
39 Chowdhury, A. Y., Tavis, J. E. & George, S. L. Human pegivirus (GB virus C) NS3 protease activity inhibits induction of the type I interferon response and is not

inhibited by HCV NS3 protease inhibitors. *Virology* **456-457**, 300-309, doi:10.1016/j.virol.2014.03.018 (2014).
40 Kell, A. M. & Gale, M., Jr. RIG-I in RNA virus recognition. *Virology* **479-480**, 110-121, doi:10.1016/j.virol.2015.02.017 (2015).
41 Li, X. D., Sun, L., Seth, R. B., Pineda, G. & Chen, Z. J. Hepatitis C virus protease NS3/4A cleaves mitochondrial antiviral signaling protein off the mitochondria to evade innate immunity. *Proc Natl Acad Sci U S A* **102**, 17717-17722, doi:10.1073/pnas.0508531102 (2005).
42 Schoggins, J. W. & Rice, C. M. Interferon-stimulated genes and their antiviral effector functions. *Curr Opin Virol* **1**, 519-525, doi:10.1016/j.coviro.2011.10.008 (2011).
43 Lindqvist, R., Kurhade, C., Gilthorpe, J. D. & Overby, A. K. Cell-type- and region-specific restriction of neurotropic flavivirus infection by viperin. *J Neuroinflammation* **15**, 80, doi:10.1186/s12974-018-1119-3 (2018).
44 Samuel, M. A. & Diamond, M. S. Alpha/beta interferon protects against lethal West Nile virus infection by restricting cellular tropism and enhancing neuronal survival. *J Virol* **79**, 13350-13361, doi:10.1128/JVI.79.21.13350-13361.2005 (2005).
45 Lobigs, M., Mullbacher, A., Wang, Y., Pavy, M. & Lee, E. Role of type I and type II interferon responses in recovery from infection with an encephalitic flavivirus. *J Gen Virol* **84**, 567-572, doi:10.1099/vir.0.18654-0 (2003).
46 Wilson, E. H., Weninger, W. & Hunter, C. A. Trafficking of immune cells in the central nervous system. *J Clin Invest* **120**, 1368-1379, doi:10.1172/JCI41911 (2010).
47 Korin, B. *et al.* High-dimensional, single-cell characterization of the brain's immune compartment. *Nat Neurosci* **20**, 1300-1309, doi:10.1038/nn.4610 (2017).
48 Klein, R. S. & Hunter, C. A. Protective and Pathological Immunity during Central Nervous System Infections. *Immunity* **46**, 891-909, doi:10.1016/j.immuni.2017.06.012 (2017).
49 Russo, M. V. & McGavern, D. B. Immune Surveillance of the CNS following Infection and Injury. *Trends Immunol* **36**, 637-650, doi:10.1016/j.it.2015.08.002 (2015).
50 Hayashida, E. *et al.* Zika virus encephalitis in immunocompetent mice is dominated by innate immune cells and does not require T or B cells. *J Neuroinflammation* **16**, 177, doi:10.1186/s12974-019-1566-5 (2019).
51 Suthar, M. S., Diamond, M. S. & Gale, M., Jr. West Nile virus infection and immunity. *Nat Rev Microbiol* **11**, 115-128, doi:10.1038/nrmicro2950 (2013).
52 Galluzzi, L. *et al.* Molecular mechanisms of cell death: recommendations of the Nomenclature Committee on Cell Death 2018. *Cell Death Differ* **25**, 486-541, doi:10.1038/s41418-017-0012-4 (2018).
53 Tait, S. W. & Green, D. R. Mitochondria and cell death: outer membrane permeabilization and beyond. *Nat Rev Mol Cell Biol* **11**, 621-632, doi:10.1038/nrm2952 (2010).
54 Elmore, S. Apoptosis: a review of programmed cell death. *Toxicol Pathol* **35**, 495-516, doi:10.1080/01926230701320337 (2007).
55 Levine, B. *et al.* Conversion of lytic to persistent alphavirus infection by the bcl-2 cellular oncogene. *Nature* **361**, 739-742, doi:10.1038/361739a0 (1993).
56 Okamoto, T. *et al.* Regulation of Apoptosis during Flavivirus Infection. *Viruses* **9**, doi:10.3390/v9090243 (2017).
57 Mamik, M. K. & Power, C. Inflammasomes in neurological diseases: emerging pathogenic and therapeutic concepts. *Brain* **140**, 2273-2285, doi:10.1093/brain/awx133 (2017).
58 Jorgensen, I., Rayamajhi, M. & Miao, E. A. Programmed cell death as a defence against infection. *Nat Rev Immunol* **17**, 151-164, doi:10.1038/nri.2016.147 (2017).

59 Lei, X. *et al.* Enterovirus 71 Inhibits Pyroptosis through Cleavage of Gasdermin D. *J Virol* **91**, doi:10.1128/JVI.01069-17 (2017).
60 Moir, S., Chun, T. W. & Fauci, A. S. Pathogenic mechanisms of HIV disease. *Annu Rev Pathol* **6**, 223-248, doi:10.1146/annurev-pathol-011110-130254 (2011).
61 Snider, W. D. *et al.* Neurological complications of acquired immune deficiency syndrome: analysis of 50 patients. *Ann Neurol* **14**, 403-418, doi:10.1002/ana.410140404 (1983).
62 Gomez, D. *et al.* Empiric neurocognitive performance profile discovery and interpretation in HIV infection. *J Neurovirol* **25**, 72-84, doi:10.1007/s13365-018-0685-6 (2019).
63 Kaul, M., Garden, G. A. & Lipton, S. A. Pathways to neuronal injury and apoptosis in HIV-associated dementia. *Nature* **410**, 988-994, doi:10.1038/35073667 (2001).
64 Mamik, M. K. *et al.* HIV-1 Viral Protein R Activates NLRP3 Inflammasome in Microglia: implications for HIV-1 Associated Neuroinflammation. *J Neuroimmune Pharmacol* **12**, 233-248, doi:10.1007/s11481-016-9708-3 (2017).
65 Asahchop, E. L. *et al.* Reduced antiretroviral drug efficacy and concentration in HIV-infected microglia contributes to viral persistence in brain. *Retrovirology* **14**, 47, doi:10.1186/s12977-017-0370-5 (2017).
66 Mamik, M. K. *et al.* Insulin Treatment Prevents Neuroinflammation and Neuronal Injury with Restored Neurobehavioral Function in Models of HIV/AIDS Neurodegeneration. *J Neurosci* **36**, 10683-10695, doi:10.1523/JNEUROSCI.1287-16.2016 (2016).
67 Morgello, S. HIV neuropathology. *Handb Clin Neurol* **152**, 3-19, doi:10.1016/B978-0-444-63849-6.00002-5 (2018).
68 Potokar, M., Jorgacevski, J. & Zorec, R. Astrocytes in Flavivirus Infections. *Int J Mol Sci* **20**, doi:10.3390/ijms20030691 (2019).
69 Laureti, M., Narayanan, D., Rodriguez-Andres, J., Fazakerley, J. K. & Kedzierski, L. Flavivirus Receptors: Diversity, Identity, and Cell Entry. *Front Immunol* **9**, 2180, doi:10.3389/fimmu.2018.02180 (2018).
70 Dick, G. W., Kitchen, S. F. & Haddow, A. J. Zika virus. I. Isolations and serological specificity. *Trans R Soc Trop Med Hyg* **46**, 509-520, doi:10.1016/0035-9203(52)90042-4 (1952).
71 Song, B. H., Yun, S. I., Woolley, M. & Lee, Y. M. Zika virus: History, epidemiology, transmission, and clinical presentation. *J Neuroimmunol* **308**, 50-64, doi:10.1016/j.jneuroim.2017.03.001 (2017).
72 Kumar, A. *et al.* Zika virus inhibits type-I interferon production and downstream signaling. *EMBO Rep* **17**, 1766-1775, doi:10.15252/embr.201642627 (2016).
73 Nowakowski, T. J. *et al.* Expression Analysis Highlights AXL as a Candidate Zika Virus Entry Receptor in Neural Stem Cells. *Cell Stem Cell* **18**, 591-596, doi:10.1016/j.stem.2016.03.012 (2016).
74 White, M. K., Wollebo, H. S., David Beckham, J., Tyler, K. L. & Khalili, K. Zika virus: An emergent neuropathological agent. *Ann Neurol* **80**, 479-489, doi:10.1002/ana.24748 (2016).
75 Garcez, P. P. *et al.* Zika virus impairs growth in human neurospheres and brain organoids. *Science* **352**, 816-818, doi:10.1126/science.aaf6116 (2016).
76 Wang, T. *et al.* Toll-like receptor 3 mediates West Nile virus entry into the brain causing lethal encephalitis. *Nat Med* **10**, 1366-1373, doi:10.1038/nm1140 (2004).
77 Li, H., Saucedo-Cuevas, L., Shresta, S. & Gleeson, J. G. The Neurobiology of Zika Virus. *Neuron* **92**, 949-958, doi:10.1016/j.neuron.2016.11.031 (2016).

78 Saxena, V., Mathur, A., Krishnani, N. & Dhole, T. N. An insufficient anti-inflammatory cytokine response in mouse brain is associated with increased tissue pathology and viral load during Japanese encephalitis virus infection. *Arch Virol* **153**, 283-292, doi:10.1007/s00705-007-1098-7 (2008).
79 Saxena, V., Mathur, A., Krishnani, N. & Dhole, T. N. Kinetics of cytokine profile during intraperitoneal inoculation of Japanese encephalitis virus in BALB/c mice model. *Microbes Infect* **10**, 1210-1217, doi:10.1016/j.micinf.2008.06.015 (2008).
80 Filgueira, L. & Lannes, N. Review of Emerging Japanese Encephalitis Virus: New Aspects and Concepts about Entry into the Brain and Inter-Cellular Spreading. *Pathogens* **8**, doi:10.3390/pathogens8030111 (2019).
81 Misra, U. K. & Kalita, J. Overview: Japanese encephalitis. *Prog Neurobiol* **91**, 108-120, doi:10.1016/j.pneurobio.2010.01.008 (2010).
82 Li, G. H., Ning, Z. J., Liu, Y. M. & Li, X. H. Neurological Manifestations of Dengue Infection. *Front Cell Infect Microbiol* **7**, 449, doi:10.3389/fcimb.2017.00449 (2017).
83 Carod-Artal, F. J., Wichmann, O., Farrar, J. & Gascon, J. Neurological complications of dengue virus infection. *Lancet Neurol* **12**, 906-919, doi:10.1016/S1474-4422(13)70150-9 (2013).
84 Verma, R., Sahu, R. & Holla, V. Neurological manifestations of dengue infection: a review. *J Neurol Sci* **346**, 26-34, doi:10.1016/j.jns.2014.08.044 (2014).
85 Madi, D. *et al.* Dengue encephalitis-A rare manifestation of dengue fever. *Asian Pac J Trop Biomed* **4**, S70-72, doi:10.12980/APJTB.4.2014C1006 (2014).
86 Johnson, T. P. *et al.* Chronic Dengue Virus Panencephalitis in a Patient with Progressive Dementia with Extrapyramidal Features. *Ann Neurol* **86**, 695-703, doi:10.1002/ana.25588 (2019).
87 Lindquist, L. & Vapalahti, O. Tick-borne encephalitis. *Lancet* **371**, 1861-1871, doi:10.1016/S0140-6736(08)60800-4 (2008).
88 Velay, A. *et al.* Tick-borne encephalitis virus: molecular determinants of neuropathogenesis of an emerging pathogen. *Crit Rev Microbiol* **45**, 472-493, doi:10.1080/1040841X.2019.1629872 (2019).
89 Cordova, S. P. *et al.* Murray Valley encephalitis in Western Australia in 2000, with evidence of southerly spread. *Commun Dis Intell* **24**, 368-372 (2000).
90 Selvey, L. A. *et al.* The changing epidemiology of Murray Valley encephalitis in Australia: the 2011 outbreak and a review of the literature. *PLoS Negl Trop Dis* **8**, e2656, doi:10.1371/journal.pntd.0002656 (2014).
91 Matthews, V. *et al.* Morphological features of Murray Valley encephalitis virus infection in the central nervous system of Swiss mice. *Int J Exp Pathol* **81**, 31-40, doi:10.1046/j.1365-2613.2000.00135.x (2000).
92 Fu, T. L., Ong, K. C., Tran, Y. D., McLean, C. A. & Wong, K. T. Viral neuronotropism is important in the pathogenesis of Murray Valley encephalitis. *Neuropathol Appl Neurobiol* **42**, 307-310, doi:10.1111/nan.12285 (2016).
93 Floridis, J. *et al.* Murray Valley Encephalitis Virus: An Ongoing Cause of Encephalitis in Australia's North. *Trop Med Infect Dis* **3**, doi:10.3390/tropicalmed3020049 (2018).
94 Knox, J. *et al.* Murray Valley encephalitis: a review of clinical features, diagnosis and treatment. *Med J Aust* **196**, 322-326, doi:10.5694/mja11.11026 (2012).
95 Stapleton, J. T. & Chaloner, K. GB virus C infection and non-Hodgkin lymphoma: important to know but the jury is out. *Int J Cancer* **126**, 2759-2761, doi:10.1002/ijc.25194 (2010).
96 Spearman, C. W., Dusheiko, G. M., Hellard, M. & Sonderup, M. Hepatitis C. *Lancet* **394**, 1451-1466, doi:10.1016/S0140-6736(19)32320-7 (2019).

97 Fletcher, N. F. & McKeating, J. A. Hepatitis C virus and the brain. *J Viral Hepat* **19**, 301-306, doi:10.1111/j.1365-2893.2012.01591.x (2012).
98 Fletcher, N. F. *et al.* Hepatitis C virus infects the endothelial cells of the blood-brain barrier. *Gastroenterology* **142**, 634-643 e636, doi:10.1053/j.gastro.2011.11.028 (2012).
99 Deinhardt, F., Holmes, A. W., Capps, R. B. & Popper, H. Studies on the transmission of human viral hepatitis to marmoset monkeys. I. Transmission of disease, serial passages, and description of liver lesions. *J Exp Med* **125**, 673-688, doi:10.1084/jem.125.4.673 (1967).
100 Adams, M. J., King, A. M. & Carstens, E. B. Ratification vote on taxonomic proposals to the International Committee on Taxonomy of Viruses (2013). *Arch Virol* **158**, 2023-2030, doi:10.1007/s00705-013-1688-5 (2013).
101 Slavov, S. N. *et al.* Human pegivirus-1 (HPgV-1) RNA prevalence and genotypes in volunteer blood donors from the Brazilian Amazon. *Transfus Clin Biol*, doi:10.1016/j.tracli.2019.06.005 (2019).
102 Feng, Y. *et al.* A novel genotype of GB virus C: its identification and predominance among injecting drug users in Yunnan, China. *PLoS One* **6**, e21151, doi:10.1371/journal.pone.0021151 (2011).
103 Liu, Z. *et al.* Prevalence of GB virus type C viraemia in MSM with or without HIV-1 infection in Beijing, China. *Epidemiol Infect* **140**, 2199-2209, doi:10.1017/S0950268812000027 (2012).
104 Taklual, W., Tang, S. & Yue, W. Effect of human pegivirus route of transmission on the genetic distribution of the virus: an institution based cross-sectional study. *Virol J* **16**, 50, doi:10.1186/s12985-019-1161-5 (2019).
105 de Lima, A. B. F. *et al.* Low prevalence of human pegivirus 1 (HPgV-1) in HTLV-1 carriers from Belem, Para, North Region of Brazil. *PLoS One* **15**, e0232783, doi:10.1371/journal.pone.0232783 (2020).
106 Stapleton, J. T., Foung, S., Muerhoff, A. S., Bukh, J. & Simmonds, P. The GB viruses: a review and proposed classification of GBV-A, GBV-C (HGV), and GBV-D in genus Pegivirus within the family Flaviviridae. *J Gen Virol* **92**, 233-246, doi:10.1099/vir.0.027490-0 (2011).
107 Kriesel, J. D. *et al.* Deep sequencing for the detection of virus-like sequences in the brains of patients with multiple sclerosis: detection of GBV-C in human brain. *PLoS One* **7**, e31886, doi:10.1371/journal.pone.0031886 (2012).
108 Bhattarai, N. & Stapleton, J. T. GB virus C: the good boy virus? *Trends Microbiol* **20**, 124-130, doi:10.1016/j.tim.2012.01.004 (2012).
109 Giulivi, A. *et al.* Prevalence of GBV-C/hepatitis G virus viremia and anti-E2 in Canadian blood donors. *Vox Sang* **79**, 201-205, doi:10.1159/000056731 (2000).
110 Papageorgiou, L., Loukatou, S., Sofia, K., Maroulis, D. & Vlachakis, D. An updated evolutionary study of Flaviviridae NS3 helicase and NS5 RNA-dependent RNA polymerase reveals novel invariable motifs as potential pharmacological targets. *Mol Biosyst* **12**, 2080-2093, doi:10.1039/c5mb00706b (2016).
111 Chivero, E. T. & Stapleton, J. T. Tropism of human pegivirus (formerly known as GB virus C/hepatitis G virus) and host immunomodulation: insights into a highly successful viral infection. *J Gen Virol* **96**, 1521-1532, doi:10.1099/vir.0.000086 (2015).
112 Xiang, J., Wunschmann, S., Schmidt, W., Shao, J. & Stapleton, J. T. Full-length GB virus C (Hepatitis G virus) RNA transcripts are infectious in primary CD4-positive T cells. *J Virol* **74**, 9125-9133, doi:10.1128/jvi.74.19.9125-9133.2000 (2000).

113 Mohr, E. L. & Stapleton, J. T. GB virus type C interactions with HIV: the role of envelope glycoproteins. *J Viral Hepat* **16**, 757-768, doi:10.1111/j.1365-2893.2009.01194.x (2009).
114 Ranjbar, M. M. *et al.* GB Virus C/Hepatitis G Virus Envelope Glycoprotein E2: Computational Molecular Features and Immunoinformatics Study. *Hepat Mon* **13**, e15342, doi:10.5812/hepatmon.15342 (2013).
115 George, S. L., Varmaz, D., Tavis, J. E. & Chowdhury, A. The GB virus C (GBV-C) NS3 serine protease inhibits HIV-1 replication in a CD4+ T lymphocyte cell line without decreasing HIV receptor expression. *PLoS One* **7**, e30653, doi:10.1371/journal.pone.0030653 (2012).
116 Bhattarai, N. *et al.* GB virus C particles inhibit T cell activation via envelope E2 protein-mediated inhibition of TCR signaling. *J Immunol* **190**, 6351-6359, doi:10.4049/jimmunol.1300589 (2013).
117 Pett, S. L., Kelleher, A. D. & Emery, S. Role of interleukin-2 in patients with HIV infection. *Drugs* **70**, 1115-1130, doi:10.2165/10898620-000000000-00000 (2010).
118 Bhattarai, N., McLinden, J. H., Xiang, J., Kaufman, T. M. & Stapleton, J. T. GB virus C envelope protein E2 inhibits TCR-induced IL-2 production and alters IL-2-signaling pathways. *J Immunol* **189**, 2211-2216, doi:10.4049/jimmunol.1201324 (2012).
119 Fama, A. *et al.* Human Pegivirus Infection and Lymphoma Risk: A Systematic Review and Meta-analysis. *Clin Infect Dis*, doi:10.1093/cid/ciz940 (2019).
120 Mellor, J., Haydon, G., Blair, C., Livingstone, W. & Simmonds, P. Low level or absent in vivo replication of hepatitis C virus and hepatitis G virus/GB virus C in peripheral blood mononuclear cells. *J Gen Virol* **79 (Pt 4)**, 705-714, doi:10.1099/0022-1317-79-4-705 (1998).
121 Fama, A. *et al.* Human Pegivirus infection and lymphoma risk and prognosis: a North American study. *Br J Haematol* **182**, 644-653, doi:10.1111/bjh.15416 (2018).
122 Krajden, M. *et al.* GBV-C/hepatitis G virus infection and non-Hodgkin lymphoma: a case control study. *Int J Cancer* **126**, 2885-2892, doi:10.1002/ijc.25035 (2010).
123 Pavlova, B. G. *et al.* Association of GB virus C (GBV-C)/hepatitis G virus (HGV) with haematological diseases of different malignant potential. *J Med Virol* **57**, 361-366, doi:10.1002/(sici)1096-9071(199904)57:4<361::aid-jmv6>3.0.co;2-o (1999).
124 Ellenrieder, V. *et al.* HCV and HGV in B-cell non-Hodgkin's lymphoma. *J Hepatol* **28**, 34-39, doi:10.1016/s0168-8278(98)80199-2 (1998).
125 Kaya, H., Polat, M. F., Erdem, F. & Gundogdu, M. Prevalence of hepatitis C virus and hepatitis G virus in patients with non-Hodgkin's lymphoma. *Clin Lab Haematol* **24**, 107-110, doi:10.1046/j.1365-2257.2002.00427.x (2002).
126 De Renzo, A. *et al.* High prevalence of hepatitis G virus infection in Hodgkin's disease and B-cell lymphoproliferative disorders: absence of correlation with hepatitis C virus infection. *Haematologica* **87**, 714-718; discussion 718 (2002).
127 Byrnes, J. J., Banks, A. T., Piatack, M., Jr. & Kim, J. P. Hepatitis G-associated aplastic anaemia. *Lancet* **348**, 472, doi:10.1016/S0140-6736(05)64562-X (1996).
128 Crespo, J. *et al.* Hepatitis G virus infection as a possible causative agent of community-acquired hepatitis and associated aplastic anaemia. *Postgrad Med J* **75**, 159-160, doi:10.1136/pgmj.75.881.159 (1999).
129 Riaz Shah, S. A., Idrees, M. & Hussain, A. Hepatitis G virus associated aplastic anemia: a recent case from Pakistan. *Virol J* **8**, 30, doi:10.1186/1743-422X-8-30 (2011).
130 Smith, D. B. *et al.* Proposed update to the taxonomy of the genera Hepacivirus and Pegivirus within the Flaviviridae family. *J Gen Virol* **97**, 2894-2907, doi:10.1099/jgv.0.000612 (2016).

131 Kennedy, J. *et al.* Genetic variability of porcine pegivirus in pigs from Europe and China and insights into tissue tropism. *Sci Rep* **9**, 8174, doi:10.1038/s41598-019-44642-0 (2019).
132 Divers, T. J. *et al.* New Parvovirus Associated with Serum Hepatitis in Horses after Inoculation of Common Biological Product. *Emerg Infect Dis* **24**, 303-310, doi:10.3201/eid2402.171031 (2018).
133 Bailey, A. L. *et al.* Pegivirus avoids immune recognition but does not attenuate acute-phase disease in a macaque model of HIV infection. *PLoS Pathog* **13**, e1006692, doi:10.1371/journal.ppat.1006692 (2017).
134 Radkowski, M., Przyjalkowski, W., Lipowski, D., Wang, L. F. & Laskus, T. Lack of GB virus C/hepatitis G virus sequences in cerebrospinal fluid in patients with central nervous system infections. *Scand J Infect Dis* **30**, 539, doi:10.1080/00365549850161647 (1998).
135 Radkowski, M., Wang, L. F., Vargas, H., Rakela, J. & Laskus, T. Lack of evidence for GB virus C/hepatitis G virus replication in peripheral blood mononuclear cells. *J Hepatol* **28**, 179-183, doi:10.1016/0168-8278(88)80002-3 (1998).
136 Liu, Z. *et al.* Detection of GB virus C genomic sequence in the cerebrospinal fluid of a HIV-infected patient in China: a case report and literature review. *Epidemiol Infect* **144**, 106-112, doi:10.1017/S0950268815001326 (2016).
137 Fridholm, H. *et al.* Human pegivirus detected in a patient with severe encephalitis using a metagenomic pan-virus array. *J Clin Virol* **77**, 5-8, doi:10.1016/j.jcv.2016.01.013 (2016).
138 Wilson, M. R. *et al.* Chronic Meningitis Investigated via Metagenomic Next-Generation Sequencing. *JAMA Neurol* **75**, 947-955, doi:10.1001/jamaneurol.2018.0463 (2018).
139 Bukowska-Osko, I. *et al.* Human Pegivirus in Patients with Encephalitis of Unclear Etiology, Poland. *Emerg Infect Dis* **24**, 1785-1794, doi:10.3201/eid2410.180161 (2018).
140 Tuddenham, R. *et al.* Human pegivirus in brain tissue of a patient with encephalitis. *Diagn Microbiol Infect Dis*, 114898, doi:10.1016/j.diagmicrobio.2019.114898 (2019).
141 Hickey, W. F. Leukocyte traffic in the central nervous system: the participants and their roles. *Semin Immunol* **11**, 125-137, doi:10.1006/smim.1999.0168 (1999).
142 Horemheb-Rubio, G. *et al.* High HPgV replication is associated with improved surrogate markers of HIV progression. *PLoS One* **12**, e0184494, doi:10.1371/journal.pone.0184494 (2017).
143 Blackard, J. T. *et al.* Cytokine/chemokine expression associated with Human Pegivirus (HPgV) infection in women with HIV. *J Med Virol* **89**, 1904-1911, doi:10.1002/jmv.24836 (2017).
144 Ng, K. T. *et al.* Co-infections and transmission networks of HCV, HIV-1 and HPgV among people who inject drugs. *Sci Rep* **5**, 15198, doi:10.1038/srep15198 (2015).
145 Ernst, D. *et al.* Impact of GB virus C viraemia on clinical outcome in HIV-1-infected patients: a 20-year follow-up study. *HIV Med* **15**, 245-250, doi:10.1111/hiv.12094 (2014).
146 Xiang, J. *et al.* Inhibition of HIV-1 replication by GB virus C infection through increases in RANTES, MIP-1alpha, MIP-1beta, and SDF-1. *Lancet* **363**, 2040-2046, doi:10.1016/S0140-6736(04)16453-2 (2004).
147 Stapleton, J. T. *et al.* GBV-C viremia is associated with reduced CD4 expansion in HIV-infected people receiving HAART and interleukin-2 therapy. *AIDS* **23**, 605-610, doi:10.1097/QAD.0b013e32831f1b00 (2009).

148 Group, I.-E. S. *et al.* Interleukin-2 therapy in patients with HIV infection. *N Engl J Med* **361**, 1548-1559, doi:10.1056/NEJMoa0903175 (2009).
149 Douglas, S. D. *et al.* TH1 and TH2 cytokine mRNA and protein levels in human immunodeficiency virus (HIV)-seropositive and HIV-seronegative youths. *Clin Diagn Lab Immunol* **10**, 399-404, doi:10.1128/cdli.10.3.399-404.2003 (2003).
150 Nunnari, G. *et al.* Slower progression of HIV-1 infection in persons with GB virus C co-infection correlates with an intact T-helper 1 cytokine profile. *Ann Intern Med* **139**, 26-30, doi:10.7326/0003-4819-139-1-200307010-00009 (2003).
151 Chang, Q., McLinden, J. H., Stapleton, J. T., Sathar, M. A. & Xiang, J. Expression of GB virus C NS5A protein from genotypes 1, 2, 3 and 5 and a 30 aa NS5A fragment inhibit human immunodeficiency virus type 1 replication in a CD4+ T-lymphocyte cell line. *J Gen Virol* **88**, 3341-3346, doi:10.1099/vir.0.83198-0 (2007).
152 Moenkemeyer, M., Schmidt, R. E., Wedemeyer, H., Tillmann, H. L. & Heiken, H. GBV-C coinfection is negatively correlated to Fas expression and Fas-mediated apoptosis in HIV-1 infected patients. *J Med Virol* **80**, 1933-1940, doi:10.1002/jmv.21305 (2008).
153 Nattermann, J. *et al.* Regulation of CC chemokine receptor 5 in hepatitis G virus infection. *AIDS* **17**, 1457-1462, doi:10.1097/00002030-200307040-00006 (2003).
154 Walsh, J. G. *et al.* Rapid inflammasome activation in microglia contributes to brain disease in HIV/AIDS. *Retrovirology* **11**, 35, doi:10.1186/1742-4690-11-35 (2014).
155 McKenzie, B. A. *et al.* Caspase-1 inhibition prevents glial inflammasome activation and pyroptosis in models of multiple sclerosis. *Proc Natl Acad Sci U S A* **115**, E6065-E6074, doi:10.1073/pnas.1722041115 (2018).
156 Maingat, F. G. *et al.* Neurosteroid-mediated regulation of brain innate immunity in HIV/AIDS: DHEA-S suppresses neurovirulence. *FASEB journal : official publication of the Federation of American Societies for Experimental Biology* **27**, 725-737, doi:10.1096/fj.12-215079 (2013).
157 Boghozian, R. *et al.* Suppressed oligodendrocyte steroidogenesis in multiple sclerosis: Implications for regulation of neuroinflammation. *Glia*, doi:10.1002/glia.23179 (2017).
158 Limonta, D. *et al.* Human Fetal Astrocytes Infected with Zika Virus Exhibit Delayed Apoptosis and Resistance to Interferon: Implications for Persistence. *Viruses* **10**, doi:10.3390/v10110646 (2018).
159 Palus, M. *et al.* Infection and injury of human astrocytes by tick-borne encephalitis virus. *J Gen Virol* **95**, 2411-2426, doi:10.1099/vir.0.068411-0 (2014).
160 Wollmann, G., Robek, M. D. & van den Pol, A. N. Variable deficiencies in the interferon response enhance susceptibility to vesicular stomatitis virus oncolytic actions in glioblastoma cells but not in normal human glial cells. *J Virol* **81**, 1479-1491, doi:10.1128/JVI.01861-06 (2007).
161 Furr, S. R. & Marriott, I. Viral CNS infections: role of glial pattern recognition receptors in neuroinflammation. *Front Microbiol* **3**, 201, doi:10.3389/fmicb.2012.00201 (2012).
162 Brunetto, G. S. *et al.* Digital droplet PCR (ddPCR) for the precise quantification of human T-lymphotropic virus 1 proviral loads in peripheral blood and cerebrospinal fluid of HAM/TSP patients and identification of viral mutations. *J Neurovirol* **20**, 341-351, doi:10.1007/s13365-014-0249-3 (2014).
163 MacMicking, J., Xie, Q. W. & Nathan, C. Nitric oxide and macrophage function. *Annu Rev Immunol* **15**, 323-350, doi:10.1146/annurev.immunol.15.1.323 (1997).
164 Takashiba, S. *et al.* Differentiation of monocytes to macrophages primes cells for lipopolysaccharide stimulation via accumulation of cytoplasmic nuclear factor kappaB. *Infect Immun* **67**, 5573-5578 (1999).

165 White, R. A., 3rd, Quake, S. R. & Curr, K. Digital PCR provides absolute quantitation of viral load for an occult RNA virus. *J Virol Methods* **179**, 45-50, doi:10.1016/j.jviromet.2011.09.017 (2012).
166 Schwartz, S. L. & Lowen, A. C. Droplet digital PCR: A novel method for detection of influenza virus defective interfering particles. *J Virol Methods* **237**, 159-165, doi:10.1016/j.jviromet.2016.08.023 (2016).
167 Li, H. *et al.* Application of droplet digital PCR to detect the pathogens of infectious diseases. *Biosci Rep* **38**, doi:10.1042/BSR20181170 (2018).
168 Mu, D., Yan, L., Tang, H. & Liao, Y. A sensitive and accurate quantification method for the detection of hepatitis B virus covalently closed circular DNA by the application of a droplet digital polymerase chain reaction amplification system. *Biotechnol Lett* **37**, 2063-2073, doi:10.1007/s10529-015-1890-5 (2015).
169 Leary, T. P., Desai, S. M., Erker, J. C. & Mushahwar, I. K. The sequence and genomic organization of a GB virus A variant isolated from captive tamarins. *J Gen Virol* **78 (Pt 9)**, 2307-2313, doi:10.1099/0022-1317-78-9-2307 (1997).
170 Boukadida, C. *et al.* NS2 proteases from hepatitis C virus and related hepaciviruses share composite active sites and previously unrecognized intrinsic proteolytic activities. *PLoS Pathog* **14**, e1006863, doi:10.1371/journal.ppat.1006863 (2018).
171 Isken, O. *et al.* A conserved NS3 surface patch orchestrates NS2 protease stimulation, NS5A hyperphosphorylation and HCV genome replication. *PLoS Pathog* **11**, e1004736, doi:10.1371/journal.ppat.1004736 (2015).
172 Ye, J., Zhu, B., Fu, Z. F., Chen, H. & Cao, S. Immune evasion strategies of flaviviruses. *Vaccine* **31**, 461-471, doi:10.1016/j.vaccine.2012.11.015 (2013).
173 Overby, A. K., Popov, V. L., Niedrig, M. & Weber, F. Tick-borne encephalitis virus delays interferon induction and hides its double-stranded RNA in intracellular membrane vesicles. *J Virol* **84**, 8470-8483, doi:10.1128/JVI.00176-10 (2010).
174 Fujinami, R. S., von Herrath, M. G., Christen, U. & Whitton, J. L. Molecular mimicry, bystander activation, or viral persistence: infections and autoimmune disease. *Clin Microbiol Rev* **19**, 80-94, doi:10.1128/CMR.19.1.80-94.2006 (2006).
175 Fujinami, R. S. & Oldstone, M. B. Amino acid homology between the encephalitogenic site of myelin basic protein and virus: mechanism for autoimmunity. *Science* **230**, 1043-1045, doi:10.1126/science.2414848 (1985).
176 Dusseaux, M. *et al.* Viral Load Affects the Immune Response to HBV in Mice With Humanized Immune System and Liver. *Gastroenterology* **153**, 1647-1661 e1649, doi:10.1053/j.gastro.2017.08.034 (2017).
177 Johnston, J. B. *et al.* Neurovirulence depends on virus input titer in brain in feline immunodeficiency virus infection: evidence for activation of innate immunity and neuronal injury. *J Neurovirol* **8**, 420-431, doi:10.1080/13550280260422721 (2002).
178 Phares, T. W., Kean, R. B., Mikheeva, T. & Hooper, D. C. Regional differences in blood-brain barrier permeability changes and inflammation in the apathogenic clearance of virus from the central nervous system. *J Immunol* **176**, 7666-7675, doi:10.4049/jimmunol.176.12.7666 (2006).
179 Sonar, S. A. & Lal, G. The iNOS Activity During an Immune Response Controls the CNS Pathology in Experimental Autoimmune Encephalomyelitis. *Front Immunol* **10**, 710, doi:10.3389/fimmu.2019.00710 (2019).
180 Jung, S. *et al.* Inhibition of HIV strains by GB virus C in cell culture can be mediated by CD4 and CD8 T-lymphocyte derived soluble factors. *AIDS* **19**, 1267-1272, doi:10.1097/01.aids.0000180097.50393.df (2005).

181 Hatton, C. F. & Duncan, C. J. A. Microglia Are Essential to Protective Antiviral Immunity: Lessons From Mouse Models of Viral Encephalitis. *Front Immunol* **10**, 2656, doi:10.3389/fimmu.2019.02656 (2019).
182 Bock, P. & Gorgas, K. [Morphology and histochemistry of Arteriae helicinae (mouse)]. *Verh Anat Ges*, 563 (1978).

Appendix

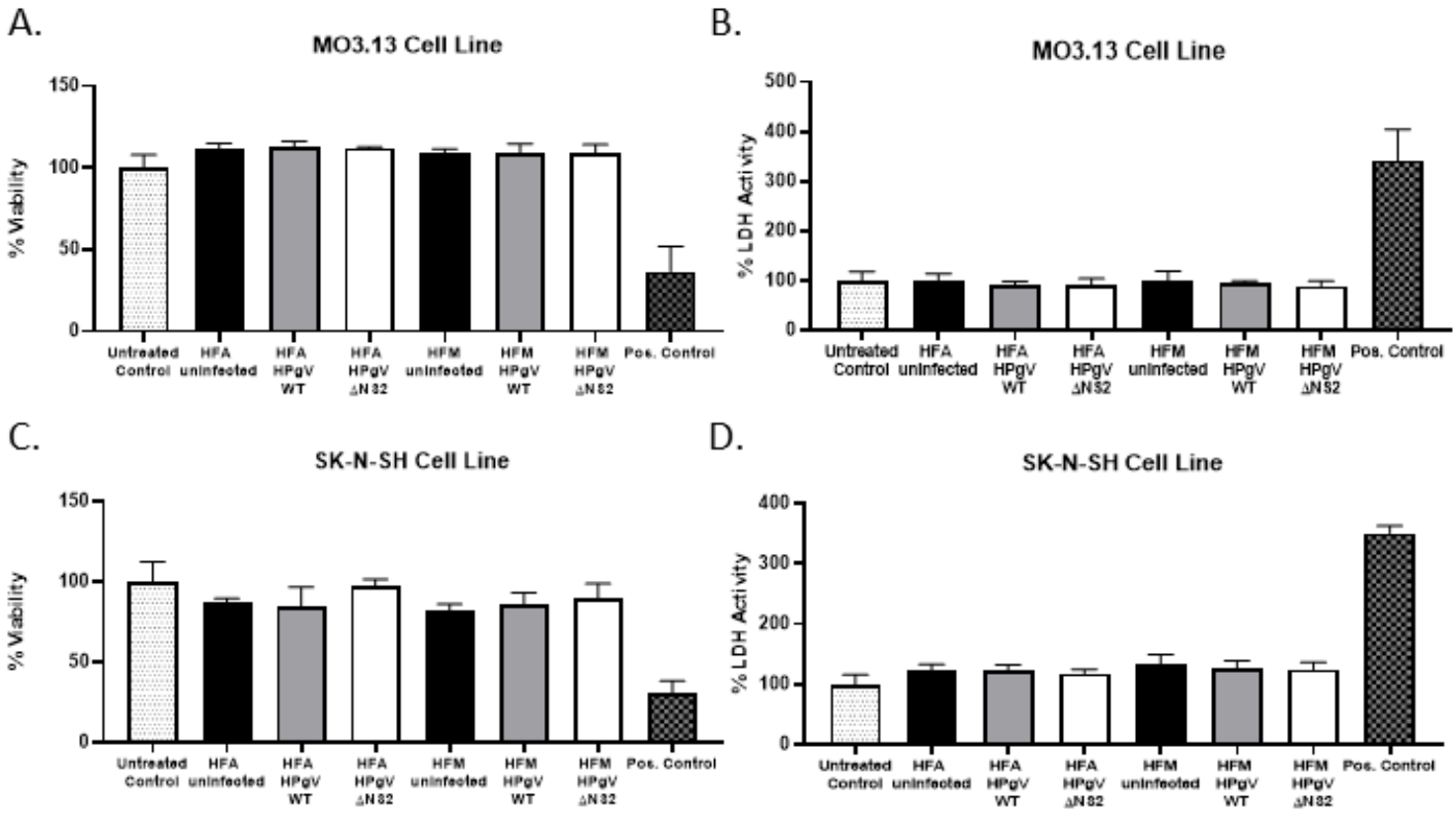

Figure A.1: Supernatants from HPgV-infected astrocytes and microglia are not toxic to human neural or oligodendrocyte cell lines.

Cell supernatants from day 4 infected human astrocytes (HFA) and microglia (HFM) were applied to human oligodendrocyte (MO3.13) or neuronal (SK-N-SH) cell lines for 48 hours and cell viability was measured in both MO3.13 [A] and SK-N-SH [C] cells and compared to untreated control cell viability. Similarly, cell supernatants from MO3.13 [B] and SK-N-SH [D] cells were collected 48 hours post-infection and LDH activity was measured and compared to untreated control levels. Positive control is a 24-hour incubation with staurosporine. n=4 technical replicates were used per condition.